Final Technical Report

Hydrodynamic and Sediment Transport Modeling Report

Revolution Wind Offshore Wind Farm

Prepared for:

Revolution Wind, LLC
56 Exchange Terrace, Suite 300
Providence, RI 02903

Prepared by:

RPS
55 Village Square Drive
South Kingstown, RI 02879

Submitted July 2022

Table of Contents

List of Figures

List of Tables

List of Abbreviations

CFE	Controlled Flow Excavator
CFL	Courant-Friedrichs-Lewis
cm	Centimeter
COP	Construction and Operations Plan
CT	Connecticut
cy	Cubic Yard
DOER	Dredging Operations and Environmental Research
ENC	Electronic Navigational Chart
ERDC	Environmental Research and Development Center
ESRI	Environmental Systems Research Institute
ft	Foot
GEBCO	General Bathymetric Chart of the Oceans
HDD	Horizontal Directional Drilling
hr	Hour
IAC	Inter-Array Cable
in	Inch
km	Kilometer
L	Liter
m	Meter
m/s	Meter/Second
MA	Massachusetts
mg	Milligram
mi	Mile
mm	Millimeter
NDBC	National Data Buoy Center
NOAA	National Oceanic and Atmospheric Administration
NY	New York
OCS	Outer Continental Shelf
OSAMP	Ocean Special Management Plan
OSS	Offshore Substation
OSU	Oregon State University
ppm	Parts per Million
RI	Rhode Island
RWEC	Revolution Wind Export Cable
RWF	Revolution Wind Farm
SCVR	Step-Wise-Continuous-Variable Rectangular
SSFATE	Suspended Sediment FATE
SSH	Sea Surface Height
TSHD	Trailing Suction Hopper Dredge
TSS	Total Suspended Solids
USACE	U.S. Army Corps of Engineers
WDPA	World Database on Protected Areas
WTG	Wind Turbine Generator

EXECUTIVE SUMMARY

This technical report provides details of the sediment effects from the offshore cable burial activities associated with the construction phase of the Revolution Wind Farm Project (Project). The details of the Project are described in Section 3.0 of the Construction and Operations Plan (COP). A description of the Project components is briefly reiterated in this document as they are vital to the cable burial assessment. The Project will include buried cables for the offshore components:

- Approximately 155 miles (mi) (250 kilometer [km]) of Inter-Array Cable (IAC) to connect the wind turbine generators (WTGs) and offshore substations (OSSs) within the Revolution Wind Farm (RWF);
- Up to two high-voltage alternating current submarine cables, located within an approximately 50-mi (80-km)-long corridor, to convey power to shore (herein referred to as the Revolution Wind Export Cable [RWEC]); and
- One offshore substation link cable (OSS-Link Cable).

The IAC and OSS-Link Cable will be located in federal waters in Lease Area OCS-A-0486 (Lease Area), while the RWEC will traverse both federal waters and state waters of Rhode Island (RI). The IAC, RWEC, and OSS-Link Cable will be buried beneath the seabed to the extent feasible as determined necessary by the Cable Burial Risk Assessment and other supporting engineering documents. Note that the OSS-Link Cable is anticipated to be installed with the same methods as the RWEC and is included as part of the RWEC in figures in this report; as such, the modeling of the RWEC in the Lease Area reflects installation of this component. Burial of the cables may be accomplished using a variety of installation methods (e.g., jet plow, controlled flow excavation [CFE], trailing suction hopper dredge [TSHD]). The resuspension of sediments from the various construction activities may cause a localized sediment plume. A sediment plume is a portion of the water column that experiences a temporary increase in the total suspended solids (TSS) concentration above ambient levels. Over time the plume settles and deposits sediment on the seabed, a process referred to as sedimentation, which is estimated as excess (i.e., above ambient) thickness of sediment accumulated on the seabed.

The objective of this assessment is to characterize the effects of the anticipated sediment-disturbing construction activities proposed to install the Project components. Based on the potential installation methods, conservative assumptions were made to complete this modeling assessment. In support of this objective, RPS performed a hydrodynamic and sediment transport modeling study to simulate the installation activities. The modeling was designed to provide results that characterize the effects of the cable burial in terms of the suspended sediment plume in the water column and the eventual seabed deposition associated with the construction methods. At the time of the modeling study, an export cable route, within the RWEC corridor, and the nearshore landing location were selected as representative locations to be evaluated.

This study assessed the installation of cables, which are presented as four distinct study components: (1) the RWEC seabed preparation alternatives, (2) the RWEC installation, (3) the IAC installation, and (4) the RWEC landfall. A brief description of each study component is provided below.

1. RWEC seabed preparation alternatives – The Project anticipates the potential need for seabed preparation of deeper sediment areas along the RWEC. The evaluation included two different methods: CFE and TSHD. For the TSHD, two disposal methods were evaluated: split bottom barge and continuous overflow.
2. Installation of the RWEC – The RWEC modeling included simulation of installation of one cable (referred to as “circuit”) from the landfall to OSS 1 (Circuit 1). While there is another cable planned from the landfall to OSS 2, the routes follow a similar path and are in proximity to one another. Therefore, the modeled route (Circuit 1) and associated results are considered representative of both routes.
3. Installation of a representative segment of the IAC – This task included simulation of a representative segment of the IAC. A section in the Lease Area with a relatively larger fraction of fine sediments was

selected for modeling to provide a conservative estimate of the plume's predicted TSS concentration. Due to the relatively short installation period, the segment was modeled twice using two different timeframes. This was done to show the potential variations induced by the different currents, and to assess the sensitivity of sediment transport to variable current regimes.

4. RWEC landfall – The Project proposes the use of horizontal directional drilling (HDD) for the last segment of the RWEC at the landfall location. While two HDD exit pits are anticipated, it is expected that the excavation of each will occur on the order of days apart. Therefore, due to the timing of the excavation, the modeled HDD exit pit is considered representative of both exit pits. The evaluation included two different landfall equipment types to excavate the HDD exit pit, which are anticipated to be implemented consecutively: a backhoe excavator and a Venturi eductor device.

This assessment was carried out using hydrodynamic and sediment transport models. Specifically, the analysis included two related modeling tasks:

1. Hydrodynamic Model – Using the HYDROMAP modeling system, develop a three-dimensional hydrodynamic model application for the southern New England OCS. The present study focused on validation of model predictions local to the RWEC and Lease Area. Current fields developed using the HYDROMAP model were used as the primary forcing for the sediment transport and dispersion model.

2. Sediment Transport Model – Using the SSFATE modeling system, model the suspended sediment fate and transport. SSFATE was applied to simulate cable burial construction activities to predict the potential sediment plumes and subsequent sedimentation. The resulting effects were presented in terms of excess TSS or sedimentation introduced from the construction activities. Therefore, the effects are associated only with the modeled construction actives and would be in addition to the natural conditions.

The hydrodynamic model produced spatially- and time-varying predictions of currents across the study area and vertically in the water column throughout the modeling domain. Currents in the RWF and along the RWEC are primarily dominated by tides, particularly near the seabed. The tidal currents continuously change speed and direction, with speeds ramping up and down in magnitude, as it cycles through the flood (move offshore to onshore), slack (minimal movement as currents shift direction) and ebb (move onshore to offshore) stages.

The sediment transport model scenarios were designed to reflect each respective construction method and installation activity. The model input parameters included scenario-specific values for the location of the sediment resuspension in the water column, the rate of resuspension, and the sediment types being resuspended. The sediment transport was simulated for an extended period to evaluate the cumulative impacts throughout the duration of the activity and to ensure sufficient time for sedimentation. The burial depth was based on an assumption which conservatively estimated the volume of sediment resuspended. The simulations produced spatially- and time-varying predictions of water column TSS and seabed deposition for each scenario. The output was post-processed to provide (1) a map of instantaneous concentration, (2) a map of the maximum concentration experienced throughout the entire simulation, (3) a map of the cumulative seabed deposition from the entire simulation, (4) tables that summarized volumes resuspended, (5) tables that summarized the area of deposition over specific thresholds, (6) tables that summarized the maximum extent of deposition thickness over specific thresholds, (7) tables that summarized the maximum extent of TSS above specific thresholds, and (8) the duration of plume exposure over specific thresholds.

The modeling predicted that the cable burial activities will result in plumes of excess TSS in the water column and seabed deposition. The term "excess" refers to above background levels. The TSS plumes are limited to the bottom of the water column for the CFE seabed preparation method, RWEC Circuit 1 burial, and IAC burial. The TSS plumes for TSHD seabed preparation and landfall are present throughout the majority of the water column due to the location of sediment introduction and, for the landfall, shallow depths. Each plume is temporary in any given

location and will change based on the sediment-disturbing activities and environmental conditions present at the time of construction.

Parameters influencing seabed deposition and TSS water column concentrations include volume and grain size distribution of disturbed sediment, local currents, installation rate, local depth, and location of sediment introduction into the water column. The bullets below describe the summary tables and key results.

Seabed Deposition

- For the seabed preparation segments, deposition exceeding 10 mm is predicted to remain within 688.8 ft (210 m), 1033.2 ft (315 m), and 852.8 ft (260 m) from the route centerline for CFE, TSHD split bottom, and TSHD continuous overflow seabed preparation activities, respectively.
- For jet plow installation along the RWEC deposition exceeding 10 mm is predicted to remain within 311.6 ft (95 m) from the route centerline.
- For the IAC, deposition exceeding 10 mm is predicted to remain within 78.7 ft (24 m) and 88.6 ft (27 m) from the route centerline for current regime 1 and current regime 2, respectively.
- Evaluation of the landfall showed that deposition exceeding 10 mm may extend up to 738 ft (225 m) from the exit pit location.

Water Column Concentrations

- For the seabed preparation segments, the predicted concentrations above background (> 0 mg/L) do not persist in any given location (grid cell) for greater than 5.5 hours, 59.2 hours, and 85 hours for CFE, TSHD split bottom, and TSHD continuous overflow seabed preparation activities, respectively. In most locations (> 75% of the affected area) concentrations return to ambient within approximately 2.5 hours for CFE and approximately 26 hours for TSHD split bottom and 37 hours for TSHD continuous overflow. Predicted concentrations greater than 100 mg/L do not persist for greater than 2.2 hours, 19.2 hours, and 17.5 hours for CFE, TSHD split bottom, and TSHD continuous overflow seabed preparation activities, respectively.
- For jet plow installation along the RWEC, predicted concentrations above background (> 0 mg/L) do not persist in any given location (grid cell) for greater than 69.7 hours. In most locations (> 75% of the affected area) concentrations return to ambient within approximately 24.5 hours. Predicted concentrations greater than 100 mg/L do not persist for greater than 4.5 hours.
- For the IAC, predicted concentrations above background (> 0 mg/L) do not persist in any given location (grid cell) for greater than 4.2 hours and 6.7 hours for current regime 1 and current regime 2, respectively. In most locations (> 75% of the affected area) concentrations return to ambient within approximately 3 hours and 4 hours for current regime 1 and current regime 2, respectively. Predicted concentrations greater than 100 mg/L do not persist for greater than 1.2 hours and 1.7 hours for current regime 1 and current regime 2, respectively.
- Evaluation of the landfall showed that predicted concentrations above background (> 0 mg/L) do not persist in any given location (grid cell) for greater than 70.3 hours. In most locations (> 75% of the affected area) concentrations return to ambient within approximately 6 hours. Predicted concentrations greater than 100 mg/L do not persist for greater than 70.2 hours.

SSFATE was used to effectively simulate four representative study components of the types of activities that are expected with the Project. The modeling predicted the potential TSS concentrations, deposition thicknesses, exposure durations, and corresponding areas and distances associated with each Project-related construction activity.

1.0 INTRODUCTION

This technical report provides the details of the sediment effects from offshore cable burial activities associated with the construction phase of the Revolution Wind Farm Project (Project). The details of the Project are described in Section 3.0 of the Construction and Operations Plan (COP). A brief description of the Project components is presented here as they are vital to the cable burial assessment. The Project will include the following buried cables for its offshore components:

- Approximately 155 miles (mi) (250 kilometer [km]) of Inter-Array Cable (IAC) to connect the wind turbine generators (WTGs) and offshore substations (OSSs) within the Revolution Wind Farm (RWF);
- Up to two high-voltage alternating current submarine cables to convey power to shore located within an approximately 50-mi (80-km)-long corridor (referred to as the Revolution Wind Export Cable [RWEC]); and
- One offshore substation link cable (OSS-Link Cable).

The IAC and OSS-Link Cable will be located in federal waters in Lease Area OCS-A-0486 (Lease Area), while the RWEC will traverse both federal waters and state waters of Rhode Island (RI). The modeling of this project was done for both federal and state waters.

The IAC, RWEC, and OSS-Link Cable will be buried beneath the seabed to the extent feasible as determined necessary by the Cable Burial Risk Assessment and other supporting engineering documents. Note that the OSS-Link Cable will be installed with the same methods as the RWEC and is included as part of the RWEC in figures in this report; as such, the modeling of the RWEC in the Lease Area reflects installation of this component. Burial of the cables may be accomplished using a variety of installation methods (e.g., jet plow, controlled flow excavation [CFE], trailing suction hopper dredge [TSHD]). The resuspension of sediments from the various construction activities may cause a localized sediment plume. A sediment plume is a portion of the water column that experiences a temporary increase in the total suspended solids (TSS) concentration above ambient levels. Over time the plume settles and deposits sediment on the seabed, a process referred to as sedimentation, which is estimated as excess (i.e., above ambient) thickness of sediment accumulated on the seabed.

The objective of this assessment is to characterize the effects of the anticipated sediment-disturbing construction activities proposed to install the Project components. Based on the potential installation methods, conservative assumptions were made to complete this modeling assessment. In support of this objective, RPS performed a hydrodynamic and sediment transport modeling study to simulate the installation activities. The modeling was designed to provide results that characterize the effects of the cable burial in terms of the suspended sediment plume in the water column and the eventual seabed deposition associated with the construction methods.

This study assessed the installation of cables, which are presented as four distinct study components: (1) the RWEC seabed preparation alternatives, (2) the RWEC installation, (3) the IAC installation, and (4) the RWEC landfall. A brief description of each study component is provided below.

1. RWEC seabed preparation alternatives – The Project anticipates the potential need for seabed preparation of deeper sediment areas along the RWEC. The evaluation included two different methods: CFE and TSHD. For the TSHD, two disposal methods were evaluated: split bottom barge and continuous overflow.
2. Installation of the RWEC – The RWEC modeling included simulation of installation of one cable (referred to as “circuit”) from the landfall to OSS 1 (Circuit 1). While there is another cable planned from the landfall to OSS 2, the routes follow a similar path and are in proximity to one another. Therefore, the modeled route (Circuit 1) and associated results are considered representative of both routes.
3. Installation of a representative segment of the IAC – This task included simulation of a representative segment of the IAC. A section in the Lease Area with a relatively larger fraction of fine sediments was

selected for modeling to provide a conservative estimate of the plume's predicted TSS concentration. Due to the relatively short installation period, the segment was modeled twice using two different timeframes. This was done to show the potential variations induced by the different currents, and to assess the sensitivity of sediment transport to variable current regimes.

4. RWEC landfall – The Project proposes the use of horizontal directional drilling (HDD) for the last segment of the RWEC at the landfall location. While two HDD exit pits are anticipated, it is expected that the excavation of each will occur on the order of days apart. Therefore, due to the timing of the excavation, the modeled HDD exit pit is considered representative of both exit pits. The evaluation included two different landfall equipment types to excavate the HDD exit pit, which are anticipated to be implemented consecutively: a backhoe excavator and a Venturi eductor device.

At the time of the modeling study, an export cable route, within the RWEC corridor, and the nearshore landing location were selected as representative locations to be evaluated. The indicative route is within the RWEC corridor as can be seen in Figure 1.1-1, which gives an overview of the RWF and RWEC areas. The map shows the RWEC corridor in yellow and the modeled RWEC route in black.

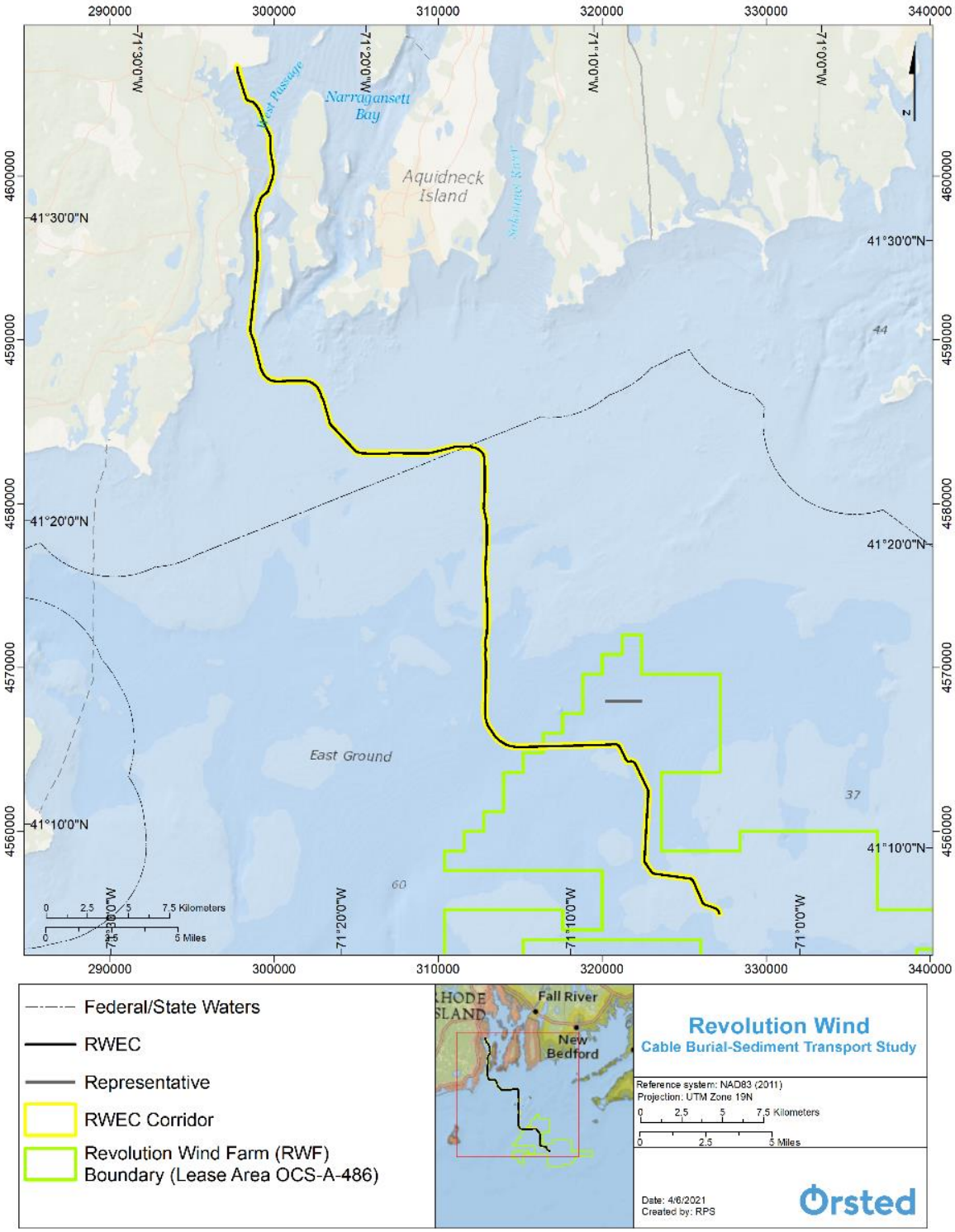

Figure 1.1-1. Location of the Indicative Export Cable Route in the RWEC Corridor.

1.1 Study Area

The study area is broadly situated within the southern New England Outer Continental Shelf (OCS), which lies south of Massachusetts, Rhode Island, and Long Island, New York, and extends from the Hudson Shelf Canyon in the west to Nantucket Shoals in the east. Components of the Project that have potential for sediment disturbance span a relatively large distance, with the RWEC route extending from the Lease Area, which is located between approximately 16-28 mi (26 – 46 km) offshore, to a proposed landfall at Quonset Point in North Kingstown, Rhode Island. The currents vary spatially and temporally throughout the domain. The general ocean circulation (currents) across the study area is complex and influenced to some extent by wind-driven processes, tides, and density gradients that arise from combined interaction with adjacent estuaries, solar effects, and heat flux through the air-sea interface (Codiga and Ullman, 2010). Yet, over most of the region, tidal currents are the dominant form of circulation (Spaulding and Gordon, 1982), with wind and density variations playing a smaller role.

Tides in the study area are predominately semi-diurnal (twice per day) with influences from diurnal (once per day) constituents. This results in approximately two high tides and two low tides daily, which cause the ocean currents to flood and ebb in response to the changing water levels. The current direction changes as it floods (moves offshore to onshore) and ebbs (moves onshore to offshore), with a semidiurnal tide resulting in approximately four changes in direction per day in response to the tides. While tidal currents are always present, at some locations they may be overcome by wind or density driven currents. However, tidal circulation dominates in nearshore environments and in Narraganset Bay. Sediments in the study area are characterized by modern marine deposits and reworked glacial and post-glacial outwash deposits. Marine deposits in this region are typically comprised of silty fine sand and are typically up to 6.6 – 9.8 ft (2 – 3 m) thick.

1.2 Regulatory Context and Resource Definition

This assessment has been performed to provide a characterization of the physical effects of the cable burial in terms of the associated suspended sediment plume in the water column and the seabed deposition of sediments disturbed during construction. This study has been performed to provide information that describes impacting factors with respect to activities that disturb the sea bottom and increase turbidity, as required by BOEM guidelines (30 CFR § 585.626(a), (2), and (4) and 30 CFR § 585.627(a), (1), and (2)) for inclusion within the Project's COP.

1.3 Significance Threshold

There are no thresholds of significance for which the effects were evaluated to determine compliance or impact. The results are presented in a manner that allows the reader to view the order of magnitude of the predicted effects. The sediment transport modeling produced predictions of excess TSS and cumulative seabed deposition. The term "excess" refers to above background levels. From this point herein all concentrations refer to excess concentrations. The term "cumulative" with respect to deposition refers to the fact that the deposition in any location may build over time during the cable installation and is the sum of deposition from the modeled activity. The thresholds used to demonstrate the results for TSS and seabed deposition are presented in Table 1.3-1 and Table 1.3-2, respectively.

Table 1.3-1. TSS Concentration Thresholds used for Presentation of Modeling Results.

Concentration Bin Ranges		
Threshold Bin	Parts per Million (ppm)	Milligram/Liter (mg/L)
1	10 - 50	10 - 50
2	50 - 100	50 - 100
3	100 - 200	100 - 200
4	200 - 500	200 - 500
5	> 500	> 500

Table 1.3-2. Seabed Deposition Thresholds used for Presentation of Modeling Results.

Deposition Bin Ranges		
Threshold Bin	Inches (in)	Millimeter (mm)
1	0.0039 – 0.039	0.1 - 1
2	0.039 – 0.39	1 - 10
3	0.39 – 3.14	10-80
4	> 3.14	> 80

1.4 Regulatory Coordination and Required Permits

This study did not include considerations of regulatory coordination or required permits. It is a stand-alone study characterizing the physical effects of the cable burial activities. The results may be referenced by other components of the Project, which may have regulatory coordination and required permits.

This study has been performed to provide information on impact-producing activities that may disturb the seabed and increase turbidity for consideration in the regulatory process.

1.5 Note on Units and Figures

The text and supporting tables and graphics are presented primarily in Imperial units (e.g., inches, feet, miles, knots) and secondarily in Metric units (e.g., meters, kilometers, meters per second) with the following exceptions:

- In figures where a parameter is presented at a set of round monotonically increasing levels that were established with respect to metric increments.
- Figures and reference to the TSS plume have been made with respect to metric units of mg/L due to this being the most widely use measurement to evaluate TSS plumes.
- Figures and reference to the sediment deposition have been made with respect to metric units of mm due to this being the most widely use measurement to evaluate sedimentation.

Map-based figures in this report have been made primarily using the Environmental Systems Research Institute (ESRI) ArcMap software and incorporate a basemap provided through the application. The map service layer credits do not easily fit on the images and are provided below.

- Main figures use the World Ocean Basemap; the service layer credits are listed below.
    - General Bathymetric Chart of the Oceans (GEBCO) GEBCO_08 Grid version 20100927 and IHO-IOC GEBCO Gazetteer of Undersea Feature Names August 2010 version (https://www.gebco.net), National Oceanic and Atmospheric Administration (NOAA) and National Geographic for the oceans; and DeLorme, HERE, and Esri for topographic content
- Main figures and insets showing figure location use the National Geographic World Map; the service layer credits are bulleted below.
    - Reference Data: National Geographic, ESRI, Garmin, HERE, INCREMENT P, NRCAN, METI
    - Land Cover Imagery: NASA Blue Marble, ESA GlobCover 2009 (Copyright notice: © ESA 2010 and UCLouvain)
    - Protected Areas: IUCN and UNEP-WCMC (2011), The World Database on Protected Areas (WDPA) Annual Release. Cambridge, UK: UNEP-WCMC. Available at: www.protectedplanet.net.
    - Ocean Data: GEBCO, NOAA

2.0 METHODOLOGY

RPS applied customized hydrodynamic and sediment transport and dispersion models to assess potential effects from sediment resuspension related to cable burial activities expected to take place during the construction phase of the Project. Specifically, the analysis included two interconnected modeling tasks:

- Develop a three-dimensional hydrodynamic model application for the southern New England OCS, using the HYDROMAP modeling system. The present study focused on validation of model predictions local to the RWEC and Lease Area. Current fields developed using the HYDROMAP model were used as the primary forcing for the sediment transport and dispersion model.

- Model the suspended sediment fate and transport using the SSFATE modeling system. SSFATE was applied to simulate cable burial construction activities to produce predictions of sediment plumes and sedimentation.

This study was performed in a manner such that the results were produced in terms of the effects as excess, referring to in excess of natural conditions. Therefore, the effects are presented as isolated effects of the construction that occur which would be added to the natural conditions.

2.1 Hydrodynamic Modeling Approach

The Project will include construction activities that disturb the seabed and result in sediment resuspension. In order to evaluate potential sediment resuspension, circulation patterns in the bottom waters were modeled using a three-dimensional hydrodynamic model application. RPS's HYDROMAP hydrodynamic model system (Isaji et al., 2001) was used to develop the model application for the southern New England OCS. The model was used to simulate water levels, circulation patterns, and water volume flux through the study area and to provide the hydrodynamic input (spatially- and temporally-varying currents) for the sediment transport model.

The hydrodynamic modeling included gathering and analyzing environmental data, development of the model grid and boundary conditions, validation of model performance for a period coincident with observations of water levels and currents, and development of currents for scenario timeframes relevant to the sediment transport simulations.

2.1.1 HYDROMAP Model Description

HYDROMAP is a globally re-locatable hydrodynamic model capable of simulating complex circulation patterns due to tidal forcing, wind stress, and freshwater flows, quickly and efficiently, anywhere on the globe. HYDROMAP employs a novel step-wise-continuous-variable rectangular (SCVR) gridding strategy with up to six levels of resolution. The term "step-wise-continuous" implies that the boundaries between successively smaller and larger grids are managed in a consistent integer step. The advantage of this approach is that large areas of widely differing spatial scales can be addressed within one consistent model application. Grids constructed by the SCVR are still "structured," so that arbitrary locations can be easily located to corresponding computational cells. This mapping facility is particularly advantageous when outputs of the hydrodynamic model are used in subsequent application programs (e.g., Lagrangian particle transport model) that use another grid or grid structure.

The hydrodynamic model solves the three-dimensional conservation equations in spherical coordinates for water mass, density, and momentum, with the Boussinesq and hydrostatic assumptions applied. These equations are solved subject to the following boundary conditions:

- At land boundaries, the normal component of velocity is set to zero;

- At the open boundaries, the sea surface elevation is specified by the dominant tidal constituents, each with its own amplitude and phase from a reference time zone, or as a time series of total surface elevation defined relative to the local surface elevation;
- At the sea surface, the applied stress due to the wind is matched to the local stress in the water column and the kinematic boundary condition is satisfied; and
- At the sea floor, a quadratic stress law, based on the local bottom velocity, is used to represent frictional dissipation and a friction coefficient parameterizes the loss rate.

The numerical solution methodology follows that of Davies (1977) and Owen (1980). The vertical variations in horizontal velocity are described by an expansion of Legendre polynomials. The resulting equations are then solved by a Galerkin-weighted residual method in the vertical and by an explicit finite difference algorithm in the horizontal. A space staggered grid scheme in the horizontal plane is used to define the study area. Sea surface elevation and vertical velocity are specified in the center of each cell, while the horizontal velocities are given on the cell face. To increase computational efficiency, a "split-mode" or "two mode" formulation is used (Owen, 1980; Gordon, 1982). In the split-mode, the free-surface elevation is treated separately from the internal, three-dimensional flow variables. The free-surface elevation and vertically integrated equations of motion (external mode), for which the Courant-Friedrichs-Lewis ("CFL") limit must be met, is solved first. The vertical structure of the horizontal components of the current then may be calculated such that the effects of surface gravity waves are separated from the three-dimensional equations of motion (internal mode). Therefore, surface gravity waves no longer limit the internal mode calculations and much longer time steps are possible. Isaji et al. (2001), and Isaji and Spaulding (1984) provide a detailed description of the model physics and numerical implementation.

HYDROMAP output includes spatially- and temporally-varying fields of current speed and direction. This output is seamlessly integrated as input in RPS' transport models, including SSFATE (sediment transport and fates model).

2.2 Sediment Transport Modeling Approach

Sediment transport associated with the cable burial activities was simulated using RPS's Suspended Sediment FATE (SSFATE) model. The model requires inputs defining the environment (e.g., water depths, currents) and the construction activity loading (e.g., sediment grain size, resuspended volume) to predict the associated sediment plume and seabed deposition. Details of the model and theory are provided in the following sections.

2.2.1 SSFATE Model Description

The Suspended Sediment FATE model (SSFATE) is a three-dimensional Lagrangian (particle) model developed jointly by the U.S. Army Corps of Engineers (USACE) Environmental Research and Development Center (ERDC) and Applied Science Associates (now part of the RPS Group) to simulate sediment resuspension and deposition from marine dredging operations. Model development was documented in a series of USACE Dredging Operations and Environmental Research (DOER) Program technical notes (Johnson et al., 2000; Swanson et al., 2000); at previous World Dredging Conferences (Anderson et al., 2001) and a series of Western Dredging Association Conferences (Swanson and Isaji, 2004). Following dozens of technical studies which demonstrated successful application to dredging, SSFATE was further developed to include the simulation of cable and pipeline burial operations using water jet trenchers (Swanson et al., 2007), and mechanical plows, as well as sediment dumping and dewatering operations. The current modeling system includes a GIS-based interface for visualization and analysis of model output.

SSFATE computes TSS concentrations and sedimentation patterns resulting from sediment disturbing activities. The model requires a spatial- and time-varying circulation field (typically from hydrodynamic model output), definition of the water column bathymetry, and parameterization of the sediment disturbance (source), and predicts the transport, dispersion, and settling of suspended sediment released to the water column. The focus of the model is on the far-field (i.e., beyond the initial disturbance) processes affecting the fate of suspended sediment. The model uses specifications for the suspended sediment source strengths (i.e., mass flux), vertical distributions of

sediments and sediment grain-size distributions to represent losses (loads) to the water column from different types of mechanical or hydraulic dredges, sediment dumping practices, or other sediment disturbing activities such as jetting or mechanical plowing for cable or pipeline burial. Multiple sediment types or fractions can be simulated simultaneously; as can discharges from moving sources.

2.2.2 SSFATE Model Theory

SSFATE addresses the short-term movement of sediments that are disturbed during processes (e.g., mechanical plowing, hydraulic jetting, dredging) where sediment is resuspended into the water column. The model predicts the path and fate of the sediment particles based on sediment properties, sediment loading characteristics and environmental conditions (bathymetry and currents). The computational model utilizes a Lagrangian (or particle-based) scheme to represent the total mass of sediments suspended over time. The particle-based approach provides a method to track suspended sediment without any loss of mass as compared to Eulerian (continuous) models due to the nature of the numerical approximation used for the conservation equations. Thus, the method is not subject to artificial diffusion near sharp concentration gradients and can easily simulate all types of sediment sources.

The model uses Lagrangian particles to represent the resuspended sediments. Sediment particles in SSFATE are divided into five size classes (Table 2.2-1) based on grain size, each having unique behaviors for transport, dispersion, and settling. The model releases a minimum of one particle per time step per sediment class, though a particle multiplier can be used to release multiple particles per sediment class per time step. The total mass of sediment in each particle reflects the operations and sediment grain size distribution. The mass reflects the amount of sediment that is expected to be resuspended for a given time interval based on sediment production rate and resuspension rate of the equipment, and this mass is further proportioned within each sediment size class based on the characterization of the sediment data at a given location.

Table 2.2-1. Sediment Size Classes used in SSFATE.

Sediment Size Classes in SSFATE			
Class	Type	Size Range Imperial Units (thou)	Size Range Metric Units (microns)
1	Clay	0 – 0.3	0-7
2	Fine silt	0.3 – 1.4	7-35
3	Coarse silt	1.4 – 2.9	35-74
4	Fine sand	2.9 – 5.1	74-130
5	Coarse sand	> 5.1	>130

Horizontal transport, settling, and turbulence-induced suspension of each particle is computed independently by the model for each time step. Particle advection is based on the relationship that a particle moves linearly (in three-dimensions) with a local velocity obtained from the hydrodynamic field for a specified model time step. Diffusion is assumed to follow a simple random walk process. The diffusion distance is defined as the square root of the product of an input diffusion coefficient and the time step is decomposed into X and Y displacements via a random direction function. The vertical Z diffusion distance is scaled by a random positive or negative direction.

Particle settling rates are calculated using Stokes equations based on the size and density of each particle class. Settling of particles mixtures is a complex process due to interaction of the different size classes, some of which tend to be cohesive and thus clump together to form larger particles that have different settling rates than would be expected from their individual sizes. Enhanced settlement rates due to flocculation and scavenging are particularly important for clay and fine-silt sized particles (Swanson et al., 2007; Teeter, 2000) and these processes have been implemented in SSFATE. These processes are bound by upper and lower concentrations limits, defined through empirical studies, which contribute to flocculation for each size class of particles. Outside these limits, particle collisions are either too infrequent to promote aggregation, or so numerous that the interactions hinder settling.

Deposition is calculated as a probability function of the prevailing bottom stress and local sediment concentration and size class. The bottom shear stress is based on the combined velocity due to waves (if used) and currents using the parametric approximation (Soulsby,1998). Matter that is deposited may be subsequently resuspended into the lower water column if critical levels of bottom stress are exceeded, and the model employs two different resuspension algorithms. The first applies to material deposited in the last tidal cycle (Lin et al., 2003). This accounts for the fact that newly deposited material will not have had time to consolidate and will be resuspended with less effort (lower shear force) than consolidated bottom material. The second algorithm is the established Van Rijn method (Van Rijn, 1989) and applies to all other material that has been deposited prior to the start of the last tidal cycle. Swanson et al. (2007) summarizes the justifications and tests for each of these resuspension schemes. Particles initially released by operations are continuously tracked for the length of the simulation, whether suspended or deposited.

For each model time step the suspended concentration of each sediment class as well as the total concentration is computed on a concentration grid. The concentration grid is a uniform rectangular grid with user-specified cell size that is independent of the resolution of the hydrodynamic data used to calculate transport, thus supporting finer spatial differentiation of plume concentrations and avoiding underestimation of concentrations caused by spatial averaging over larger volumes/areas. Model outputs include water-column concentrations in both horizontal and vertical planes, time-series plots of suspended sediment concentrations at points of interest, and thickness contours of sediment deposited on the sea floor. Deposition is calculated as the mass of sediment particles that accumulate over a unit area. Because the amount of water in the sediment deposited is not known, SSFATE by default converts deposition mass to thickness by assuming no water content.

For detailed description of the SSFATE model equations governing sediment transport, settling, deposition, and resuspension, the reader is directed to Swanson et al. (2007).

3.0 HYDRODYNAMIC MODELING

This section describes the environmental data used to develop the hydrodynamic model application and details of the hydrodynamic model application including model setup, the validation of the hydrodynamic model performance, and the use of the hydrodynamic model application to generate current fields for use in the sediment dispersion modeling.

3.1 Environmental Data

Environmental data including shoreline, bathymetry, winds, tidal elevations, and currents were acquired in order to understand and characterize the circulation local to the Project components in marine waters. The data were used both in developing model forcing as well as for validating the model predictions. The locations of various data sources in relation to the Project components are shown in Figure 3.1-1. Further details on the data sources are provided below. Analysis and presentation of the data used for the study are presented in subsequent sections as appropriate.

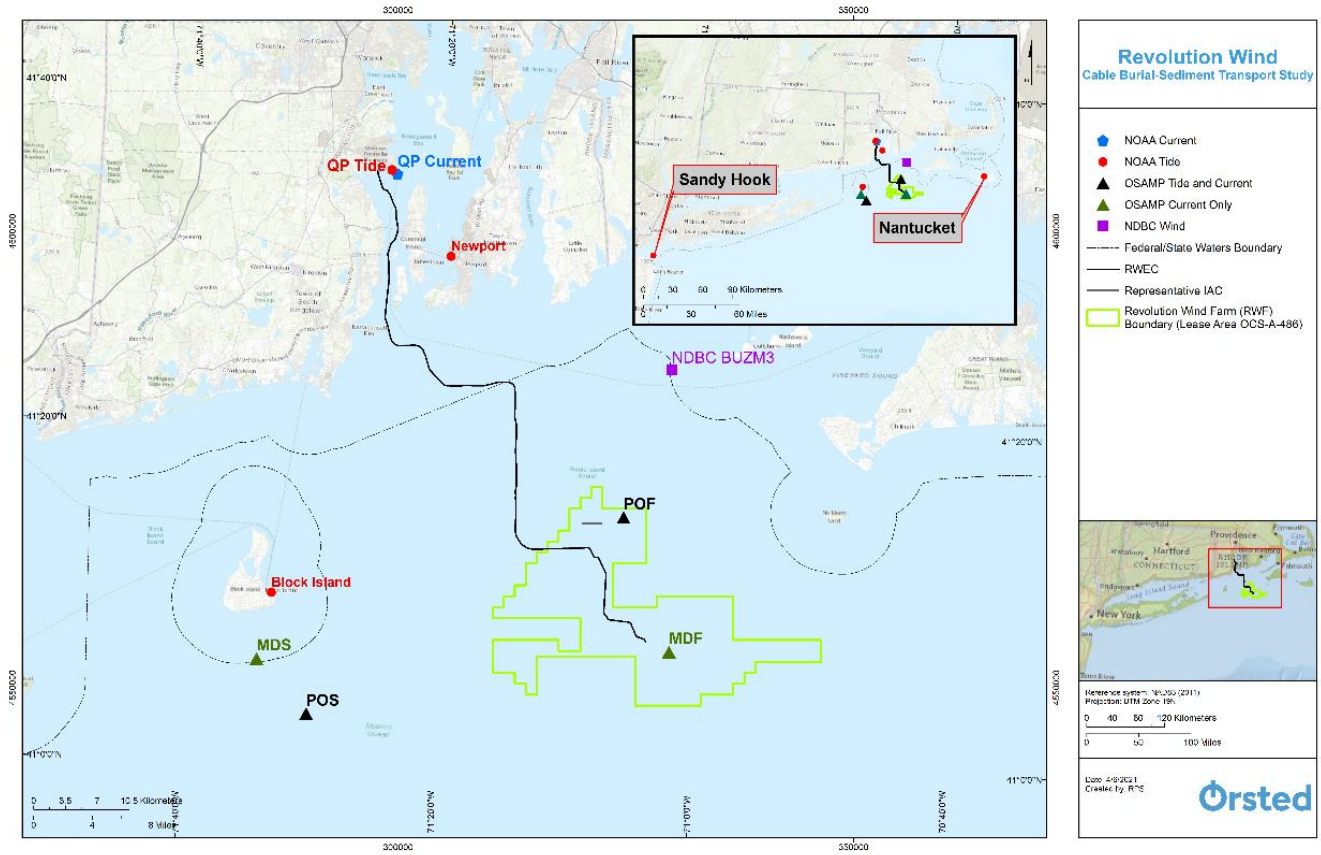

Figure 3.1-1. Location of Environmental Data Observations and Project Components.

3.1.1 Shoreline and Bathymetry

The hydrodynamic model domain extends from New York Harbor to Cape Cod and is significantly larger than the Project footprint. This extent was necessary to accurately locate and define open boundary conditions. The shoreline for the domain was developed based on merging shoreline data from each of the relevant states (Massachusetts [MA; MassGIS, 2017], RI [RIGIS, 2010], Connecticut [CT; CT DEEP, 2017], and New York [NY; NY GIS, 2017]). Bathymetry data was gathered from publicly available data provided by the National Oceanic and Atmospheric Administration (NOAA) for coastal and offshore waters of MA, CT, RI, and NY. NOAA soundings (water depth measurements) were downloaded from the NOAA's Electronic Navigational Chart (ENC) Direct to GIS portal (NOAA, 2019a) and were obtained for the harbor, coastal, and approach ENC band levels. Soundings are available from their native positioning, which is irregular in spacing. The irregular spaced soundings were interpolated to the hydrodynamic grid to provide a complete coverage of water depths within the study area.

3.1.2 Sea Surface Height (Tide) and Current Data

Sea surface height (SSH) and current data were gathered and analyzed for this study. SSH data was used for both developing model forcing and for verification of the hydrodynamic model predictions. Current data was used solely to validate the model predictions.

Sea Surface Height

Multiple sources of SSH data were used in this study. The data were available either as time histories of observations of water surface elevation or in the form of harmonic constituents from either a global model or analysis of observational data. Harmonic constituents represent the amplitude and phase of defined periodic constituents of the tidal signal (sine waves with different wave lengths), where the tidal signal is the sum of all constituents added together by superposition. The amplitude describes the difference between a mean sea level datum and the peak water level for a constituent, and the phase describes the timing of the signal relative to a time datum. The constituent period determines the time for one full oscillation of the signal. Tidal harmonic constituents' names indicate the approximate period (e.g., M2 is approximately twice daily and O1 is approximately once daily).

Output from the TPXO7 global tidal model developed by Oregon State University (OSU) was used to characterize the tides at the hydrodynamic model open boundaries. The TPX07 model output contains tidal harmonic constituent data on a ¼ degree resolution across the globe. The model is based on data from the TOPEX/Poseidon and Jason satellites, and the model methodology is documented in Egbert et al. (1994) and Egbert and Erofeeva (2002). A summary of the constituents obtained, and their specific periods, is provided in Table 3.1-1. Details on the spatially-varying amplitude and phase used as boundary forcing are provided in Section 3.2.2.

Table 3.1-1. Tidal Constituents Used at Hydrodynamic Model Boundaries.

Tidal Boundary Characteristics			
Name	Constituent	Speed (Degrees/Hour)	Period (Hours)
M2	Principal lunar semidiurnal constituent	28.98	12.42
S2	Principal solar semidiurnal constituent	30.00	12.00
N2	Larger lunar elliptic semidiurnal constituent	28.44	12.66
K1	Lunar diurnal constituent	15.04	23.93
O1	Lunar diurnal constituent	13.94	25.82

Observational based tide data was obtained from NOAA Center for Operational Oceanographic Products and Services (CO-OPS) or from activities associated with the Rhode Island Ocean Special Management Plan (OSAMP). The location of observation stations used in this study are shown in Figure 3.1-1.The NOAA CO-OPS program provides historical observations of water level, along with published harmonic constituents of the tides based on their analysis of the observations. The OSAMP included a temporary field program during which four buoys (POF, POS, MDS, MDF) were deployed to collect metocean observation data. Two of those buoys (POF and POS) included observations of pressure which was converted to water depth; the oscillating water depth was used to determine the tidal characteristics at these locations. The harmonic constituents of these stations were published in Grilli et al. (2010). The time history of observations from the OSAMP stations had also been previously provided to RPS through the researches working on the OSAMP. The observations of water levels were used to evaluate the model predictions (Section 3.2.3.1).

Current Data

Observations of currents were obtained from four OSAMP stations (MDF, MDS, POF, POS) and from one NOAA CO-OPS station (NOAA station nb0301 located offshore Quonset Point [QP]). The location of these stations are shown in Figure 3.1-1. The OSAMP buoys included observations at multiple depths throughout the water column processed to provide a value in discrete bins. The NOAA CO-OPS station has only one point of measurement in the upper water column (12 ft [3.6 m] below the surface). A summary of metrics for each station is provided in Table

3.1-2. Further details and discussions on the OSAMP oceanographic instrumentation and observations can be found in Codiga and Ullman (2010). The current observations were used for verification of model predictions. These are presented in Section 3.2.3.1.

Table 3.1-2. Current Observations.

Current Observation Data				
Source	Location	Point or Profile	Bin Resolution, Feet (ft) (Meters [m])	Time Step (Hours)
NOAA	Quonset Point, RI	Point – Upper Water Column	NA	0.10
OSAMP	POS	Profile	2.46 (0.75)	2.00
OSAMP	POF	Profile	2.46 (0.75)	2.00
OSAMP	MDF	Profile	3.28 (1.00)	1.00
OSAMP	MDS	Profile	3.28 (1.00)	1.00

Wind Data

The hydrodynamic model forcing also includes surface winds, and thus a record describing the wind speed and direction during the simulation period was needed. Additionally, wind data was used to select representative timeframes with typical wind characteristics for running the model to develop currents for use in the sediment transport modeling. Winds observed at the National Data Buoy Center (NDBC) Buzzards Bay station BUZM3 were obtained and used in this study. This data was available at an hourly time step and the most recent ten years of data (2009 – 2018) was obtained for analysis (NDBC, 2019).

3.2 HYDROMAP Hydrodynamic Model Application

A model application of the study area was developed using the HYDROMAP hydrodynamic model system. This included development of a model grid and grid bathymetry, development of boundary forcing (tides and wind), and selection of numerical parameters. The model set-up allows for three-dimensional simulations, which were utilized for this study. The vertical structure is represented by Legendre polynomials; in this instance four polynomials were used to represent the vertical variability in the currents from tidal and wind forcing. The model application was first verified against observations for a period of November 25 – December 25, 2009 and then subsequently run for a period of time identified as having typical winds that was sufficient for model simulations of cable installation (April 1 – May 15, 2016).

3.2.1 Model Grid

The complete model domain extends from New York Harbor at the westernmost extent, to Cape Cod at the eastern extent. Although this domain is significantly larger than the study area, the extent was chosen to best locate and define open boundary conditions. The computational grid for the entire domain, consisting of 24,506 active water cells, is shown in Figure 3.2-1. The hydrodynamic model grid was mapped to the shoreline with grid cell resolution ranging from approximately 3,281 – 820 ft. (1.0 km – 250 m); the resolution is coarse further from the shore and becomes finer in the areas closest to the shore to capture the physical characteristics of the shoreline/bathymetry. The model grid bathymetry was assigned by interpolating a set of individual data points onto the model grid. For grid cells that contain multiple soundings, the values are averaged; grid cells without soundings are interpolated based on the closest soundings. The final gridded bathymetry is shown in Figure 3.2-2 and a zoomed-in view of the grid is presented in Figure 3.2-3.

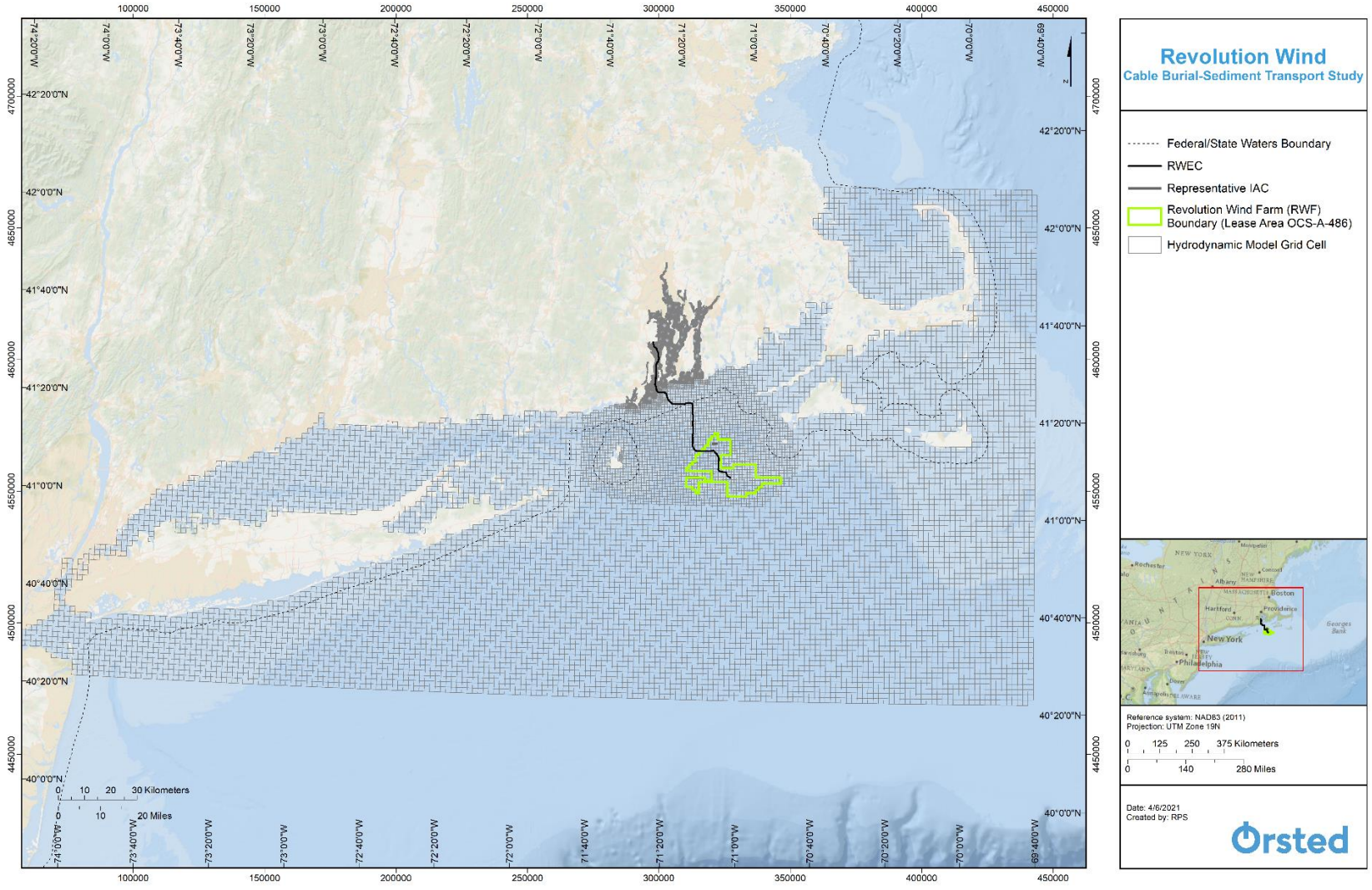

Figure 3.2-1. Hydrodynamic Model Grid.

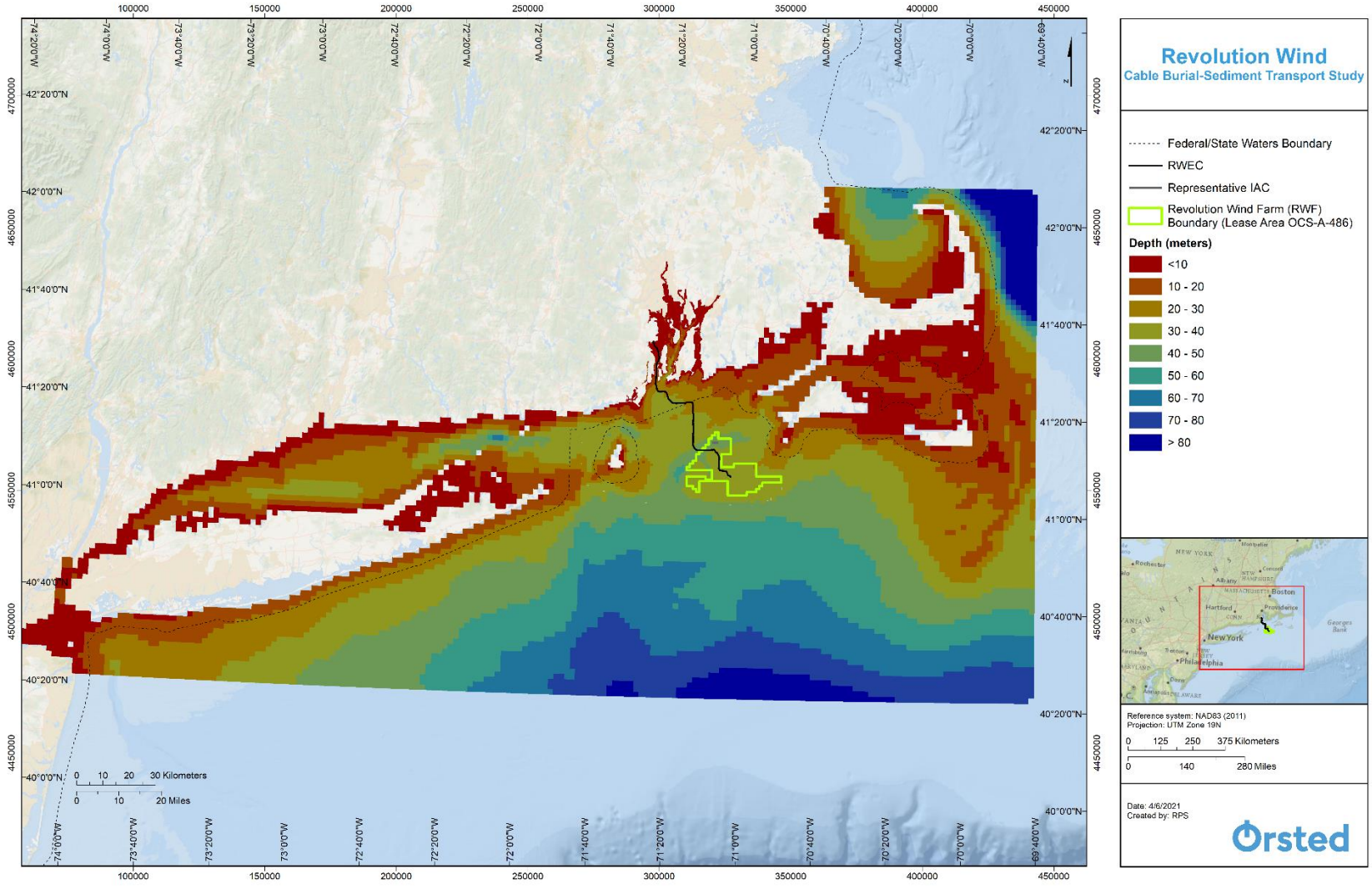

Figure 3.2-2. Hydrodynamic Model Grid Bathymetry.

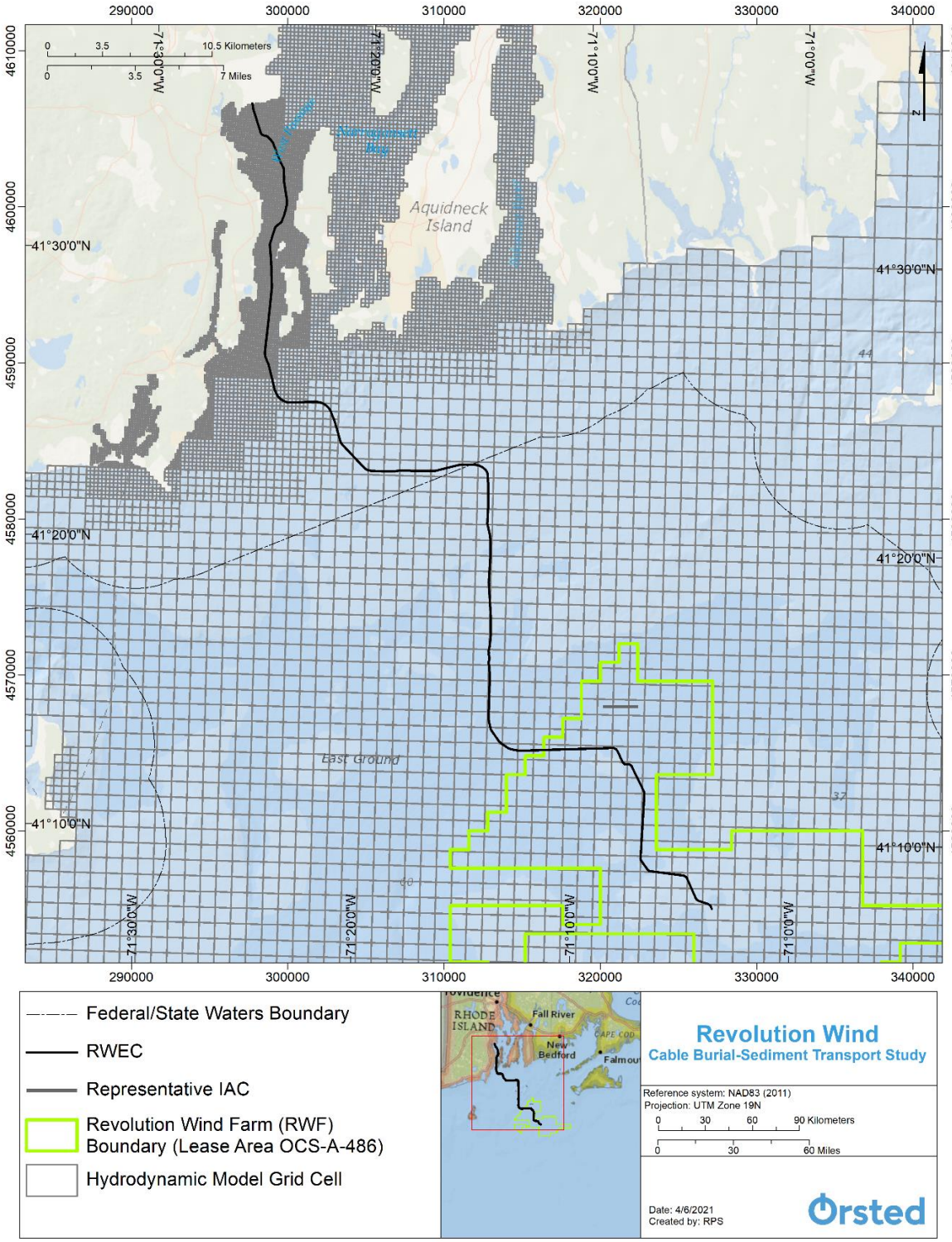

Figure 3.2-3. Zoomed-in View of Hydrodynamic Model Grid Focused on Project Components.

3.2.2 Model Boundary Conditions

Model boundary conditions for this application included specification of tidal characteristics at open boundary water cells at the edge of the domain and surface winds applied to all cell surfaces.

Tidal Boundary Conditions

The circulation in the study area is tidally dominated, and therefore an important feature of the model application is the characterization of tidal boundary conditions. Harmonic constituent data extracted from the TPXO global tidal model was used at the model open boundaries. Each boundary cell was assigned a unique set of the harmonic constituent amplitudes and phases, interpolated from the TOPEX model predictions. In total, the open boundary was specified for the five predominant tidal constituents in the area: three semi-diurnals (M2, N2, and S2) and two diurnals (K1 and O1). The dominant tidal constituent in this region is the M2-principal lunar semi-diurnal (twice daily) constituent. Illustrations of amplitude and phase of the M2 constituent along the model grid open boundaries are shown in Figure 3.2-4 and Figure 3.2-5, respectively. Figure 3.2-4 illustrates that the M2 amplitude is greater than 1.31 ft (0.4 m) in most places, with the exception of the southeast region of the domain. Figure 3.2-5 illustrates how the M2 phase is generally similar parallel to Long Island and Narragansett Bay.

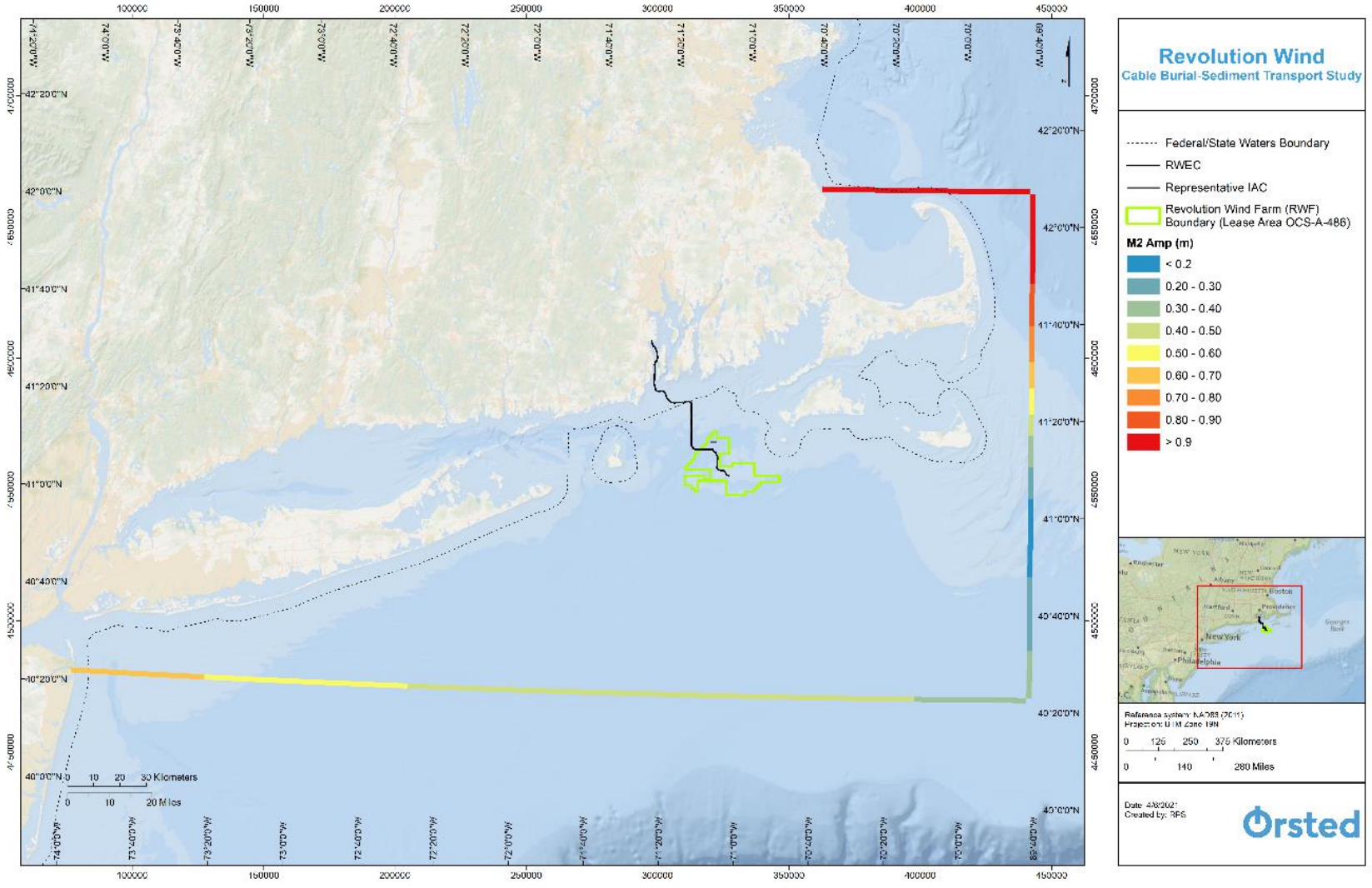

Figure 3.2-4. Tidal Boundary Forcing: M2 Amplitude.

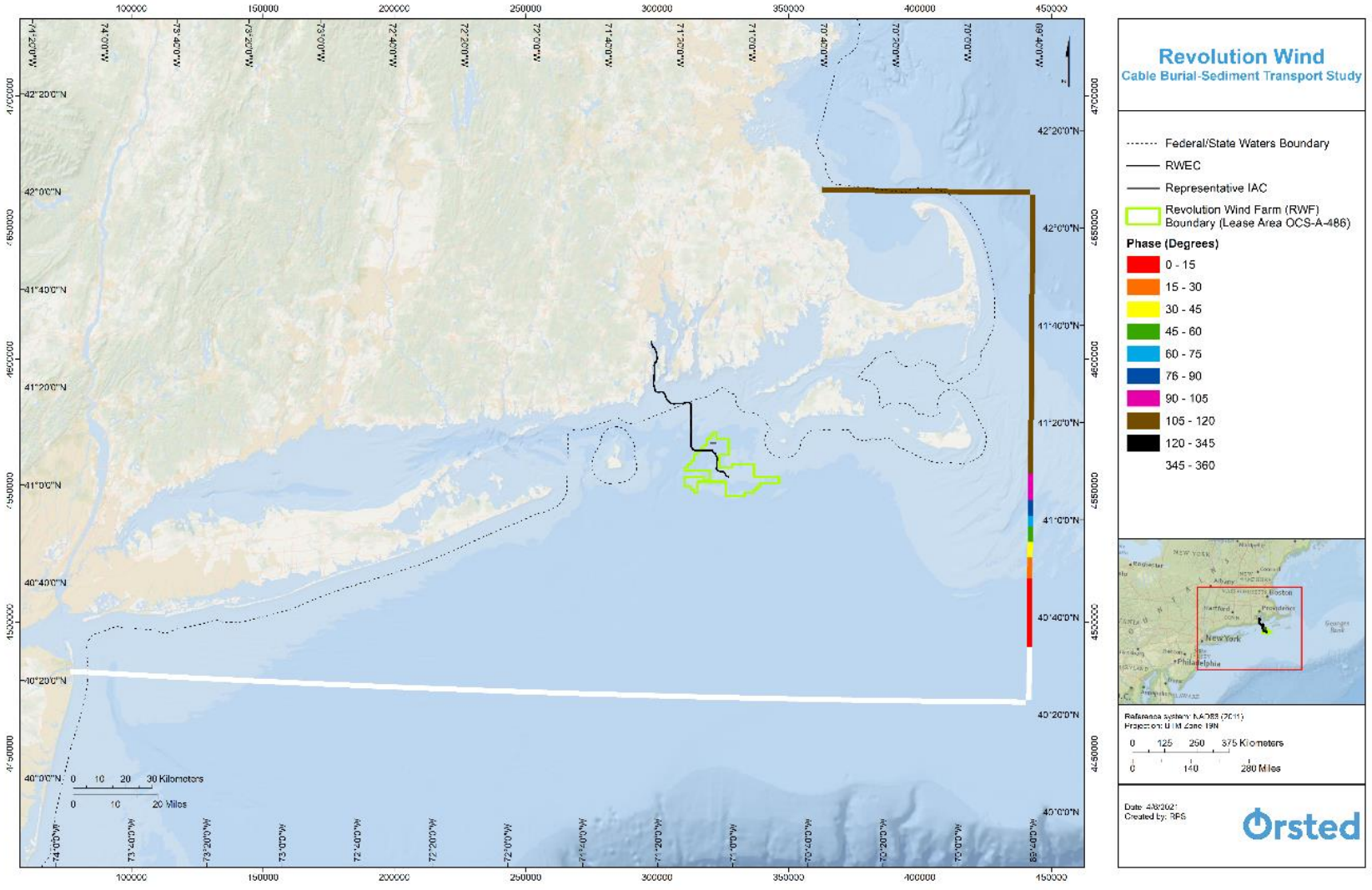

Figure 3.2-5. Tidal Boundary Forcing: M2 Phase.

Meteorological Boundary Conditions

The water surface boundary covers the entire gridded area and is influenced by wind speed and direction. Meteorological data was obtained from the NDBC Buzzards Bay Station (NDBC, 2019) and was applied to the entire grid surface. The wind rose from the validation period is shown in Figure 3.2-6. The wind rose generated from the record of winds within the most recent ten (2009-2018) is presented in Figure 3.2-7. The wind rose represents speed with colors and direction by the size of the rose 'petals', with each petal representing a directional field (e.g., Northeast) and located within the compass rose in accordance with the direction from which the wind is coming. The winds at this location come predominantly from the southwest. Details of the winds used for the different modeling periods are presented in Section 3.2.1.4.2.

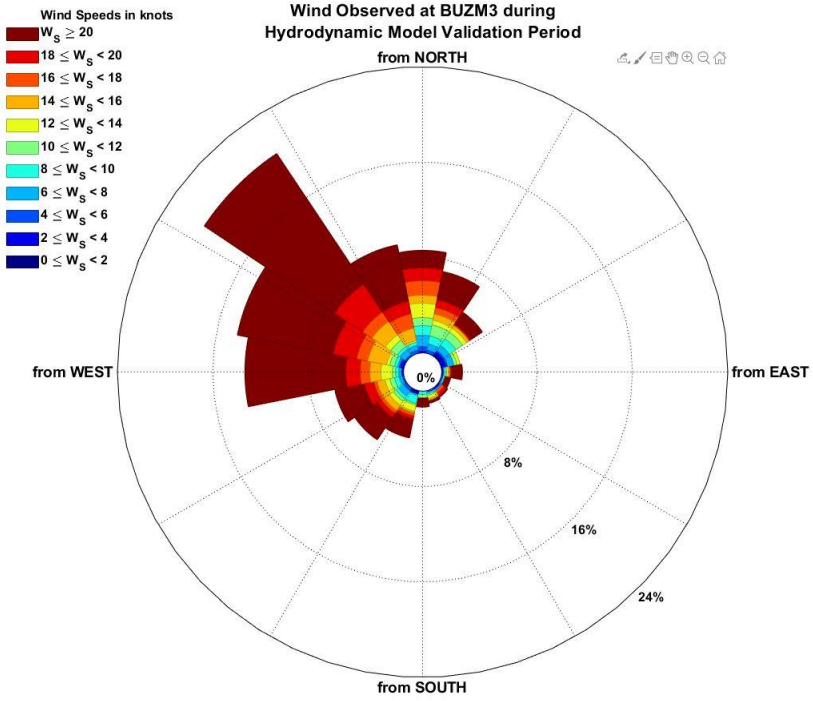

Figure 3.2-6. Wind Rose from Observed NDBC Station BUZM3 from the Hydrodynamic Model Validation Period of November 25, 2009 – December 25, 2009.

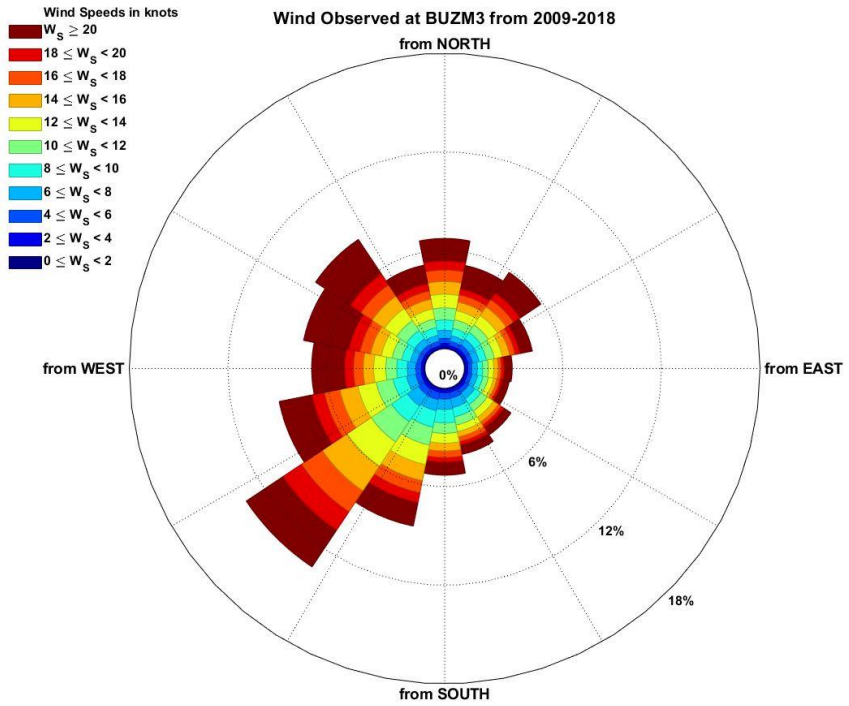

Figure 3.2-7. Wind Rose from Observed NDBC Station BUZM3 from 2009-2018.

Selection of Representative Periods for Sediment Transport Modeling Based on Wind

The exact timing of the Project cable burying activities is not known at this time. The approach for the cable burial modeling is to use currents that reflect a typical timeframe. Currents local to the planned cable burial activities vary primarily due to tides and winds. Since tides do not vary seasonally, an analysis of monthly wind records was conducted to define the scenario timeframes.

The most recent ten-year record of winds at BUZM3 (2009-2018) was analyzed to evaluate the wind characteristics and to select a typical timeframe. Monthly average speeds were calculated for the full record and were assessed quantitatively and qualitatively to determine which year had monthly averages that most closely represented the full record. The monthly average wind speed ranges from 7.45 knots (3.8 m/s) to 20 knots (10.3 m/s) and the annual speed at this location is 14.9 knots (7.6 m/s). The trends of individual years were investigated through analysis of the monthly average wind speeds. A two-plot figure showing (1) the differences in monthly average wind speed from the full 10-year record, and (2) the selected typical year (2016) along with the record average, is presented in Figure 3.2-8.

As shown in Figure 3.2-9, the monthly averages during 2016 remain close to the record averages throughout the year with no extreme outliers. It can also be seen that April 2016 has winds close to the annual average from the 10-year record. Based on this analysis, a scenario simulation period used to develop currents for the sediment transport modeling of April 1, 2016 – May 15, 2016 was established to generate currents for use in the sediment transport modeling. The wind roses for the long term ten-year record and this scenario simulation period are shown in Figure 3.2-9. The long term record shows that winds are predominately from the southwest followed by a relatively high frequency of occurrences from the northwest (though the wind rose indicates that the winds blow from all directions for some portions of the year). The scenario simulation period captures the southwest predominance, though it does have a relatively greater fraction of winds from the northeast.

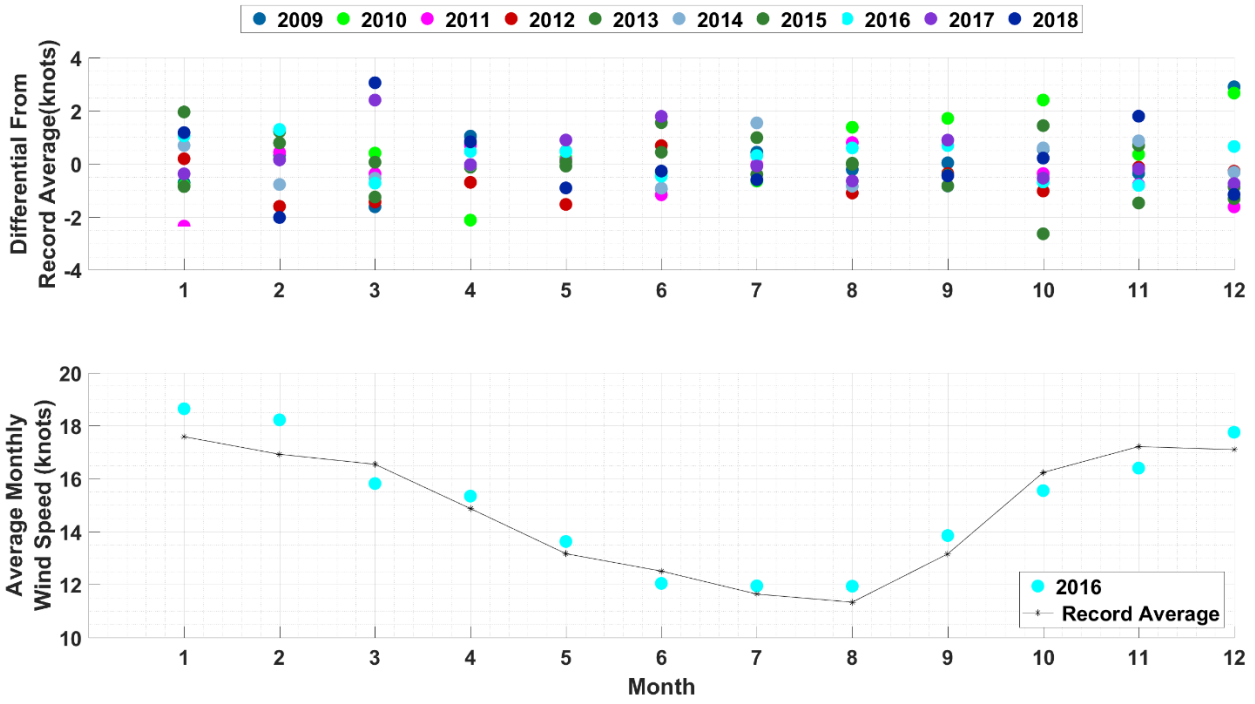

Figure 3.2-8. Monthly Average Wind Speeds. Differential Between Monthly Average Wind Speed for a Given Year and the Record Monthly Average (Top) and Monthly Average Wind Speeds for the Selected Typical Year (2016) as well as the Record Average (Bottom).

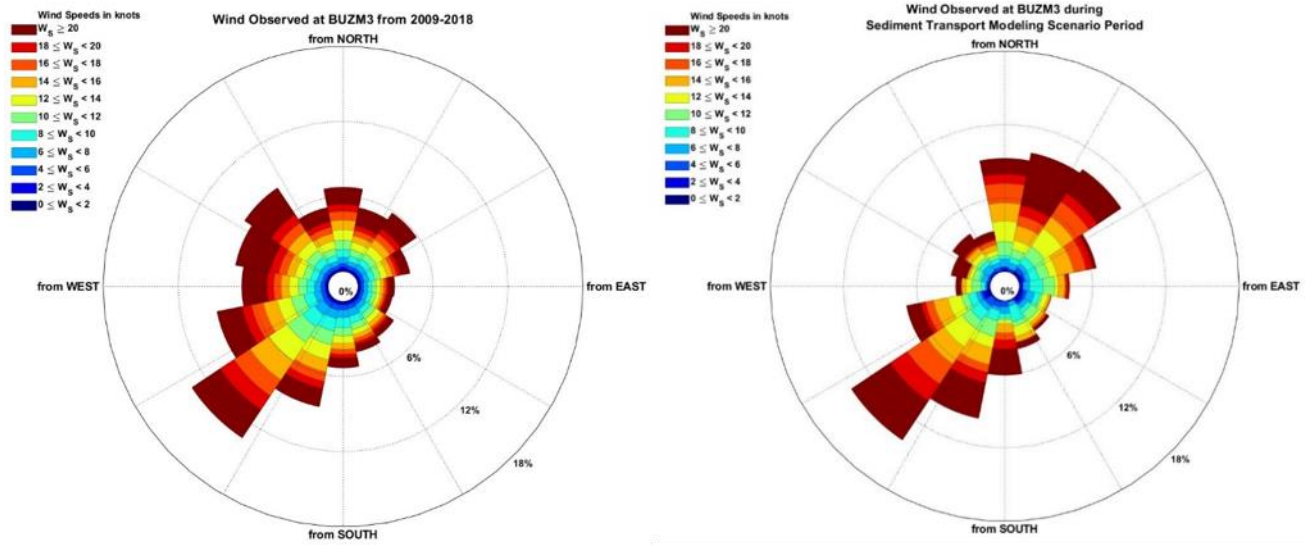

Figure 3.2-9. Wind Rose from Observed NDBC Station BUZM3 from the Most Recent 10 Year Record of 2009-2018 (Left) and the Scenario Period of April 1, 2016 – May 15, 2016 (Right).

3.2.3 HYDROMAP Hydrodynamic Model Results

The hydrodynamic model application was first run to verify model performance and subsequently to generate currents for use in the sediment transport model simulations. The following sections provide the results from both simulations.

3.2.3.1 Model Validation Results

The model was run from November 25, 2009 through December 25, 2009 to verify model performance. This period was chosen because it lies within the time period of available tide and current observations from the OSAMP.

HYDROMAP predictions of water elevation are shown along with observations of water levels in Figure 3.2-10 and Figure 3.2-11. Note that the Block Island station did not have observations available for this time period. However, a record of expected water level was generated based on the harmonic constituents using the publicly available T_Tide Matlab Toolbox and the NOAA published data. Methodologies of the T_Tide toolbox are described in Pawlowicsz et al. (2002). The generated time history was used for comparisons of the model predictions of water level at these locations. Figure 3.2-10 and Figure 3.2-11 show that the model was able to recreate the spatial and temporal variability in the tide across the domain. The model recreated the semidiurnal nature of the tides and further was able to reproduce the spring/neap cycle of changing tidal amplitude. The model response to wind driven setup and surge is less pronounced. However, the daily variations in tidal energy is captured well.

HYDROMAP predictions of currents were compared to observed currents at five locations through comparison of current roses; these are presented in Figure 3.2-12 through Figure 3.2-16. The OSAMP stations had observations throughout the water column and therefore comparisons of surface, mid, and bottom currents were made (Figure 3.2-12 - Figure 3.2-15). The NOAA CO-OPS station measures only upper water column currents near Quonset Point, therefore a comparison of only surface current roses were made (Figure 3.2-16). These figures show that the model was able to recreate general circulation patterns. The order of magnitude of the speeds was recreated, and the spatial variability was captured. For example, both the model and observations showed that current speeds were stronger at the OSAMP MDS and MDF stations compared to the OSAMP POS and POF stations. The model was able to recreate the trend in variability in current direction. For example, with respect to bottom currents, the model recreated the predominate northeast current at OSAMP POS, the predominate southeast current at OSAMP MDF, the less singularly predominate direction of OSAMP MDS, and the predominately eastern current at OSAMP POF. Similarly, at the surface, the Quonset Point station the model was able to recreate the predominately rectilinear nature of the currents that oscillate between northeast and southwest, though the observations showed a southern residual that was not captured in the model. Differences in predicted directions are likely due to influences from larger scale circulation features in the region at large that are not simulated with this model application.

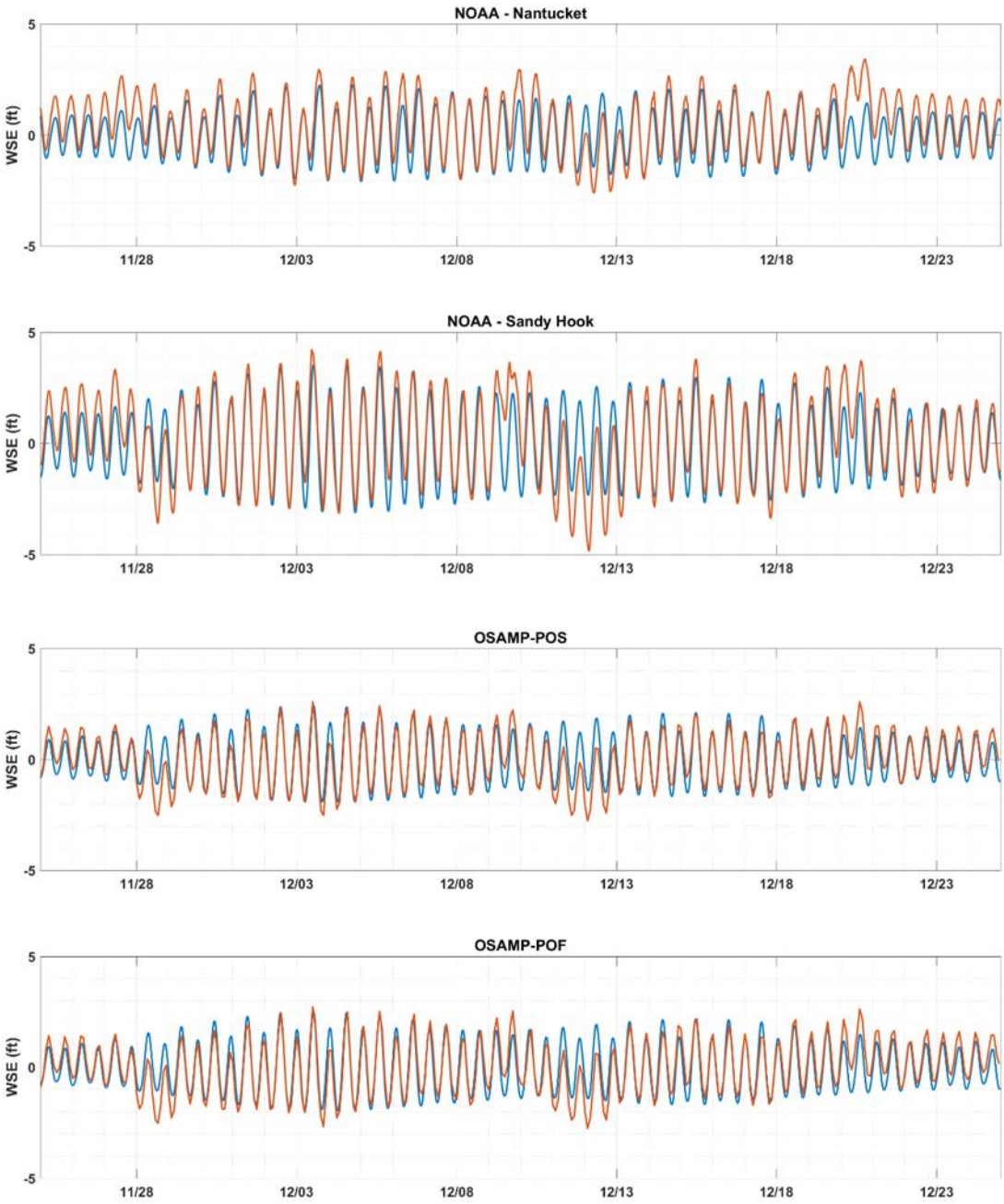

Figure 3.2-10. Model-Predicted (Blue) vs. Observed (Orange) Surface Water Elevations at Locations within the Model Domain (1 of 2).

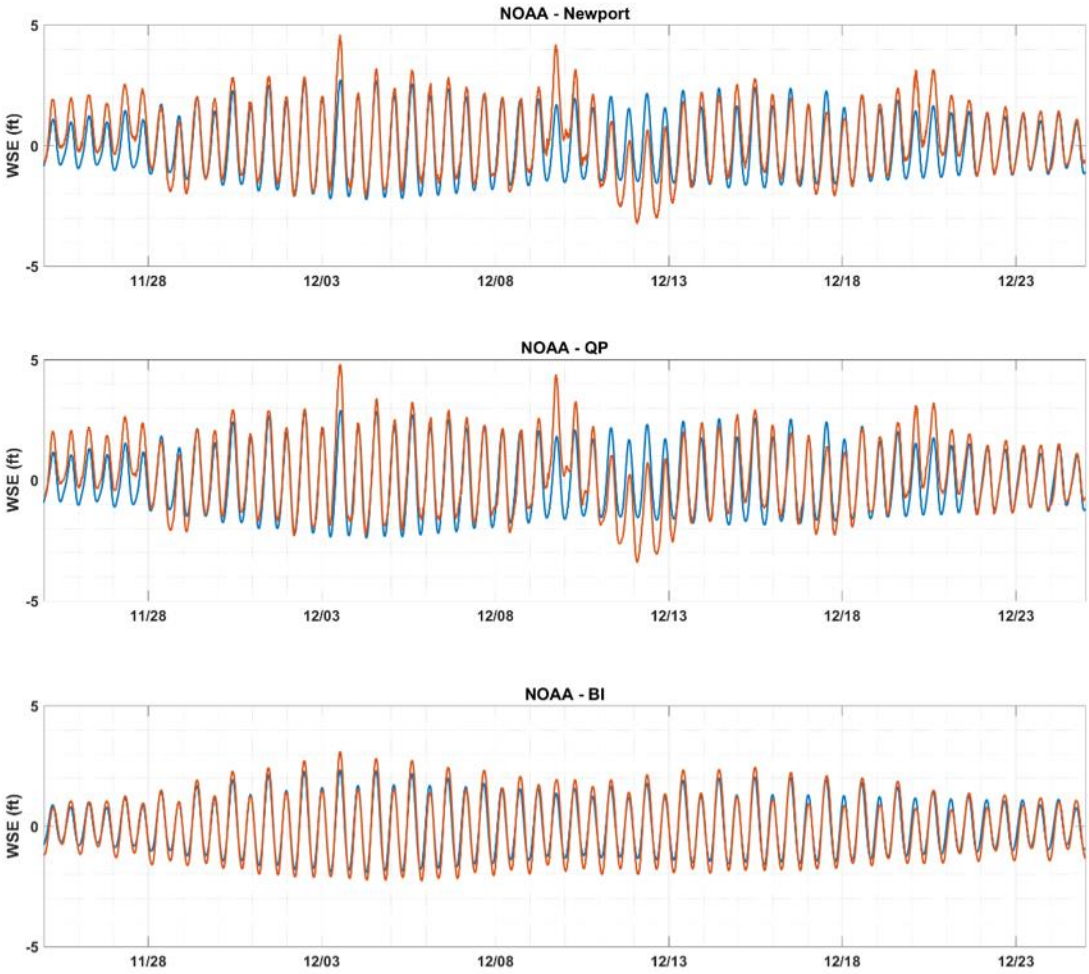

Figure 3.2-11. Model-Predicted (Blue) vs. Observed (Orange) Surface Water Elevations at Locations within the Model Domain (2 of 2).

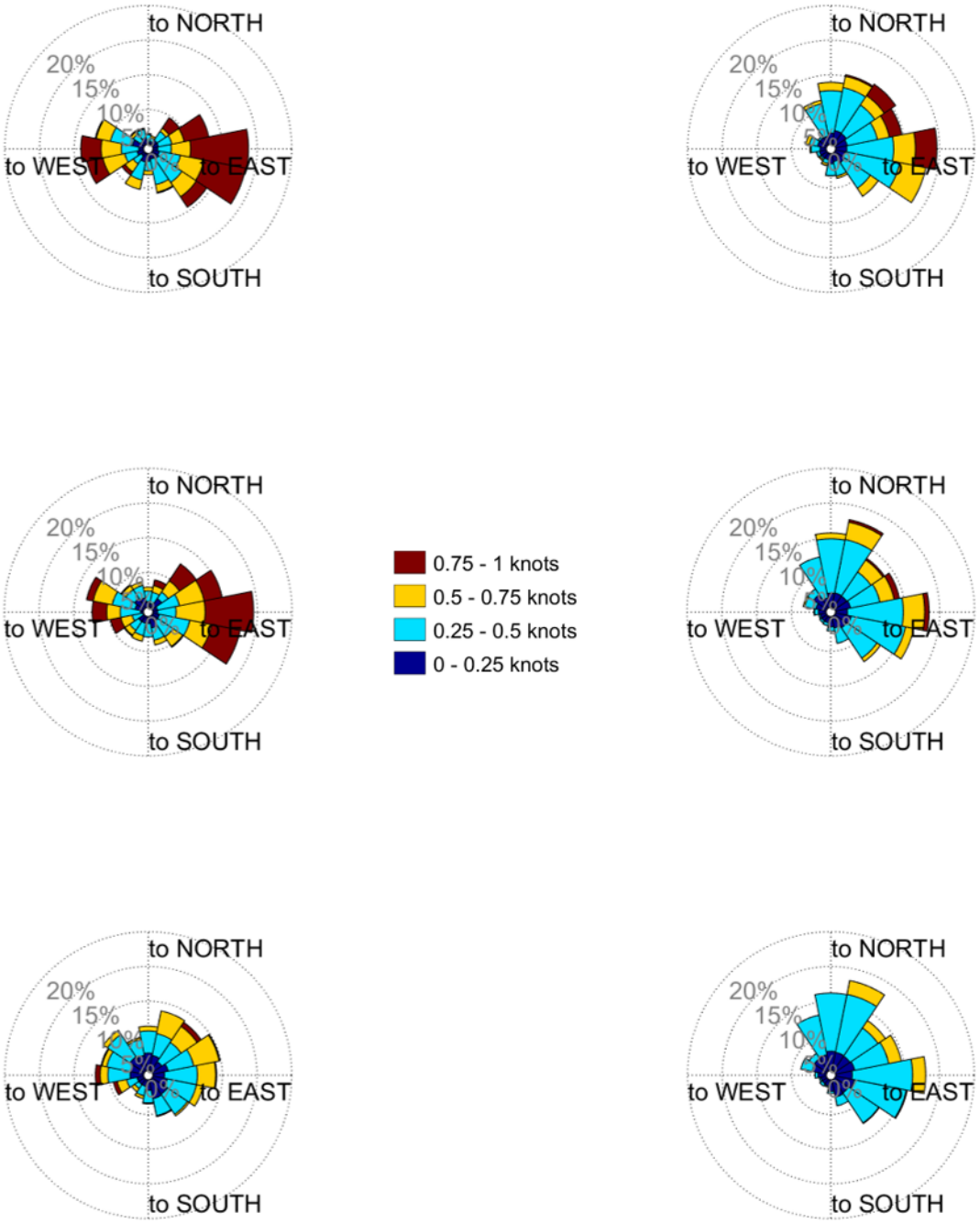

Figure 3.2-12. Model-Predicted (Right) vs Observed Currents (Left) at OSAMP MDS Station Location for Surface (Top), Mid (Middle) and Bottom (Bottom) of the Water Column.

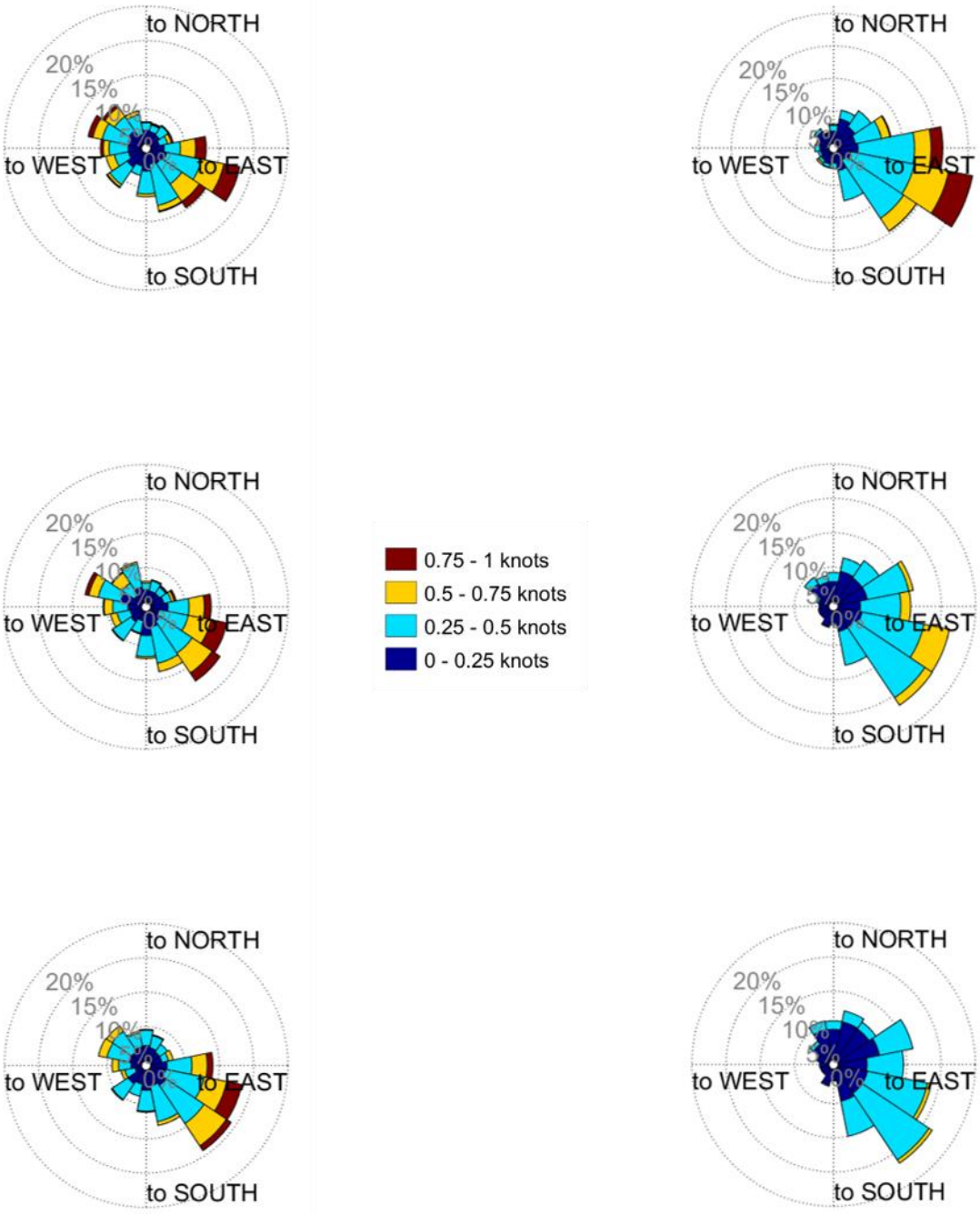

Figure 3.2-13. Model-Predicted (Right) vs. Observed (Left) Currents at OSAMP MDF Station Location for Surface (Top), Mid (Middle) and Bottom (Bottom) of the Water Column.

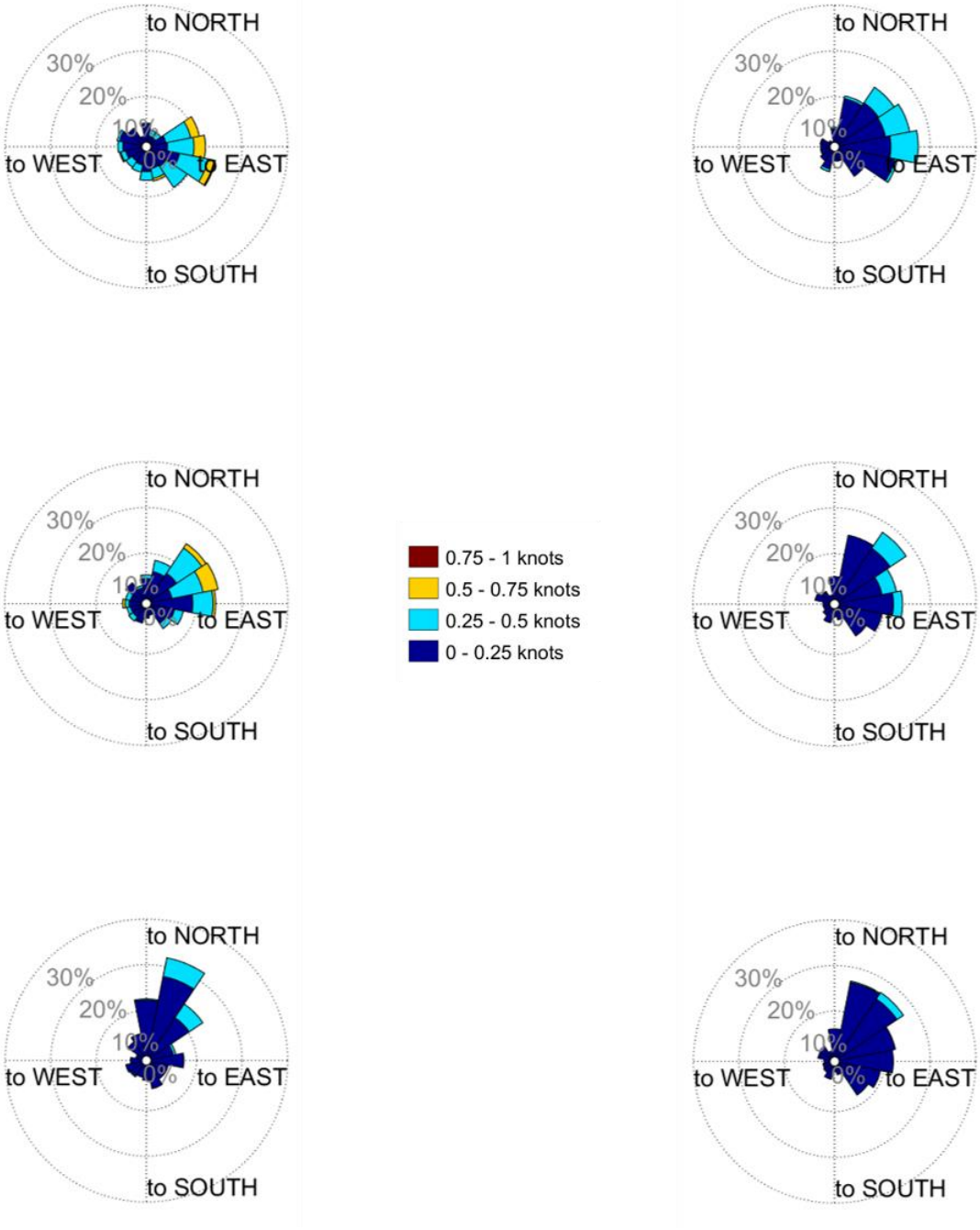

Figure 3.2-14. Model-Predicted (Right) vs. Observed (Left) Currents at OSAMP POS Station Location for Surface (Top), Mid (Middle) and Bottom (Bottom) of the Water Column.

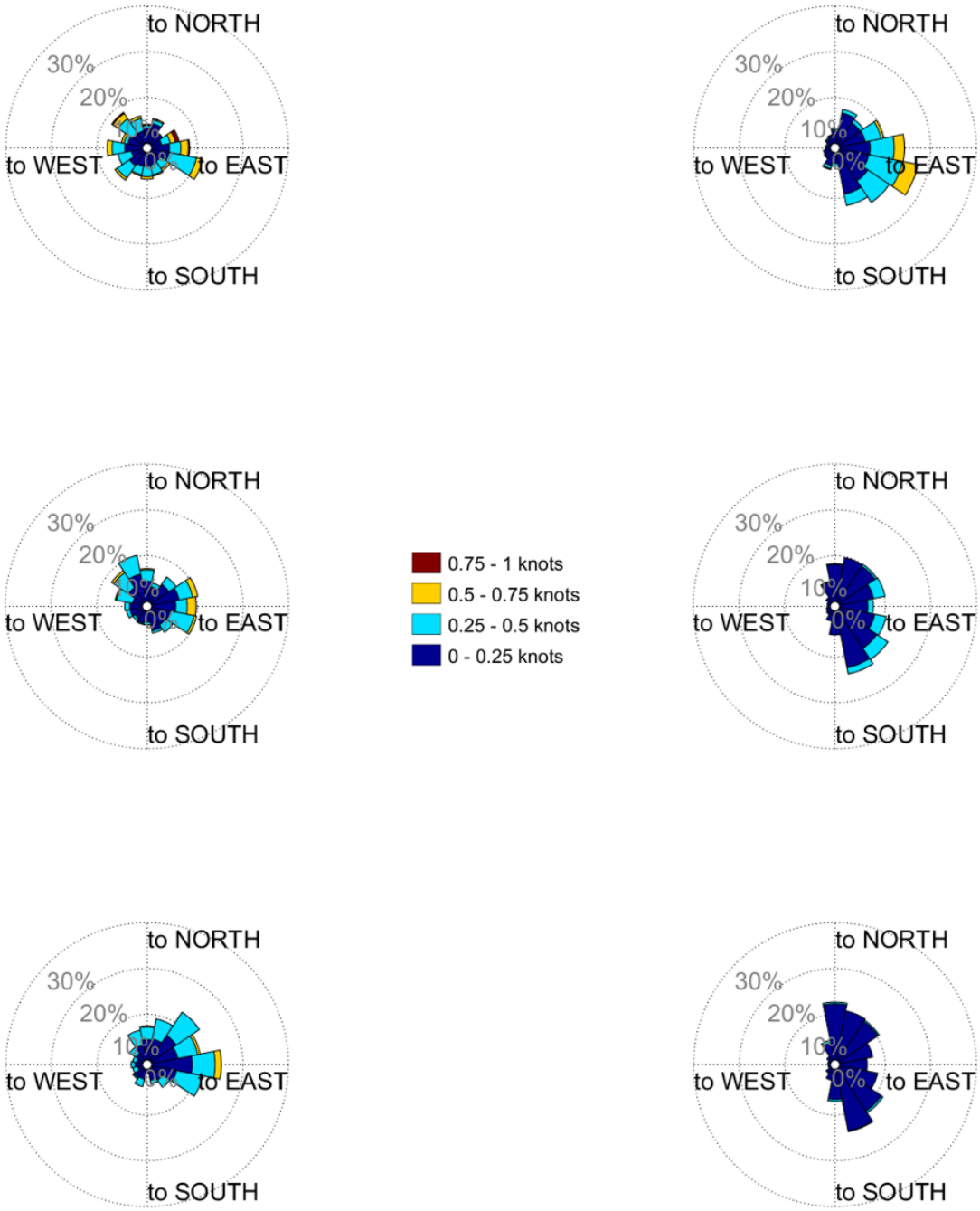

Figure 3.2-15. Model-Predicted (Right) vs Observed (Left) Currents at OSAMP POF Station Location for Surface (Top), Mid (Middle) and Bottom (Bottom) of the Water Column.

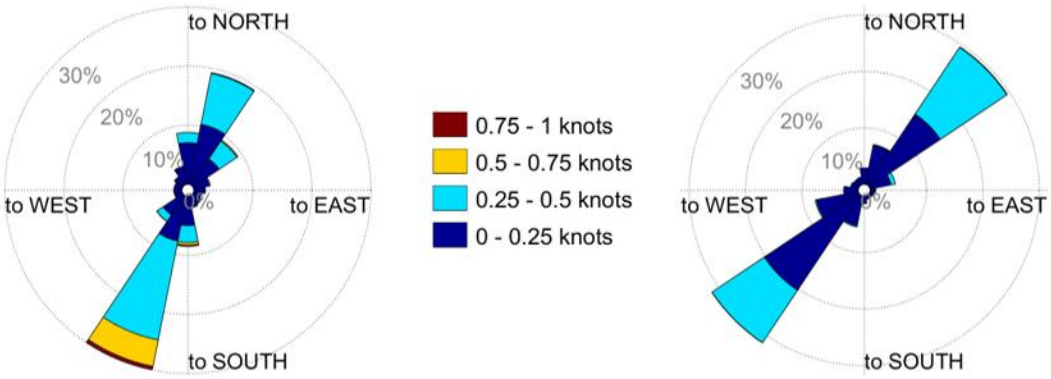

Figure 3.2-16. Model-Predicted (Right) vs Observed (Left) Currents at NOAA nb0301 Station Location for Upper Water Column Currents.

3.2.3.2 Model Results for Use in Sediment Transport Modeling Scenarios

Following model validation, HYDROMAP was used to develop currents for a scenario time period with typical winds established as April 1, 2016 through May 15, 2016. The purpose of this application was to generate a window of time that could be used as forcing for the sediment dispersion modeling. Snapshots of the bottom currents during ebb and flood from this time period are shown in Figure 3.2-17 and Figure 3.2-18, respectively. These figures have color coded arrows where the color represents the speed in knots and the orientation represents the direction the current is moving. These figures are taken at moments of near peak speeds, and do not reflect the speeds at all times. The currents oscillate in and out of the domain, with lower speeds offshore (peaking at approximately 0.4 knots [0.2 m/s] in these snapshots) and along the RWEC until it enters Narragansett Bay where currents increase (approaching approximately 0.8 knots [0.4 m/s] at these snapshots).

Based on the cable installation parameters, the total duration for installation of the cables was known. For the simulation of the RWEC burial, the duration of construction is sufficient to adequately capture variability of the tides and currents in the region since the activities will take place over multiple weeks. Simulations of the representative IAC were notably shorter (< 1 day) than the RWEC and was simulated twice to sample a different tidal regime.

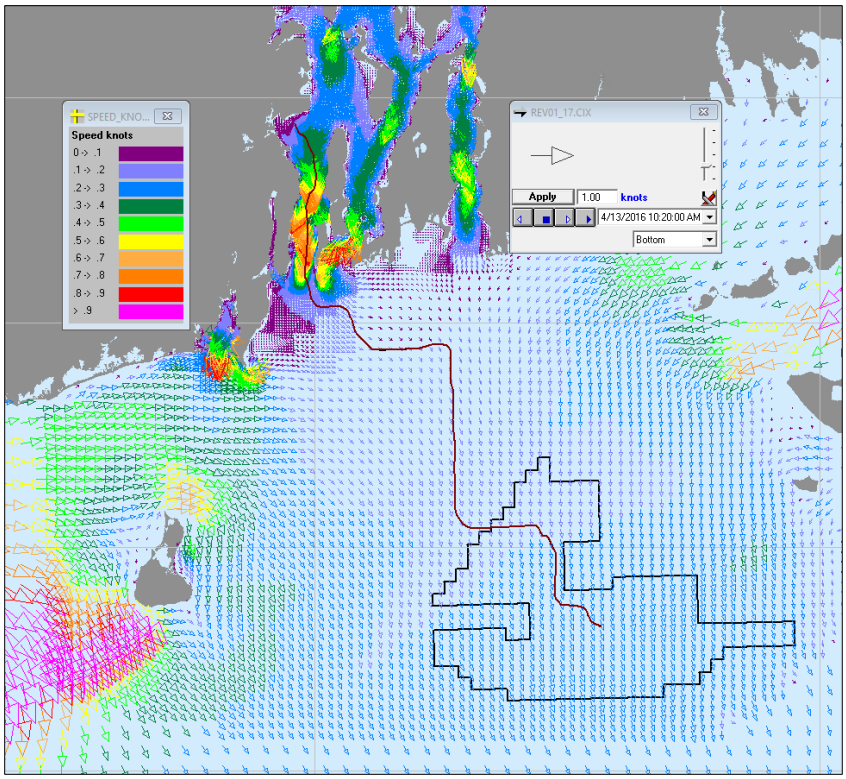

Figure 3.2-17. Example Snapshot of Ebb Bottom Currents Local to Project Boundaries.

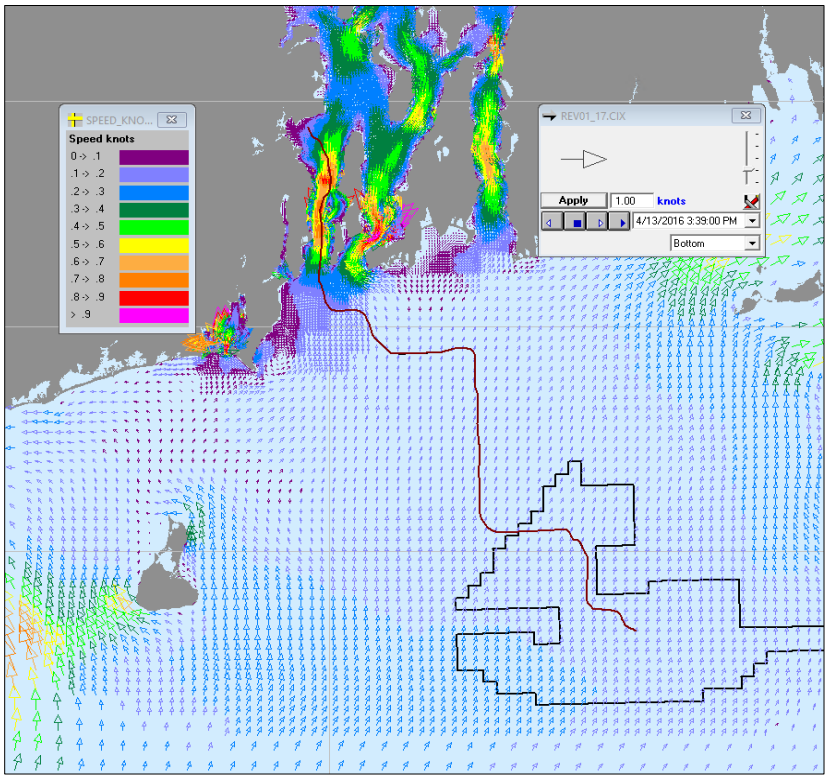

Figure 3.2-18. Example Snapshot of Flood Bottom Currents Local to Project Boundaries.

4.0 SEDIMENT TRANSPORT MODELING

SSFATE was used to perform a series of simulations to assess suspended sediment concentration and seabed deposition resulting from anticipated cable burial activities. This study has four components: (1) seabed preparation alternatives, (2) RWEC Circuit 1, (3) IAC, and (4) landfall. This section includes details of the study components, the model application and the model results.

4.1 SSFATE Model Components and Scenario Descriptions

A set of scenarios was developed to capture the various activities. Figure 4.1-1 depicts the study components associated with each modeling scenario and Table 4.1-1 provides a summary of each modeling scenario and associated methods modeled. The model scenarios along with their key parameters are described below.

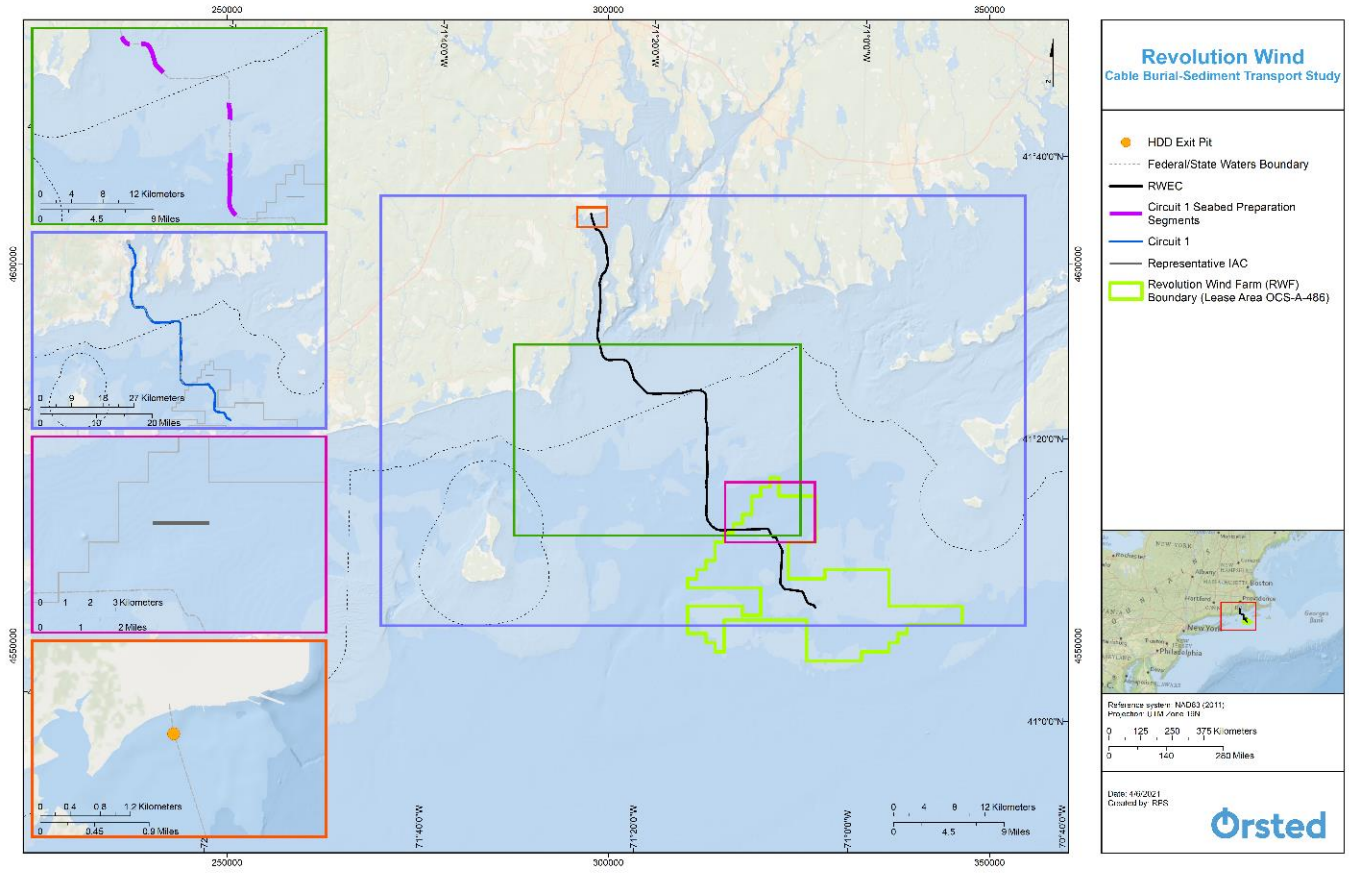

Figure 4.1-1. Study Components.

Table 4.1-1. Description of Activities Being Simulated.

RWEC Modeling Scenarios		
Project Component	Description of Scenario	Methods Modeled
RWEC Seabed Preparation	Circuit 1 – Seabed Preparation Segments	CFE
	Circuit 1 – Seabed Preparation Segments	TSHD – Split Bottom
	Circuit 1 – Seabed Preparation Segments	TSHD – Continuous Overflow
RWEC	Circuit 1	Jet Plow
RWF – IAC	IAC – Current Regime 1	Jet Plow
	IAC – Current Regime 2	Jet Plow
Landfall	HDD Exit Pit	Backhoe Excavator followed by Venturi Eductor Device

4.1.1 Study Component 1: Seabed Preparation Alternatives, Segments of the RWEC Circuit 1

Prior to cable burial, four segments along the RWEC route (approximately 10.5 mi [16.9 km]) may require seabed preparation. Seabed preparation may be necessary in regions where the sediment is deeper to ensure that the sediment clearance is sufficient before commencing the cable burial process. If required, it is assumed that the seabed preparation will occur consecutively and be completed along the segments before cable burial begins. This assessment evaluated three different modeling scenarios which reflect alternative seabed preparation equipment types and parameters: (1) CFE, (2) TSHD using periodic overflow and split bottom barge disposal, and (3) TSHD using continuous overflow. Note that the seabed preparation equipment types were modeled separately to compare the potential impacts from each alternative method, and all methods are not anticipated to be used.

The CFE method mobilizes the cross-sectional area of the trench and introduces sediment along the route centerline near the seabed. Alternatively, the TSHD method removes sediment and introduces it along the route centerline at, and/or near, the water surface. The two TSHD simulations, split bottom and continuous overflow, differed in the way sediment was introduced to the water column. The split bottom method includes periodic overflow and split bottom barge disposal, which would occur as the hopper becomes full. It was assumed that overflow and disposal occurred along the RWEC with overflow composed primarily of fine sediment and split bottom disposal consisting of primarily coarse sediment. This difference in grain size is due to the settlement of coarse sediment within the hopper. Sediment was introduced as overflow at the water surface, and a few meters below the water surface as split bottom disposal. The continuous overflow method conservatively assumed the dredged sediments were immediately introduced to the water column at the surface, bypassing hopper storage. Therefore, the grain size distribution entering the water from the continuous overflow was representative of *in-situ* material. An overview of the scenarios associated with the seabed preparation modeling is presented in Table 4.1-2. Figure 4.1-2 depicts the four seabed preparation segments.

Table 4.1-2. Description of Activities Modeled for RWEC Seabed Preparation.

RWEC Seabed Preparation Modeling Scenarios				
Project Component	Description of Scenario	Methods Modeled	Total Length Modeled, Miles (mi) (Kilometers [km])	Total Dredge Duration (Days)
RWEC Seabed Preparation	Circuit 1 – Seabed Preparation Segments	CFE	10.5 (16.9)	1.76
	Circuit 1 – Seabed Preparation Segments	TSHD – Split Bottom	10.5 (16.9)	13.64
	Circuit 1 – Seabed Preparation Segments	TSHD – Continuous Overflow	10.5 (16.9)	10.88

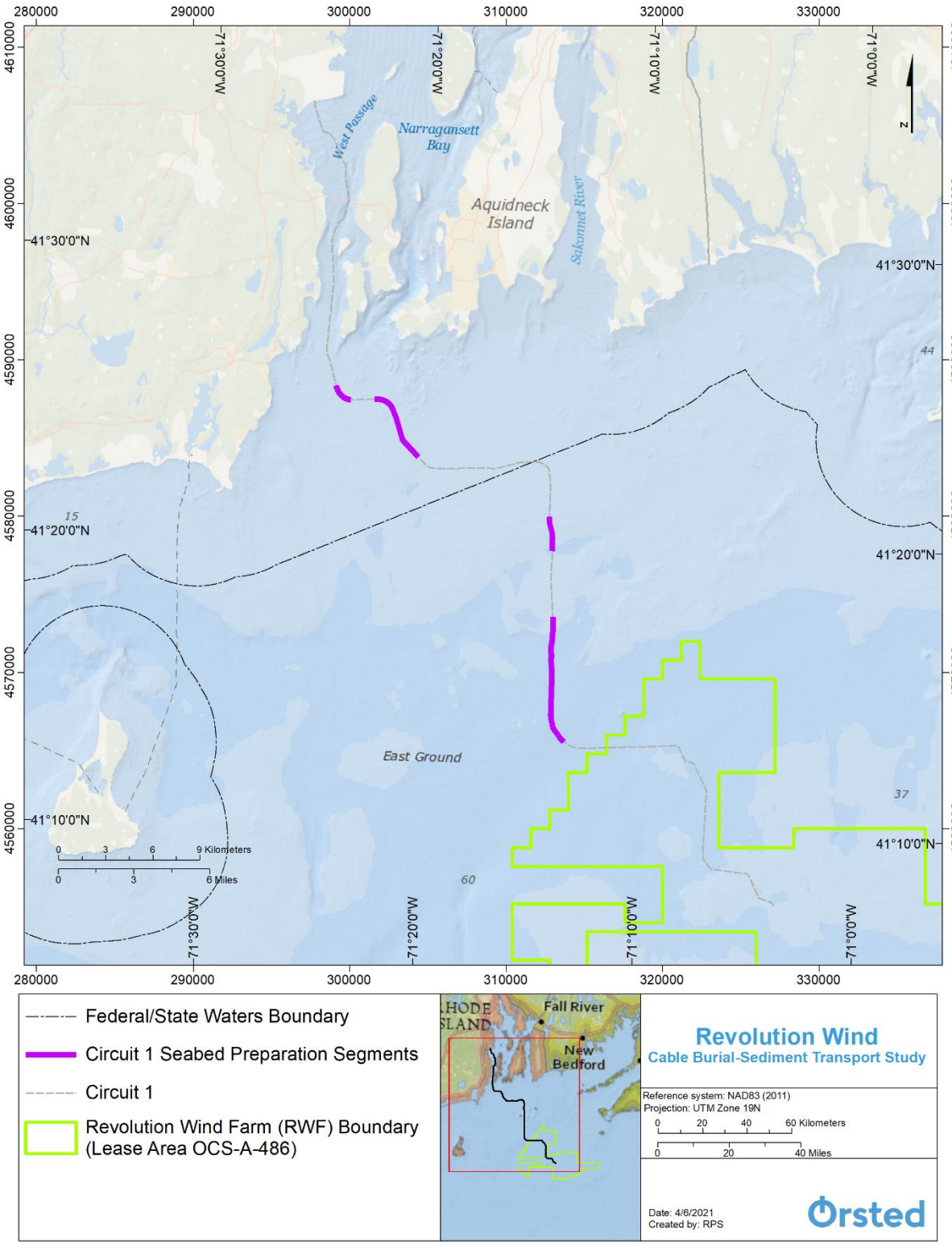

Figure 4.1-2. Seabed Preparation Segments of RWEC Circuit 1 Route.

4.1.2 Study Component 2: RWEC Circuit 1 Cable Burial

The Project includes approximately 46.7 mi (75.1 km) of RWEC corridor. The RWEC may include up to two circuits, but because the circuits follow a similar path and are in proximity to one another only Circuit 1 was modeled as a representative case. An overview of the scenarios associated with the RWEC modeling is presented in Table 4.1-3. Figure 4.1-3 depicts the modeled RWEC Circuit 1.

Table 4.1-3. Description of Activities Modeled for RWEC Circuit 1 Cable Burial.

RWEC Circuit 1 Modeling Scenarios				
Project Component	Description of Scenario	Methods Modeled	Total Length Modeled, mi (km)	Total Dredge Duration (Days)
RWEC	Circuit 1	Jet Plow	46.7 (75.1)	7.82

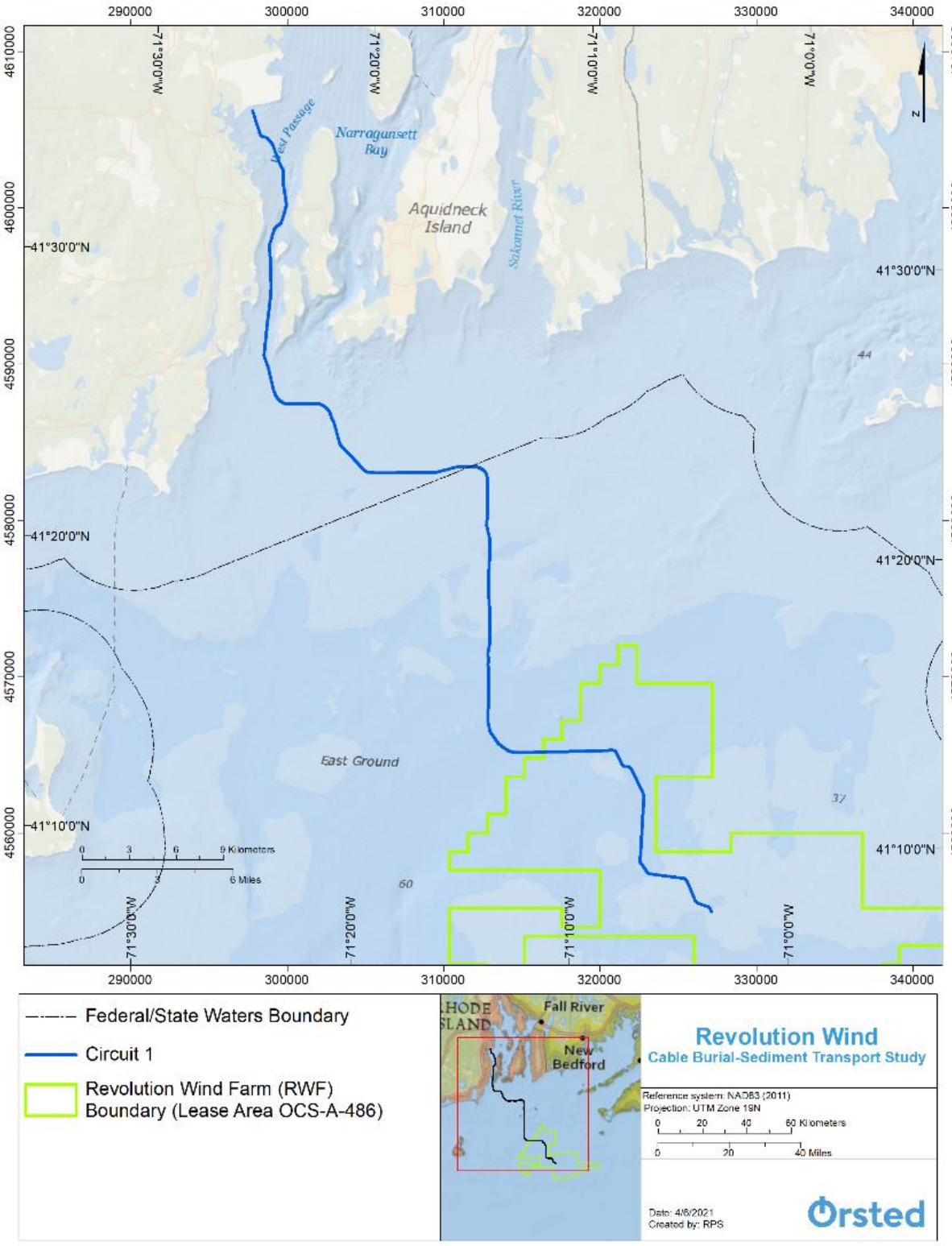

Figure 4.1-3. RWEC Circuit 1.

4.1.3 Study Component 3: Representative IAC Cable Burial

Within the RWF, approximately 155 mi (250 km) of buried cable is anticipated for the IAC. Burial of a representative 1.4 mi (2.3 km) segment was modeled for two different current conditions (i.e., spring tide and neap tide) using two different timeframes due to the relatively short installation period. This was done to show the potential variations induced by the different currents, and to assess the sensitivity of sediment transport to variable current regimes. The modeled IAC section was selected as a representative section because it is located in an area with a relatively larger fraction of fine sediments. Based on the assumption that fine sediments take longer to settle, this conservatively predicts the worst-case scenario for water column TSS concentrations. An overview of the scenarios associated with the representative IAC modeling is presented in Table 4.1-4. Figure 4.1-4 depicts the representative IAC location.

Table 4.1-4. Description of Activities Modeled for IAC Burial.

IAC Modeling Scenarios					
Project Component	Description of Scenario	Methods Modeled	Total Length Modeled, mi (km)	Total Dredge Duration (Days)	Current Condition
IAC	IAC – Current Condition 1	Jet Plow	1.4 (2.3)	0.23	Spring Tide
	IAC – Current Condition 2	Jet Plow	1.4 (2.3)	0.23	Neap Tide

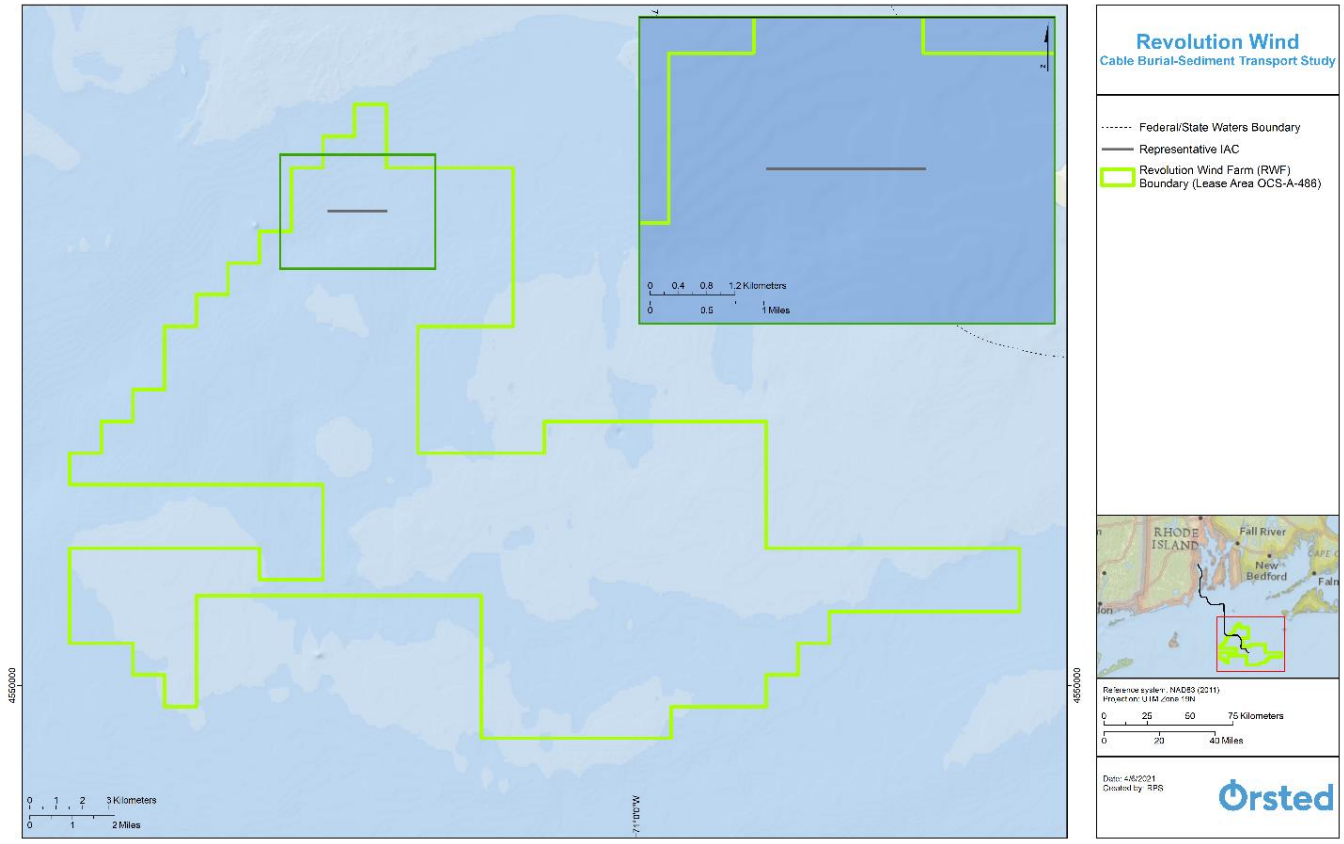

Figure 4.1-4. RWF Representative IAC Route.

4.1.4 Study Component 4: RWEC Landfall

The RWEC study evaluated two different landfall equipment types to excavate the HDD exit pit, which are anticipated to be implemented consecutively: a backhoe excavator to clear the majority of the material and a Venturi eductor device for more precise clearing. The pit would be cleared and subsequently backfilled after tie-in. Although the volume cleared is expected to be the same as the volume backfilled, it is anticipated that the backfilling process will begin on the order of hours to days after the pit has been cleared, thus allowing sufficient time for sediment to disperse and settle. Therefore, only the clearance was modeled and is considered representative of the backfill process. A summary of the scenarios is presented in Table 4.1-5. Figure 4.1-5 depicts the HDD exit pit location along the RWEC.

Table 4.1-5. Description of Activities Modeled for Landfall.

Landfall Scenario			
Project Component	Description of Scenario	Methods Modeled	Total Dredge Duration (Days)
Landfall	HDD Exit Pit	Backhoe Excavator followed by Venturi Eductor Device	2.9

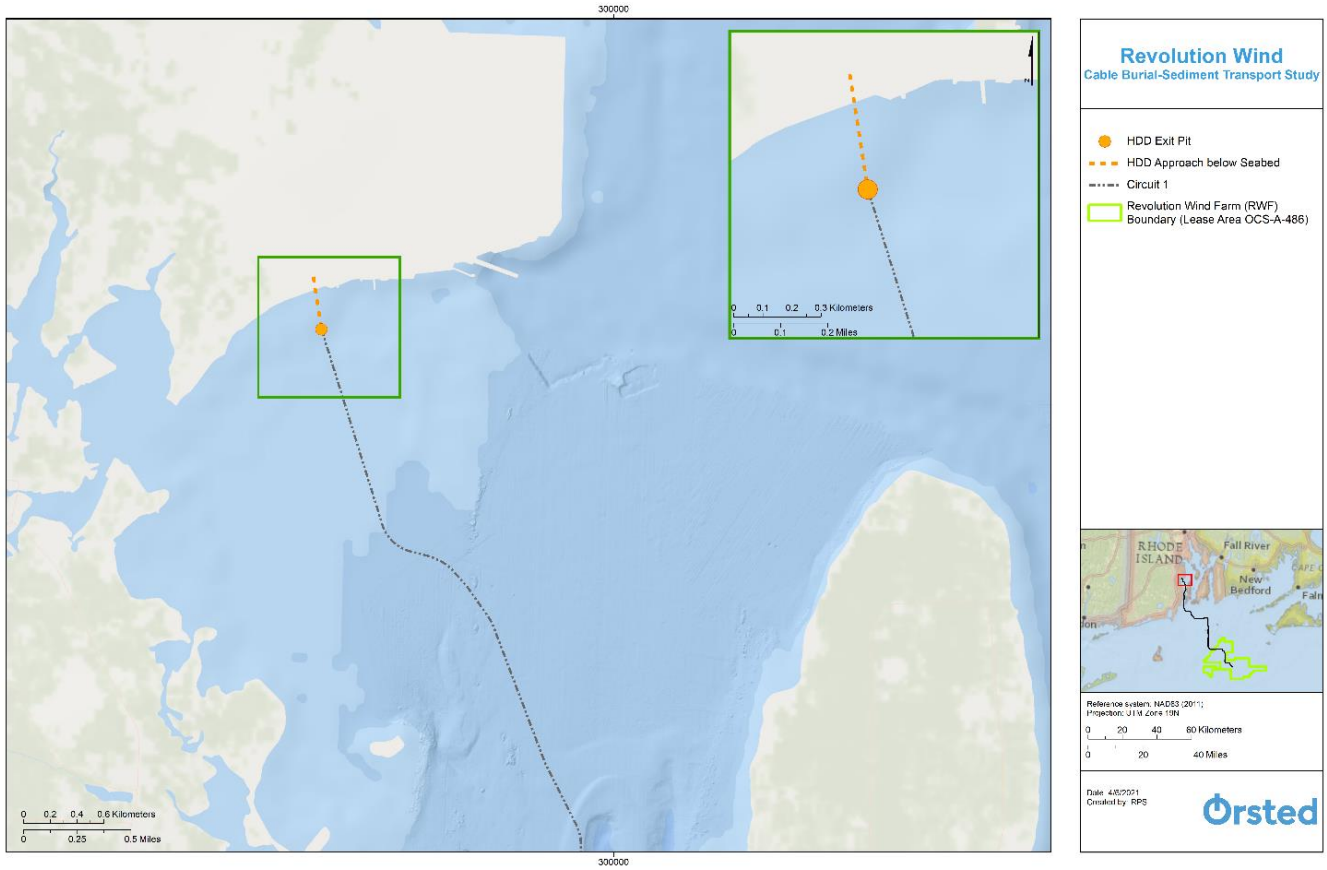

Figure 4.1-5. RWEC Landfall HDD Exit Pit Location.

4.2 SSFATE Sediment Transport Model Application

Setup of the SSFATE model consists of defining the environmental conditions, the construction scenario, and computational parameters. For each scenario, this includes:

- The study area environmental conditions
    - Shoreline and bathymetry
    - Tides and currents
- The construction activity source terms
    - The geographic extent of the activity (point release vs. line source)
    - The dates and duration of the activity
    - The volumes and cross-sectional areas of the trench or excavation pit
    - The production rate for each dredge/trenching method
    - Loss rates for each dredge/trench method
    - The grain size distribution along the route
    - The vertical distribution of sediments as they are initially released to the water column
- Specification of model run parameters
    - The concentration and deposition grid resolution
    - Model calculation and output timesteps

4.2.1 Environmental Conditions in SSFATE

The SSFATE model uses hydrodynamics and bathymetry sources from the HYDROMAP application described in Section 3. Concentration and deposition gridding in SSFATE is independent of the resolution of the hydrodynamic data used to calculate sediment transport.

4.2.2 Sediment Source Terms

The sediment loading was developed for each scenario based on conservative assumptions about the construction activities and the associated trench size (i.e., the disturbed sediment volume). A summary of the trench dimensions, installation rate, production rate, and 'loss rate' for each trench type associated with seabed preparation and installation of the RWEC and IAC is presented in Table 4.2-1. The loss rate is the percentage of the trench volume that is assumed to be resuspended into the water column. A 30% loss rate was assumed for jet plow installation, while a loss rate of 100% was assumed for all other construction methods (i.e., CFE, TSHD). For both the CFE and jet plow it was assumed that the resuspension would be evenly distributed within the bottom 8.2 ft (2.5 m) of the water column. For the TSHD split bottom method, it was assumed 20% of the resuspension would occur at the water surface as periodic overflow, and 80% would occur 16.4 ft (5 m) below the water surface as periodic disposal from the split bottom. For the TSHD continuous overflow method, it was assumed that 100% of the dredged sediment would be introduced at the water surface.

Table 4.2-1. Installation Details Assumed for the RWEC and IAC Modeling.

Trenching Parameters for RWEC and IAC						
Project Component	Equipment	Total Length Modeled, mi (km)	Disturbance Depth, ft (m)	Disturbance Cross-Sectional Area, ft^2 (m^2)	Installation Rate, ft/hr (m/hr)	Loss Rate
RWEC Seabed Preparation	CFE	10.5 (16.9)	6.6 (2.0)	301.4 (28.0)	1312 (400)	100%
	TSHD – Split Bottom	10.5 (16.9)	6.6 (2.0)	301.4 (28.0)	215 (65.5)	100%
	TSHD – Continuous Overflow	10.5 (16.9)	6.6 (2.0)	301.4 (28.0)	215 (65.5)	100%
RWEC	Jet Plow	46.7 (75.1)	9.8[1] (3.0)	88.3 (8.2)	1312 (400)	30%
RWF - IAC	Jet Plow	1.4 (2.3)	8.2 (2.5)	65.7 (6.1)	1312 (400)	30%

Two construction methods to clear the HDD exit pit were modeled for the landfall simulations: a backhoe excavator and a Venturi eductor device. The landfall approach includes drilling underneath the seabed, from the shore to the HDD exit pit, eliminating sediment resuspension to the water column. The pit would be cleared and subsequently

[1] As stated in Section 3 of the COP, the maximum depth of disturbance along the RWEC is 4 m. If the RWEC disturbance depth exceeds the modeled 3 m this would result in additional sediment volume released to the environment. Assuming the same production rate, this would increase the duration of sediment loading because it would take longer to remove the larger sediment volume. This would likely change the timing of the currents to produce a slightly different plume and depositional footprint. Additional volume released has the potential to result in higher maximum concentrations, thicker depositional footprints, and longer duration of exposure above thresholds. However, when modeling RWEC installation multiple conservative assumptions were made to evaluate a maximum effect scenario. For example, the loss rate used in modeling was conservatively assumed to be 30%, when in reality the loss rate may be much lower (i.e., 15% or less depending on the sediment type). Using a 3.5 m trench depth and a loss rate of ~23% or a 4 m trench depth and loss rate of ~19% results in a similar mass of sediments predicted to be released, both of which remain above the lower threshold of 15%. So, although increasing the disturbance depth would release more sediments to the environment, the RWEC modeling remains representative as it bounded the potential impacts by assuming a conservative loss rate.

backfilled after tie-in. However, as previously discussed in Section 4.1, only the clearance was modeled and is considered representative of the backfill process. A summary of scenario parameters for the landfall simulation is presented in Table 4.2-2. It was assumed that 100% of the sediments excavated by the backhoe were introduced near the surface and 30% of the sediments removed by the Venturi eductor device were evenly distributed within the bottom 3.28 ft (1 m) of the water column.

Table 4.2-2. Installation Details Assumed for the Landfall Modeling.

Sediment Transport Modeling Scenarios Overview				
Project Component	Equipment	Trench or Pit Volume Excavated, Cubic Yards (cy) (Meters Cubed [m^3])	Production Rate, cy/hr (m^3/hr)	Loss Rate
Landfall	HDD Exit Pit – Backhoe Excavator followed by Venturi Eductor Device	4,901 (3,750)	78 (60)	100%
		980 (750)	131 (100)	30%

4.2.2.1 Sediment Grain Size Distribution

The sediment characteristics and grain size distribution are key input parameters in the SSFATE model when predicting sediment transport. Based on the sediment samples (e.g., vibracores, grab samples) collected during multiple offshore surveys, the spatial variability of the sediment characteristics and grain size distribution were captured in the modeled scenarios. Once collected, the samples underwent further laboratory analysis, as documented in Section 4.3.2 of the COP, and results from these analyses were then refined by RPS as it pertained to the sediment characterization used in the SSFATE model. Sediment data was divided into classes based on the grain size, and the depth-dependent samples were weighted to represent *in-situ* conditions for the various installation activities. Specifically, the objective was to determine the distribution within the five delineated classes used in SSFATE (Table 2.2-1) and the percentage of the upper seabed that is solid based on the measure of sediment water content, a measure of the interstitial pore waters in the sediments.

The sediment characteristics along the RWEC and in the RWF, as used in the modeling, are presented in Figure 4.2-1, Figure 4.2-2, and Figure 4.2-3. As shown in these figures, the sediments are predominately coarse-grained in the RWF and along the RWEC in federal waters but have a relatively larger fraction of fine-grained sediments closer to shore. In the RWF, the simulated IAC is representative of a worst-case plume because this location has a relatively high fraction of fine sediments. Fine sediments (e.g., clays, silts) tend to last longer in the water column, whereas coarse sediment (e.g., fine sand, coarse sand) will settle at a faster rate.

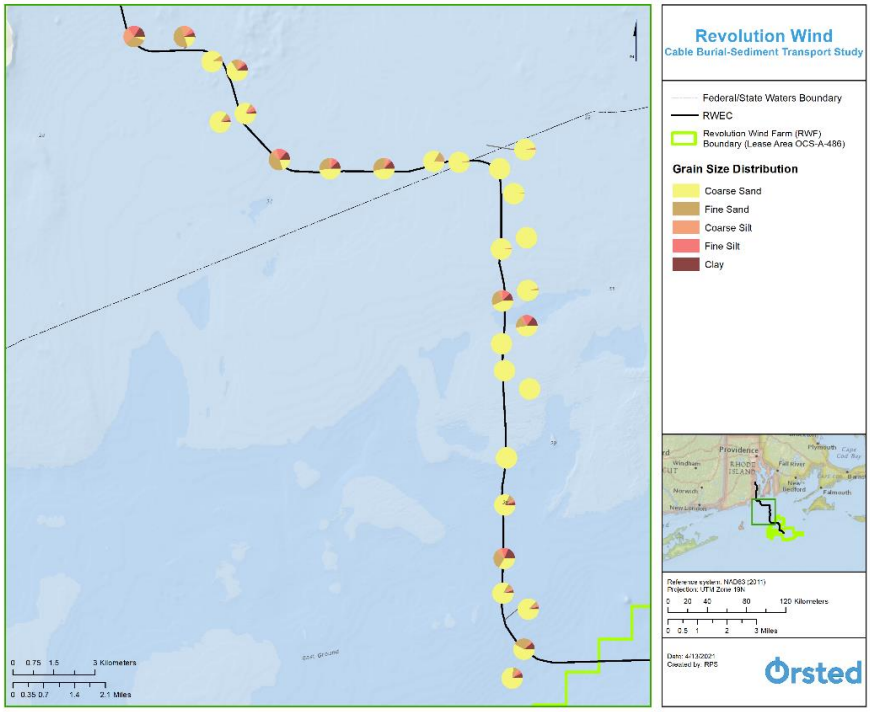

Figure 4.2-1. Sediment Grain Size Distributions for Seabed Preparation Modeling.

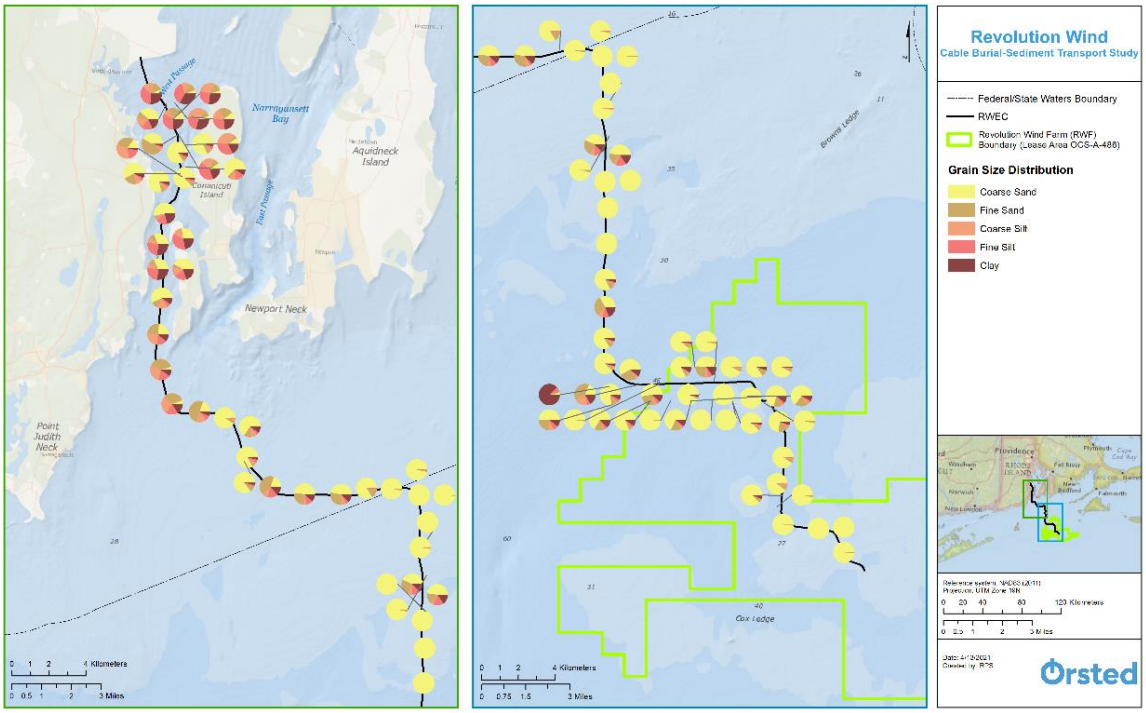

Figure 4.2-2. Sediment Grain Size Distributions for Modeling along the RWEC.

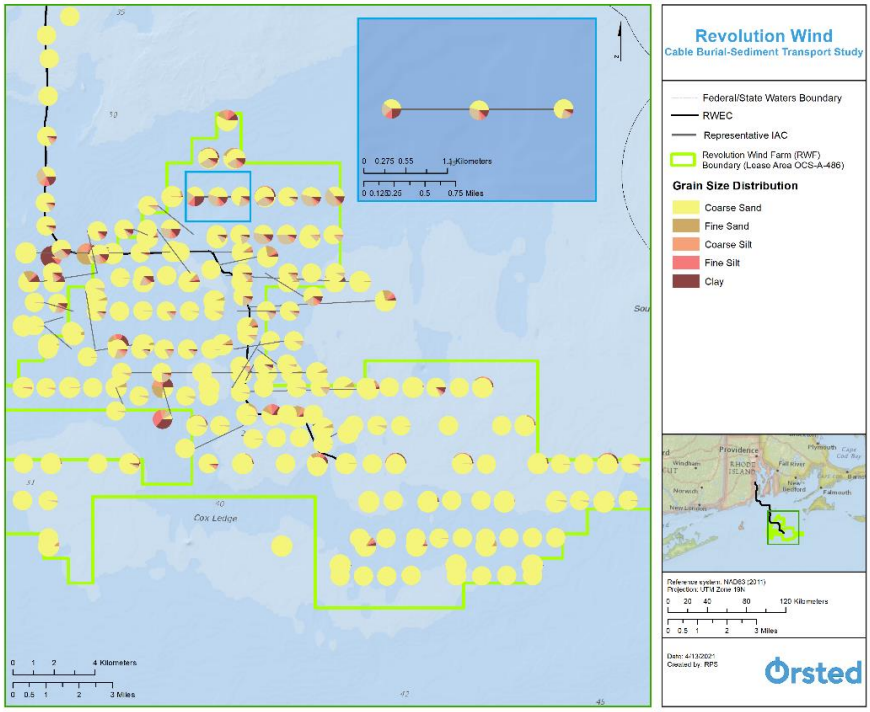

Figure 4.2-3. Sediment Grain Size Distributions for IAC Burial Modeling.

4.2.3 Model Run Parameters

For the entire RWEC and associated cable burial activities, model computations were performed every 10 minutes, with output saved at a 10-minute time step. For the seabed preparation, IAC burial, and landfall activities, model computations were performed every 5 minutes and model output was saved every 10 minutes. Sediment concentrations were computed on a grid with resolution of 197 ft x 197 ft (50 m x 50 m) in the horizontal dimension and 3.3 ft (1.0 m) in the vertical dimension for the entire RWEC cable burial activities and 66 ft x 66 ft (20 m x 20 m) in the horizontal dimension and 1.6 ft (0.5 m) in the vertical dimension for landfall activities. Seabed preparation and IAC burial activities were computed on a grid with resolution of 82 ft x 82 ft (25 m x 25 m) in the horizontal dimension and 1.6 ft (0.5 m) in the vertical dimension.

4.3 SSFATE Model Results

SSFATE simulations were performed for each construction activity. All modeling assumed continuous operation for each phase of the construction. Note that reported concentrations are those predicted above the background concentration in the study area.

The results from the model runs are presented below in maps showing the predicted TSS concentrations and subsequent deposition for each activity. Specifically, three sets of graphics were developed for each scenario:

- **Maps of Instantaneous TSS Concentrations**: These figures present the predicted instantaneous excess TSS concentrations at a moment in time for line sources. The concentrations are depicted as contours using mg/L. The plan view shows the maximum concentration throughout the water column (i.e., maximum value at any depth).

- **Maps of Time-integrated Maximum TSS Concentrations**: These figures present the predicted maximum time-integrated excess water column concentration from the entire water column (i.e., maximum value at

any point in time at any depth). The concentrations are depicted as contours using mg/L. The entire area within the contour was predicted to be at or above the concentration defined by the contour itself. Most importantly, it should be noted that these maps portray the maximum TSS concentration that occurred throughout the entire simulation at all depths and that: (1) these concentrations do not persist throughout the entire simulation and may be just one time step; and (2) these concentrations do not occur concurrently throughout the entire modeled area. Therefore, results are time-integrated spatial views of maximum predicted concentrations.

- **Maps of Seabed Deposition**: These figures present the predicted deposition on the seabed that would occur following completion of the construction activity and after suspended sediments settled out of the water column. The thickness levels are shown as contours (in mm) and the entire area within the contour is at or above the thickness defined by the contour itself.

4.3.1 Study Component 1: Seabed Preparation Alternatives, Segments of the RWEC Circuit 1

Seabed Preparation – CFE

A snapshot of the instantaneous concentration from the modeled CFE seabed preparation illustrates that highest concentrations are predicted to be adjacent to the route centerline, with lower concentrations extending further towards the northwest due to transport from local currents (Figure 4.3-1). The insets show the instantaneous plume along the first segment, with the cross-section showing the introduction of sediment near the seabed. Figure 4.3-2 shows the time-integrated maximum TSS for seabed preparation using the CFE method. The plume footprint tends to remain close to the route due to the resuspension of the entire cross-sectional area near the bottom of the water column and a relatively quick installation rate. The cumulative deposition along the seabed preparation segments is presented in Figure 4.3-3, which depicts a similar footprint to the time-integrated maximum TSS.

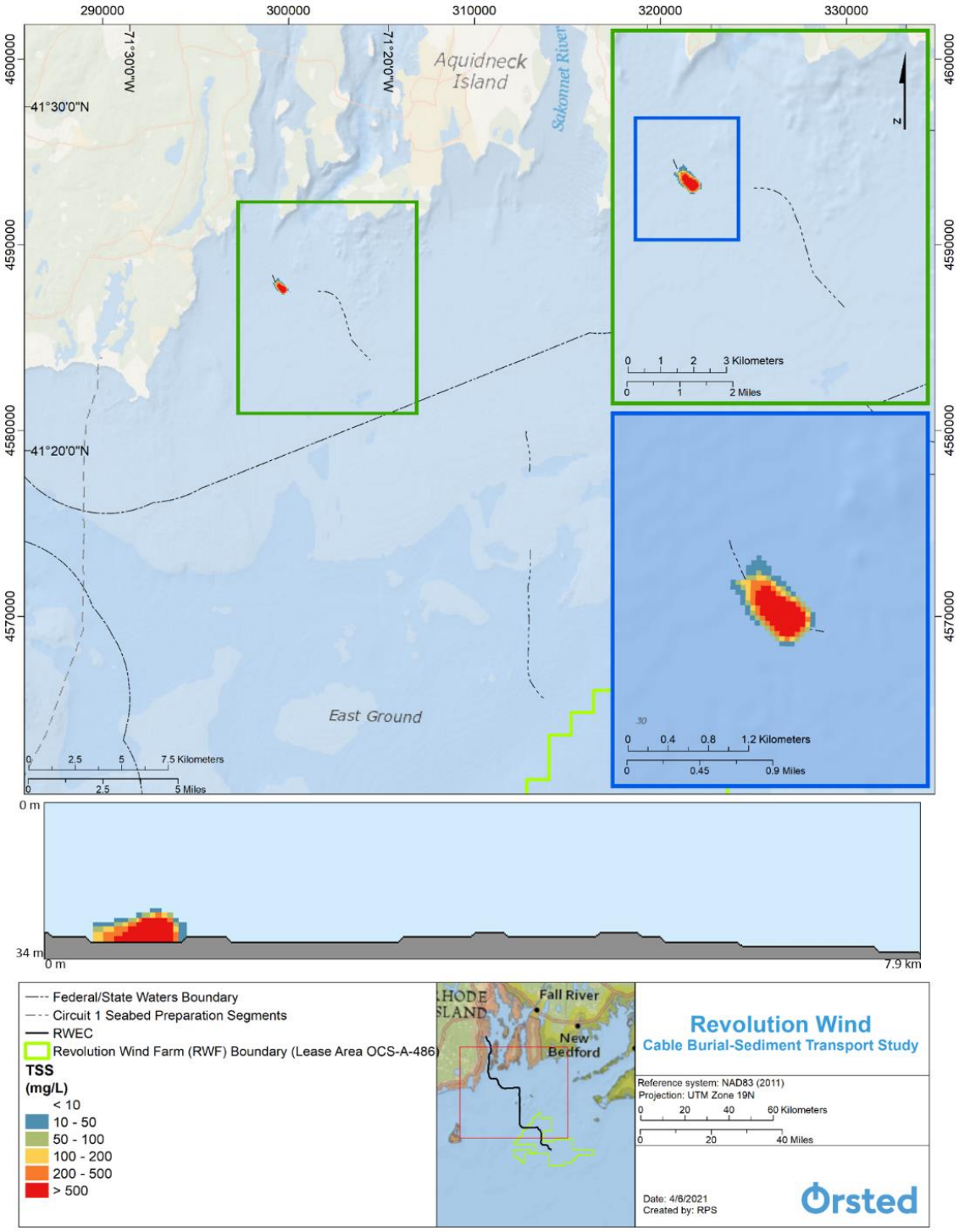

Figure 4.3-1. Snapshot of Predicted Instantaneous TSS Concentrations Associated with CFE Seabed Preparation.

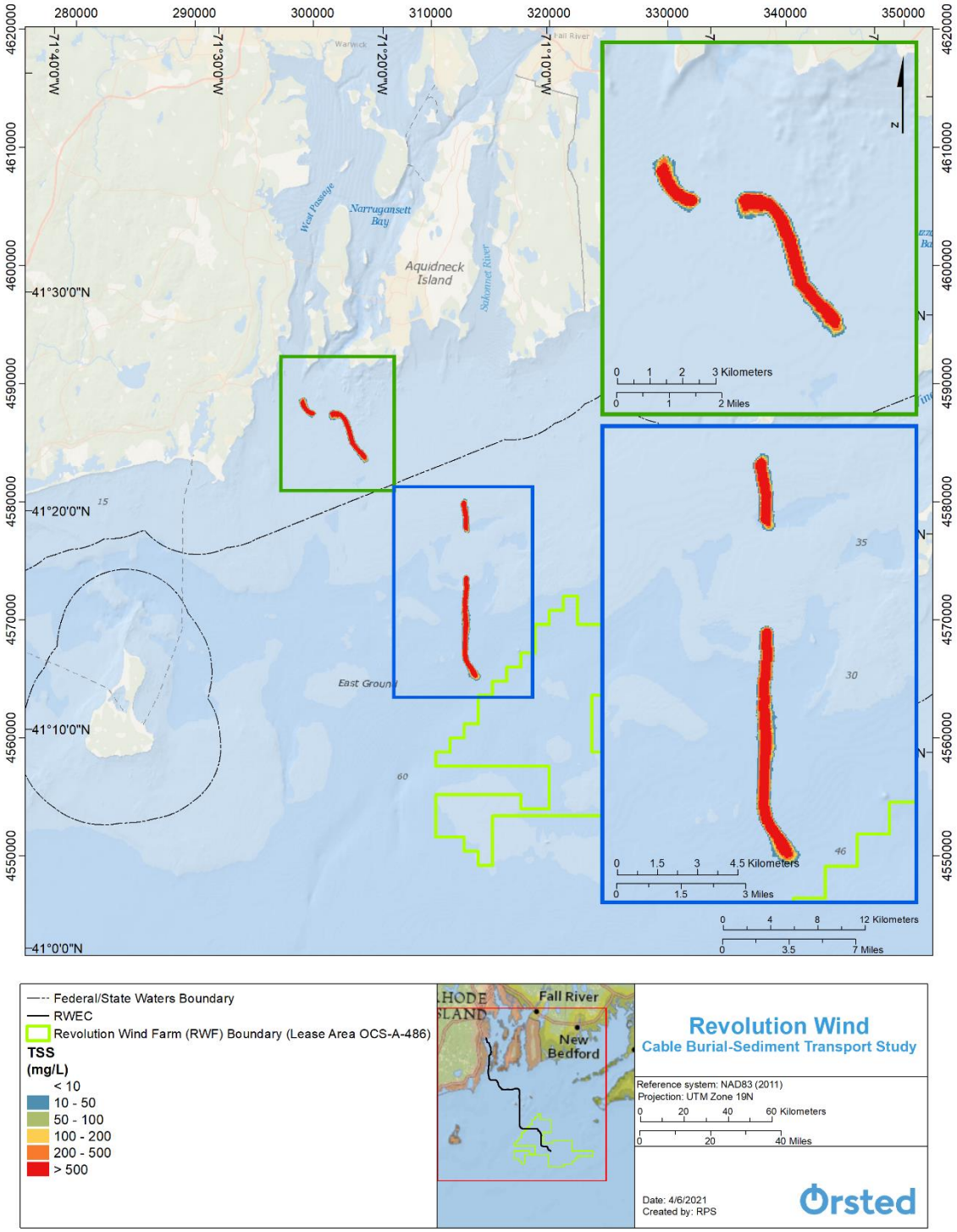

Figure 4.3-2. Map of Predicted Time-Integrated Maximum TSS Concentrations Associated with CFE Seabed Preparation.

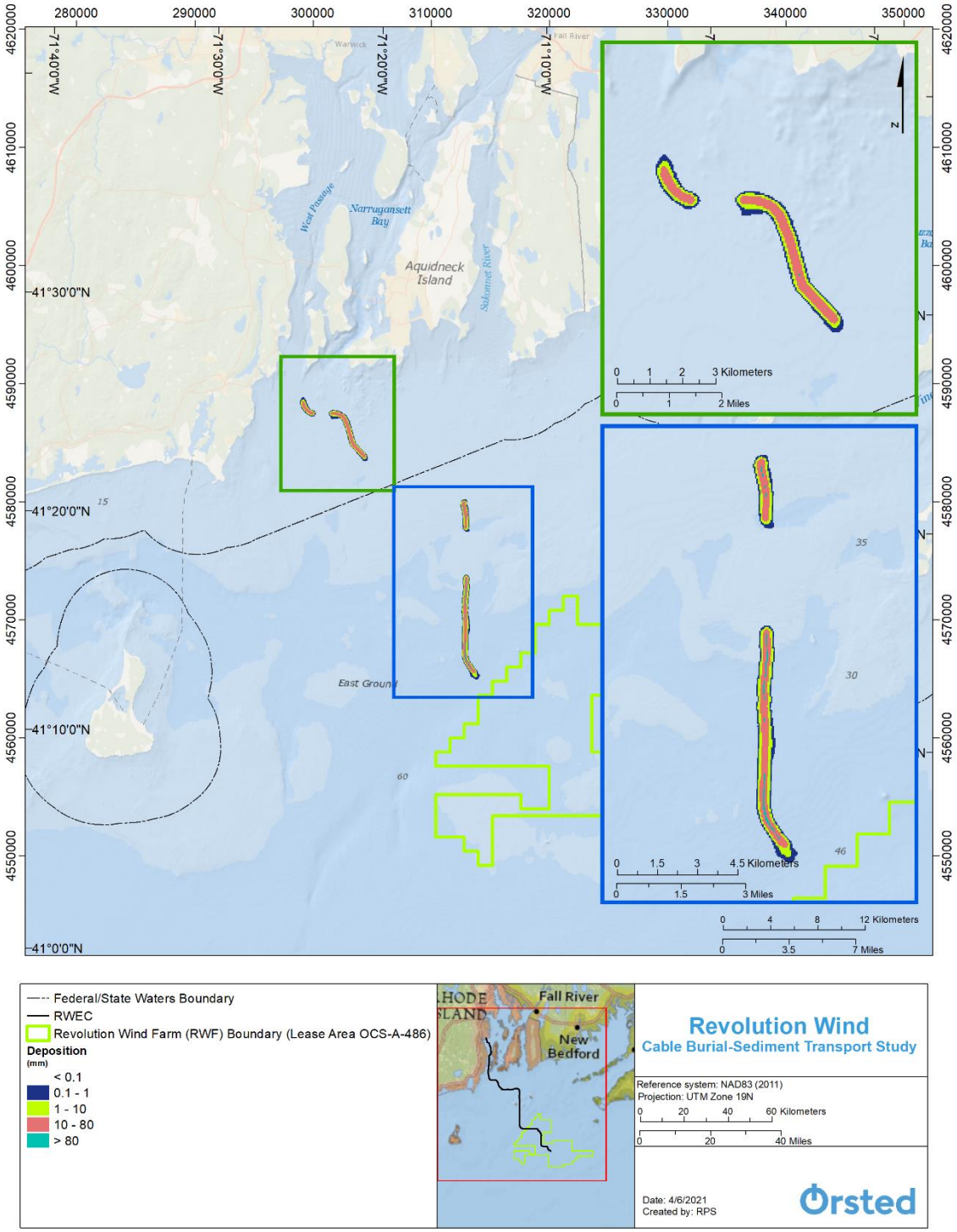

Figure 4.3-3. Map of Predicted Deposition Thickness Associated with CFE Seabed Preparation.

Seabed Preparation – TSHD, Split Bottom

A snapshot of the instantaneous concentration from the modeled TSHD split bottom seabed preparation illustrates that highest concentrations are predicted to be directly adjacent to the route centerline, with lower concentrations extending further south due to transport from local currents (Figure 4.3-4). The insets show the instantaneous plume along the first segment, with the cross-section showing the introduction of sediment at, and just below, the water surface. The plume footprint is reflective of the periodic overflow and split bottom disposal. Figure 4.3-5 shows the time-integrated maximum TSS for seabed preparation using the TSHD split bottom method. Because sediment is introduced at or near the water surface with a relatively slow installation rate, the plume footprint experiences multiple tidal cycles and tends to oscillate with the currents. The cumulative deposition along the seabed preparation segments is presented in Figure 4.3-6, which depicts a similar footprint to the time-integrated maximum TSS.

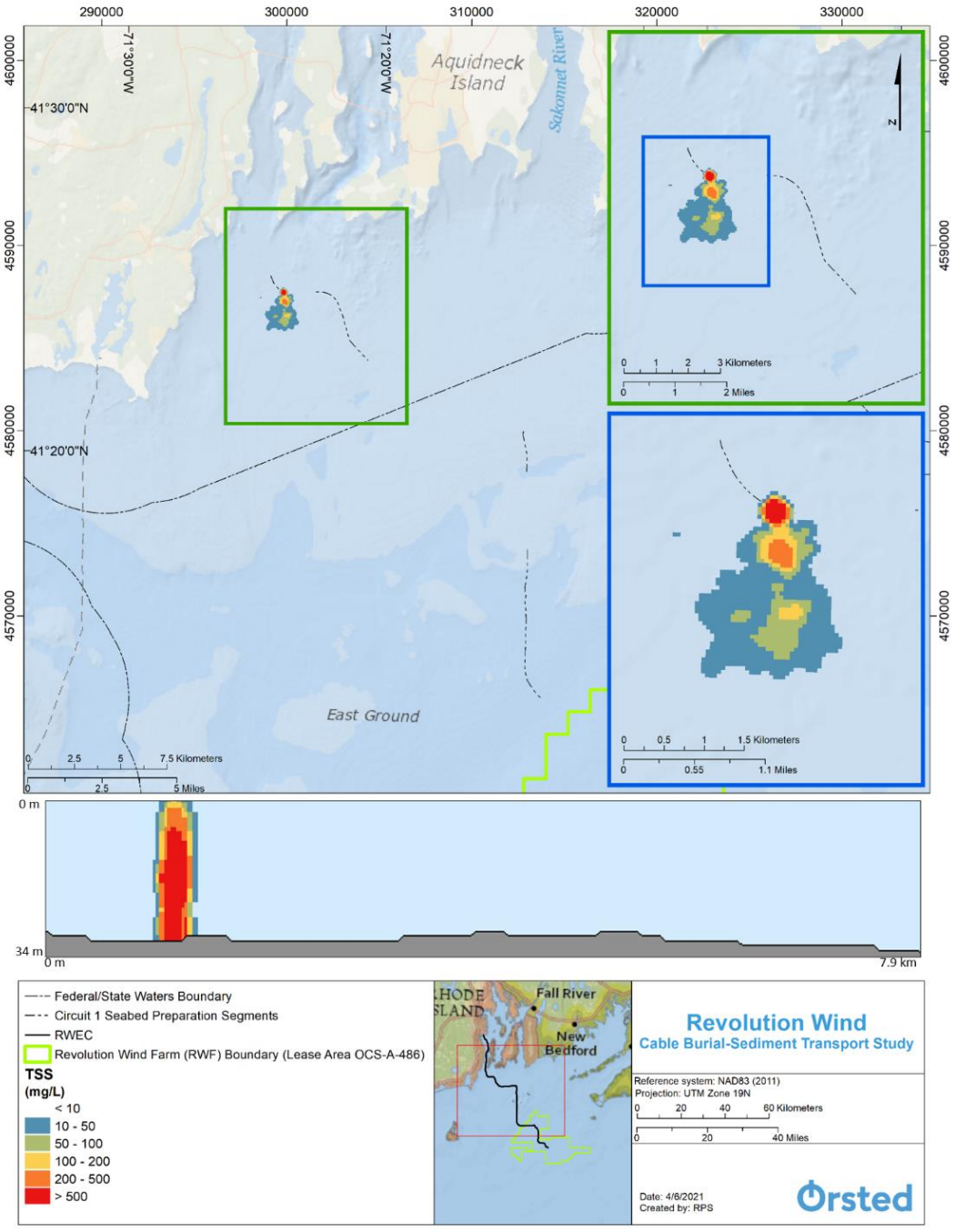

Figure 4.3-4. Snapshot of Predicted Instantaneous TSS Concentrations Associated with TSHD, Split Bottom Seabed Preparation.

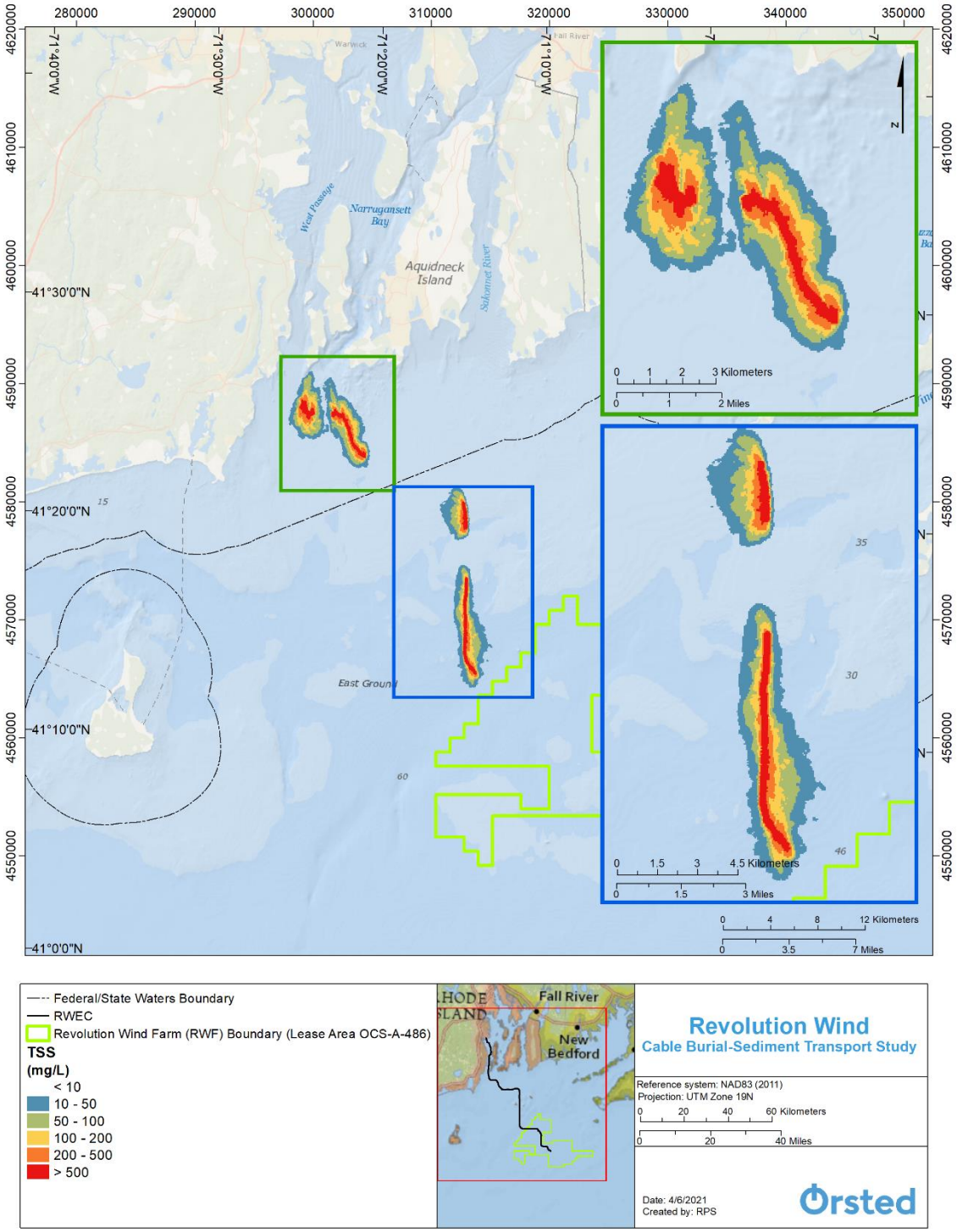

Figure 4.3-5. Map of Predicted Time-Integrated Maximum TSS Concentrations Associated with TSHD, Split Bottom Seabed Preparation.

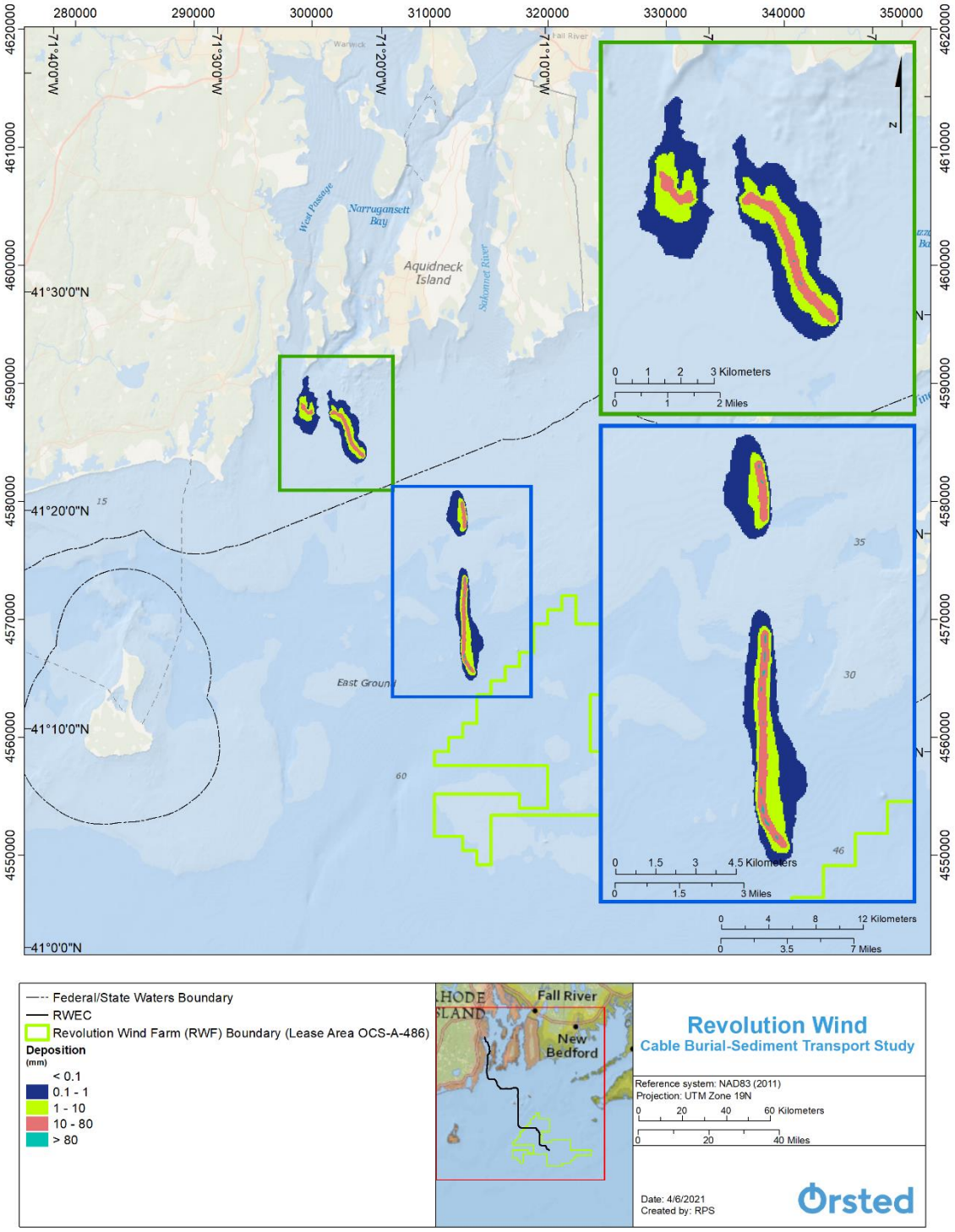

Figure 4.3-6. Map of Predicted Deposition Thickness Associated with TSHD, Split Bottom Seabed Preparation.

Seabed Preparation – TSHD, Continuous Overflow

A snapshot of the instantaneous concentration from the modeled TSHD continuous overflow seabed preparation illustrates that highest concentrations are predicted to be directly adjacent to the route centerline, with lower concentrations extending further towards the south due to transport from local currents (Figure 4.3-7). The insets show the instantaneous plume along the first segment, with the cross-section showing the introduction of sediment at the water surface. Figure 4.3-8 shows the time-integrated maximum TSS for seabed preparation using the TSHD continuous overflow method. Because sediment is introduced at the water surface with a relatively slow installation rate, the plume footprint experiences multiple tidal cycles and tends to oscillate with the currents. The cumulative deposition along the seabed preparation segments is presented in Figure 4.3-9, which depicts a similar footprint to the time-integrated maximum TSS.

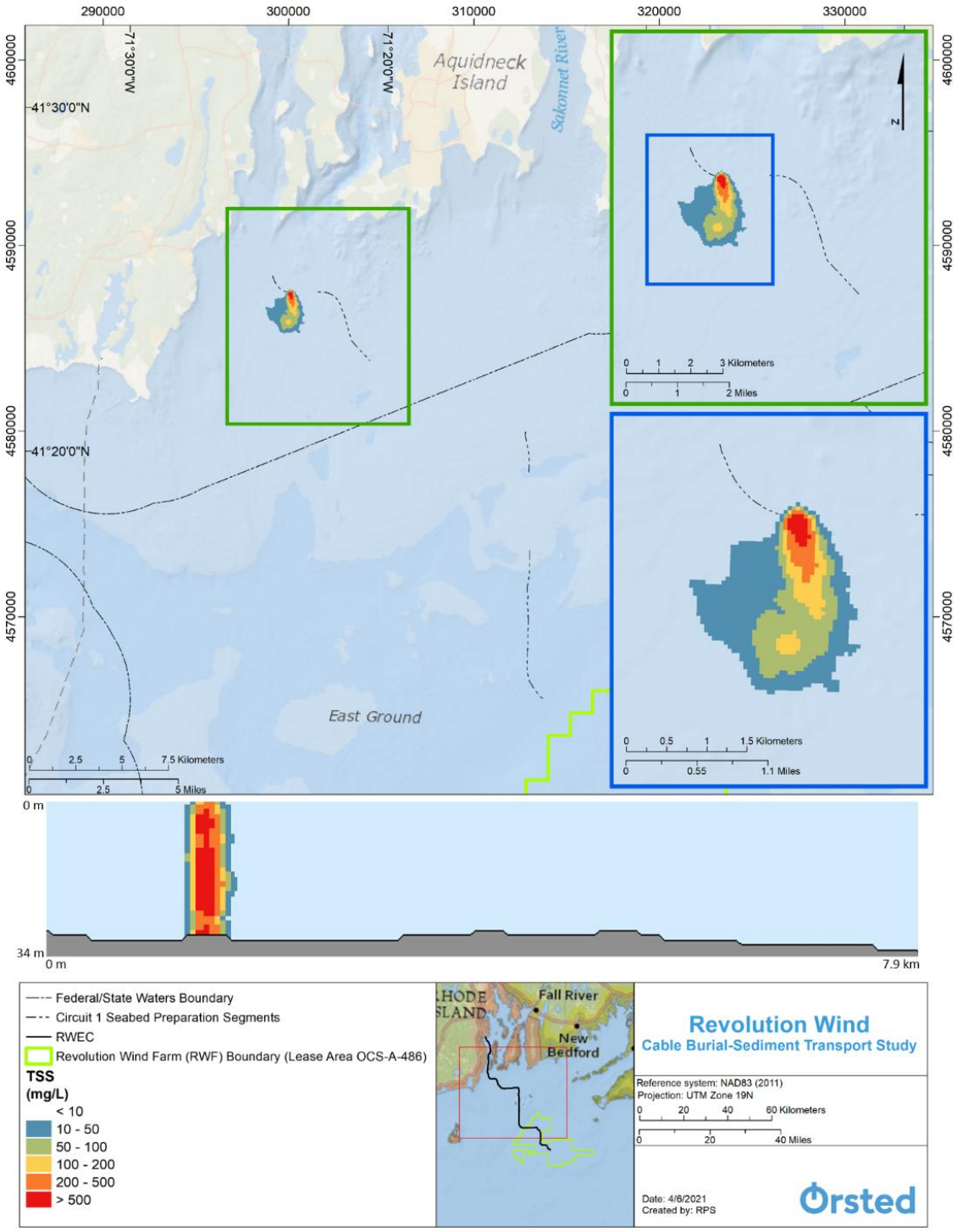

Figure 4.3-7. Snapshot of Predicted Instantaneous TSS Concentrations Associated with TSHD, Continuous Overflow Seabed Preparation.

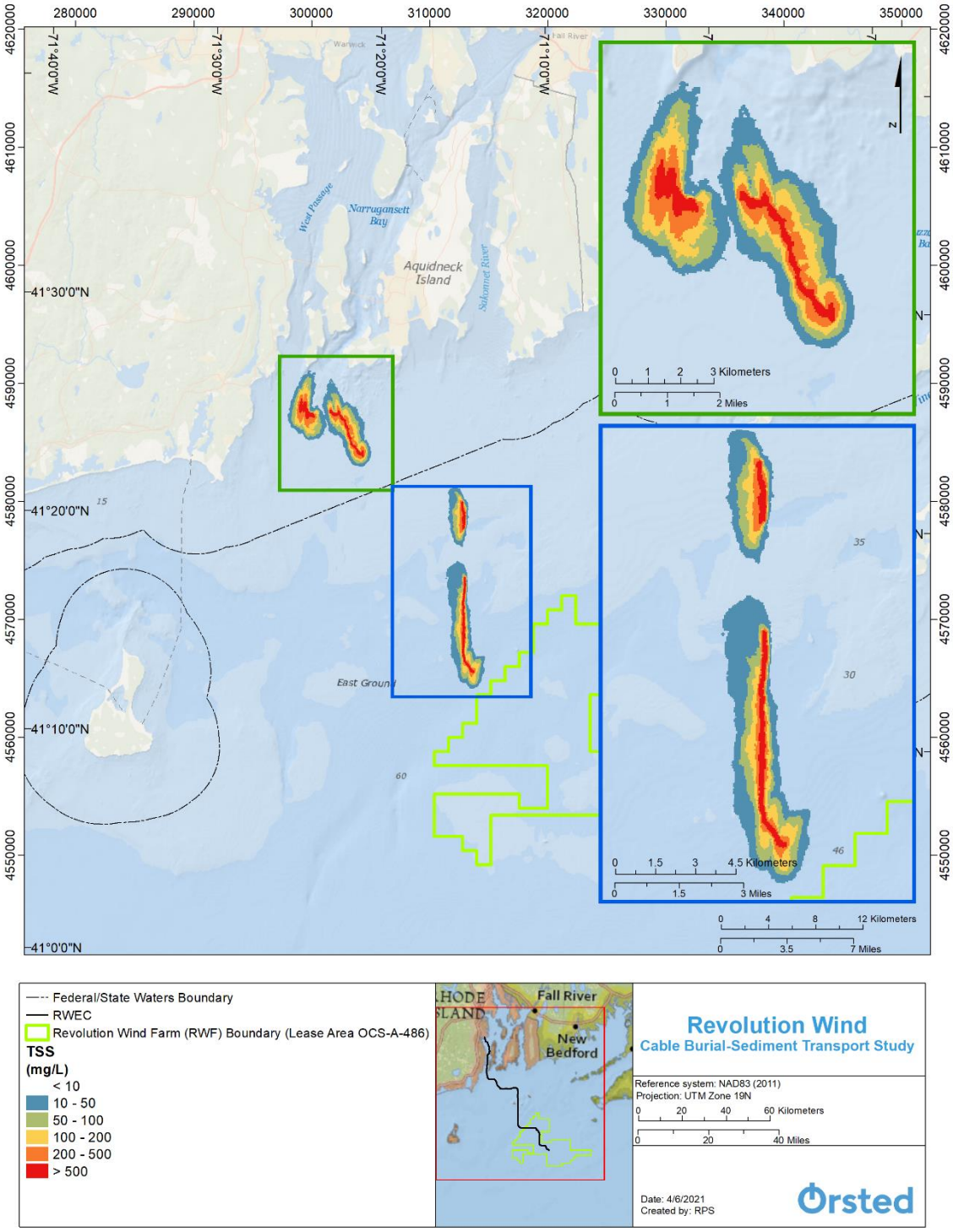

Figure 4.3-8. Map of Predicted Time-Integrated Maximum TSS Concentrations Associated with TSHD, Continuous Overflow Seabed Preparation.

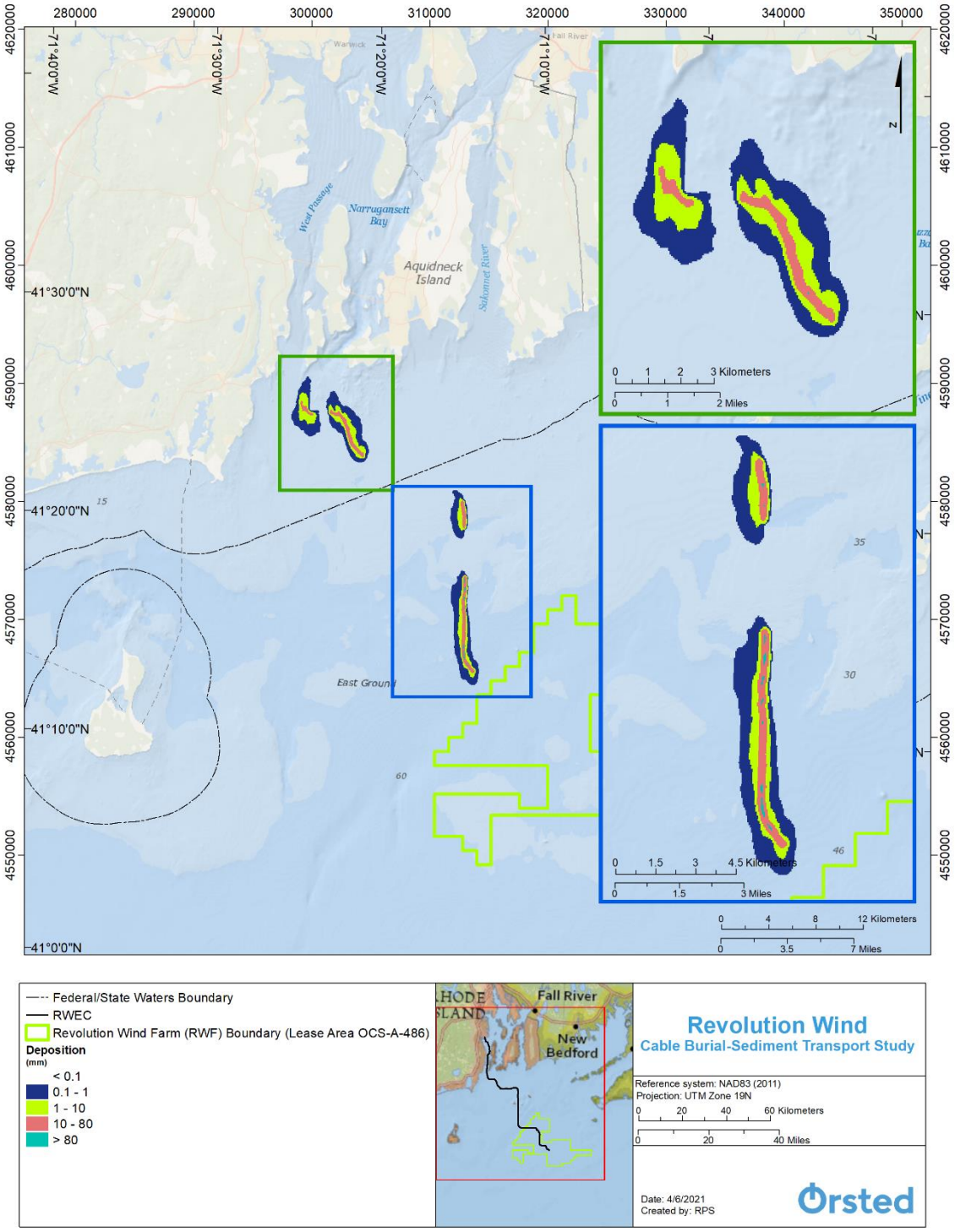

Figure 4.3-9. Map of Predicted Deposition Thickness Associated with TSHD, Continuous Overflow Seabed Preparation.

Seabed Preparation – Alternatives Comparison

Example comparisons of instantaneous TSS concentration, time-integrated maximum TSS concentration, and deposition thickness for each seabed preparation alternative are provided in Figure 4.3-10, Figure 4.3-11, and Figure 4.3-12, respectively. Predictions show the plume of the CFE method tends to remain closer to the route centerline, with relatively higher concentrations, than the TSHD methods. The localization of sediment plumes for the CFE method is likely due to the introduction of sediment closer to the seabed and faster installation rate. The TSHD split bottom method instantaneous plume reflects the periodic overflow and split bottom disposal in comparison to the TSHD continuous overflow. However, the footprints of both TSHD methods appear alike due to the similar disposal locations within the water column and same installation speed. The slight differences are most likely due to the periodic introduction of finer sediment at the surface and coarser sediment a few meters below the surface for the split bottom method, whereas all sediment is disposed of at the surface for the continuous overflow method. These differences are evident in the results tables presented in Section 4.4.

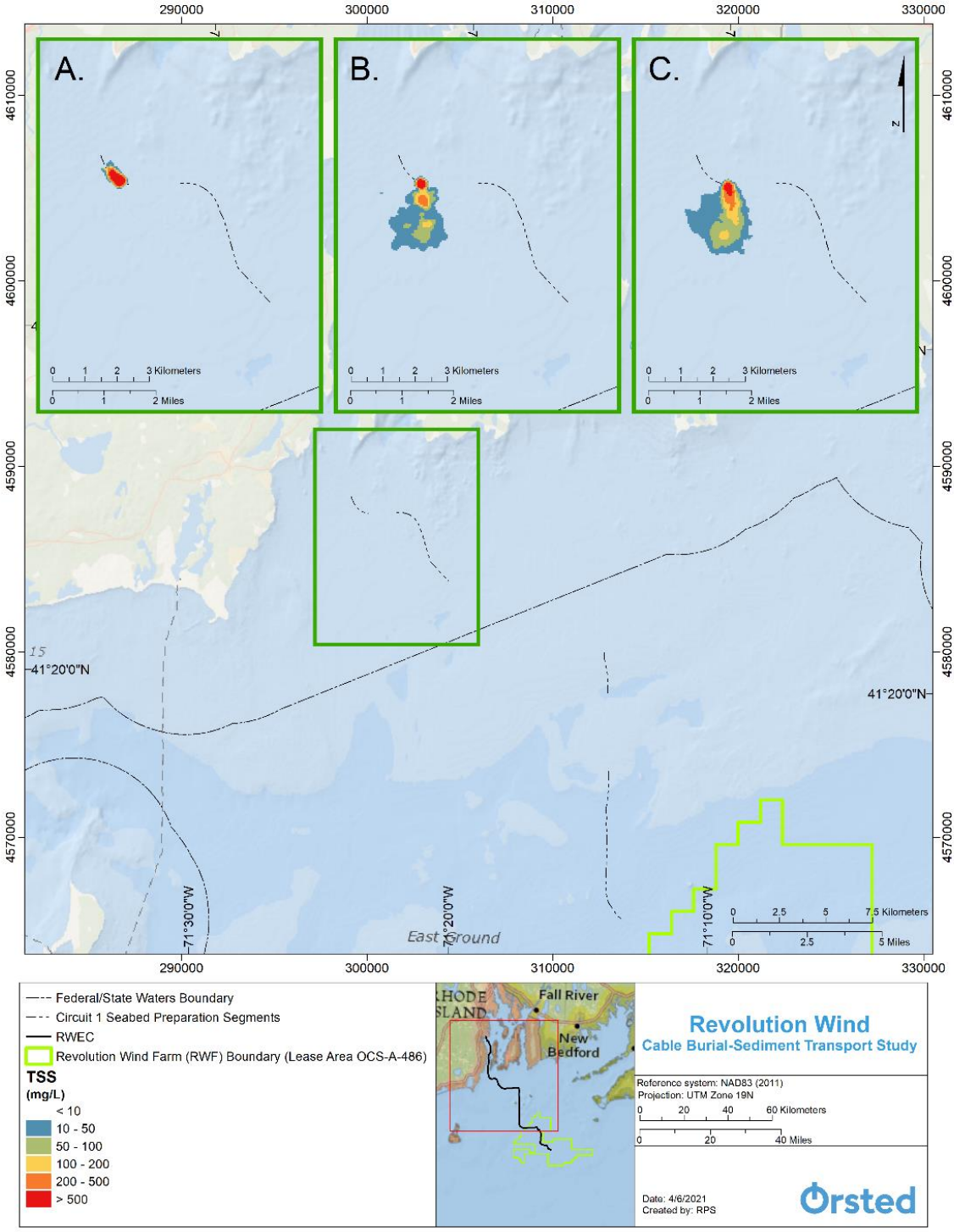

Figure 4.3-10. Snapshot of Predicted Instantaneous TSS Concentrations Associated with (A) CFE, (B) TSHD, Split Bottom, and (C) TSHD, Continuous Overflow Seabed Preparation.

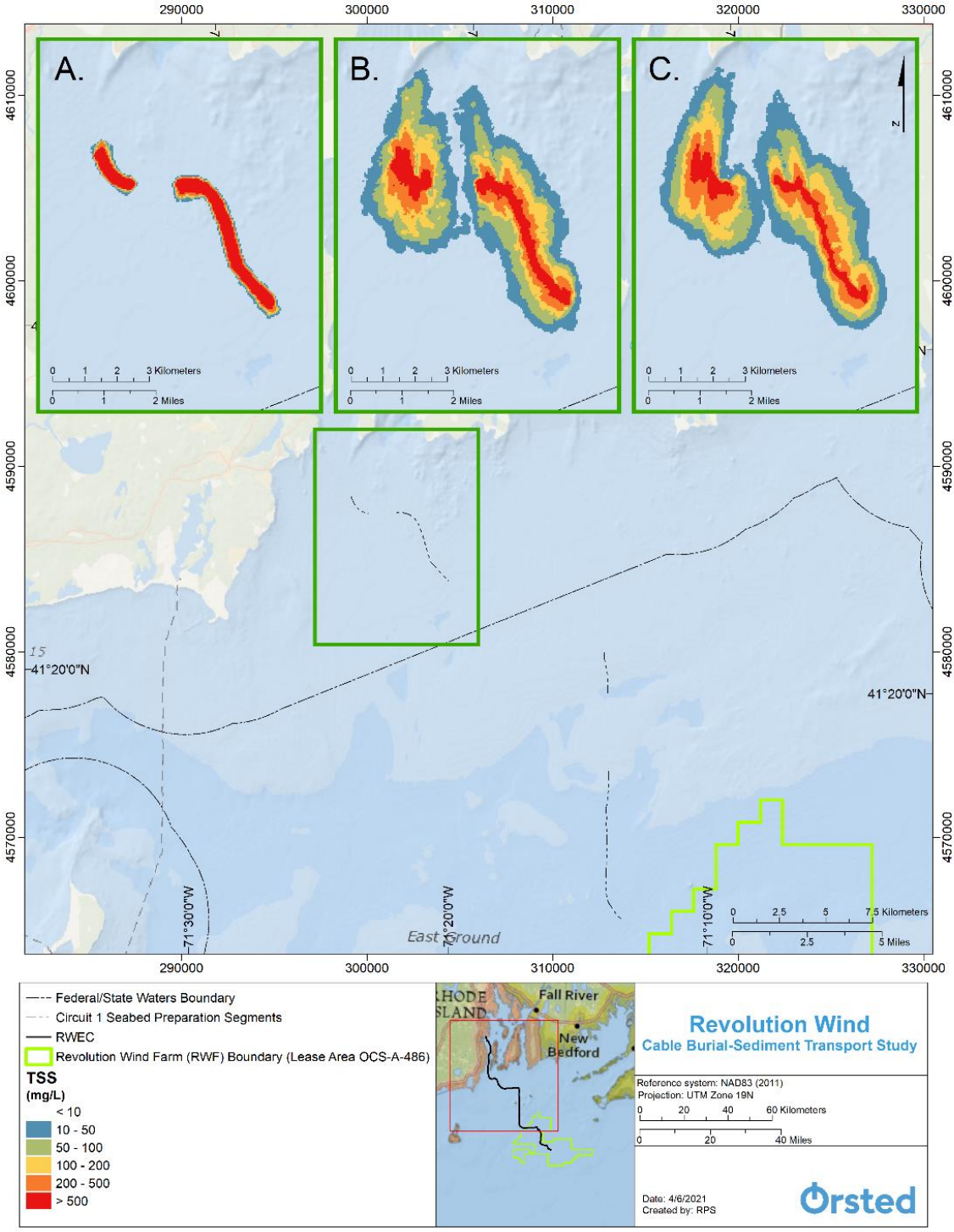

Figure 4.3-11. Map of Predicted Time-Integrated Maximum TSS Concentrations Associated with (A) CFE, (B) TSHD, Split Bottom, and (C) TSHD, Continuous Overflow Seabed Preparation.

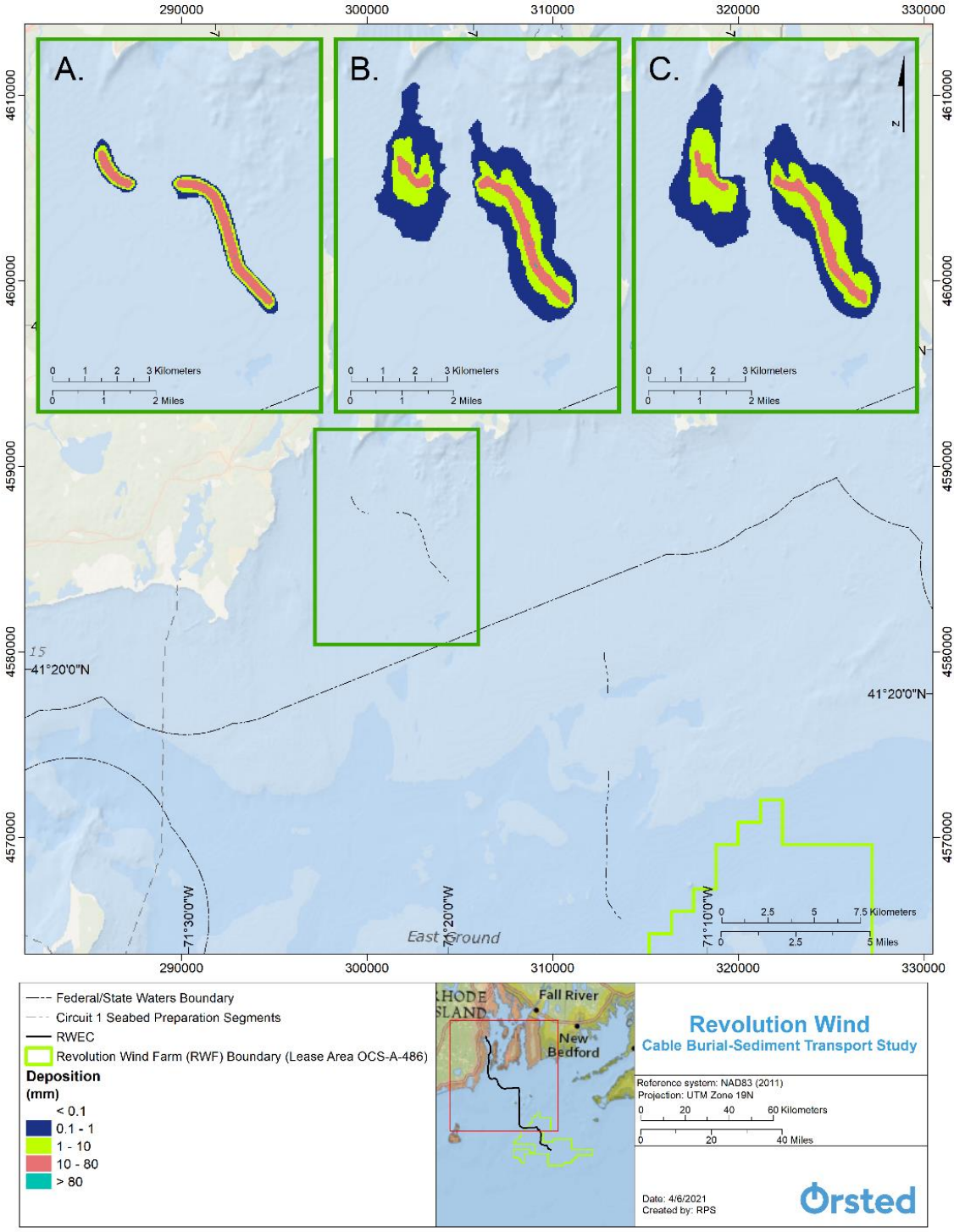

Figure 4.3-12. Map of Predicted Deposition Thickness Associated with (A) CFE, (B) TSHD, Split Bottom, and (C) TSHD, Continuous Overflow Seabed Preparation.

4.3.2 Study Component 2: RWEC Circuit 1 Cable Burial

A snapshot of the instantaneous concentration from the modeled RWEC Circuit 1 cable burial illustrates that highest concentrations are predicted to be directly adjacent to the route centerline, with lower concentrations extending further towards the south due to transport from local currents (Figure 4.3-13). The cross-section shows sediment is introduced and remains near the seabed.

The results from the entire simulation are provided in Figure 4.3-14 and Figure 4.3-15. Figure 4.3-14 shows the time integrated maximum TSS for installation of the entire circuit. The response of the plume to the oscillating currents is evident in the footprint, particularly in sections where the route is perpendicular to the predominate current direction. It is also evident that, in areas of almost all coarse sand, the plume is smaller and the footprint does not extend as far from the route centerline. The cumulative deposition along the circuit is presented in Figure 4.3-15.

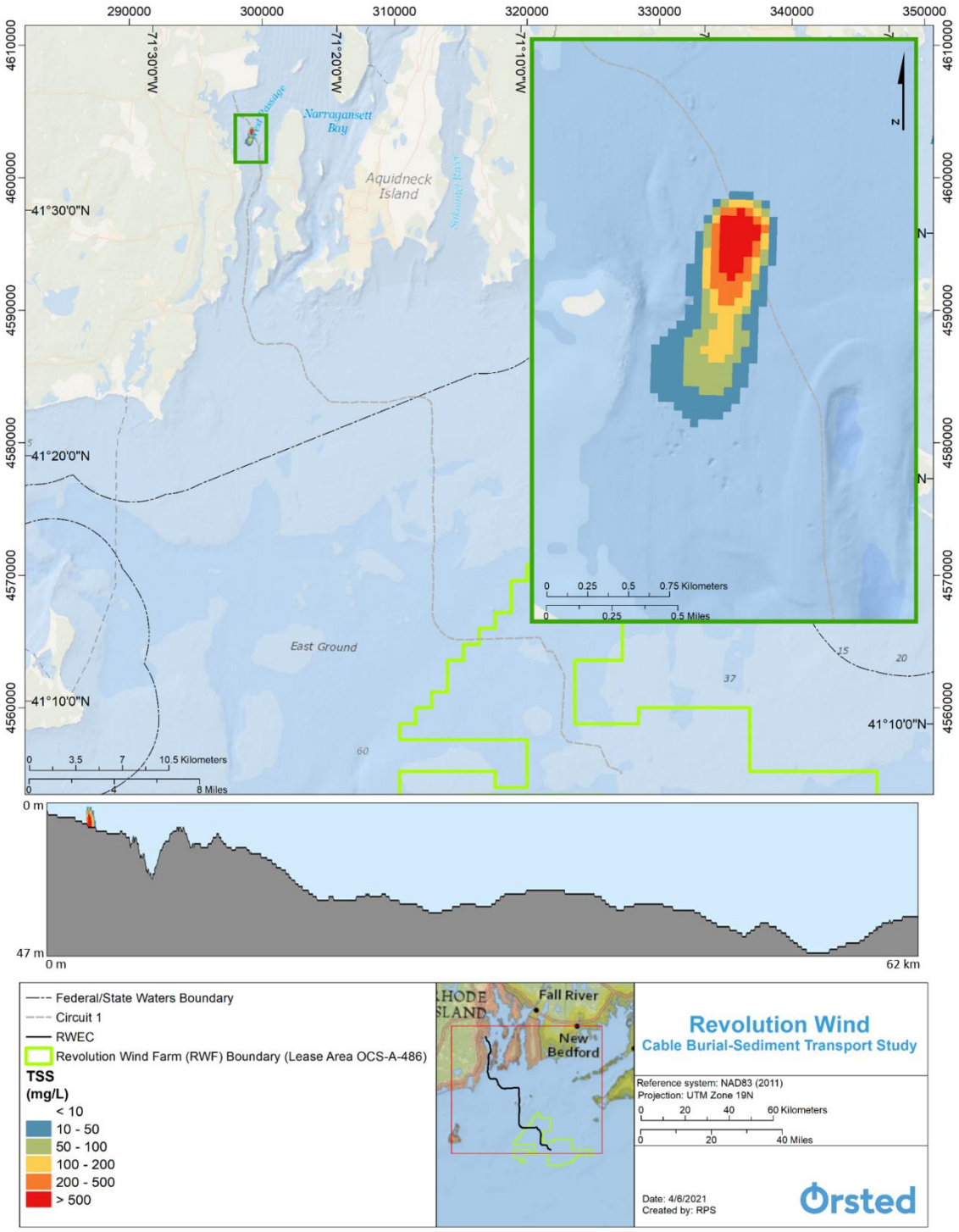

Figure 4.3-13. Snapshot of Predicted Instantaneous TSS Concentrations Associated with RWEC Circuit 1 Cable Burial.

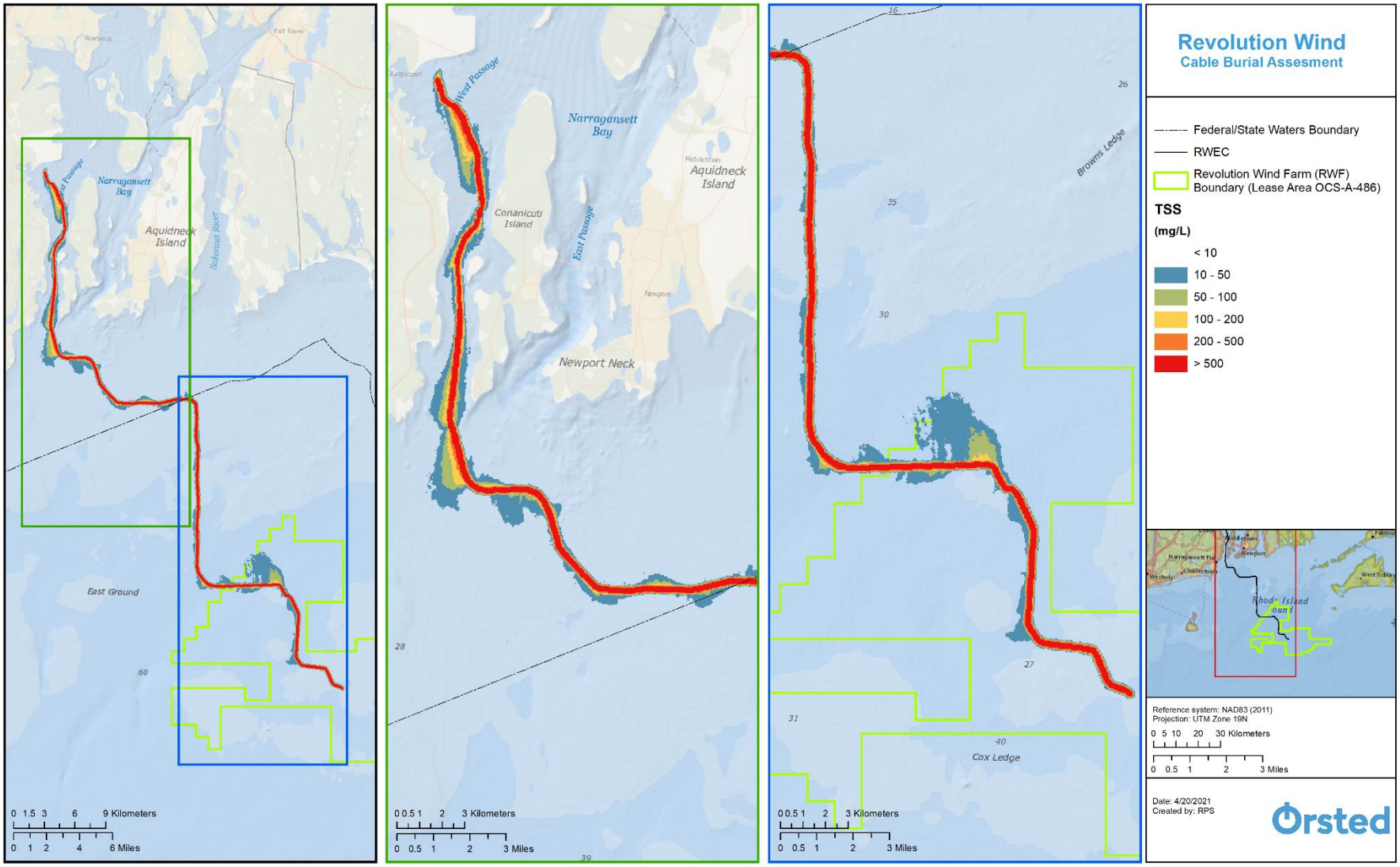

Figure 4.3-14. Map of Predicted Time-Integrated Maximum TSS Concentrations Associated with RWEC Circuit 1 Cable Burial.

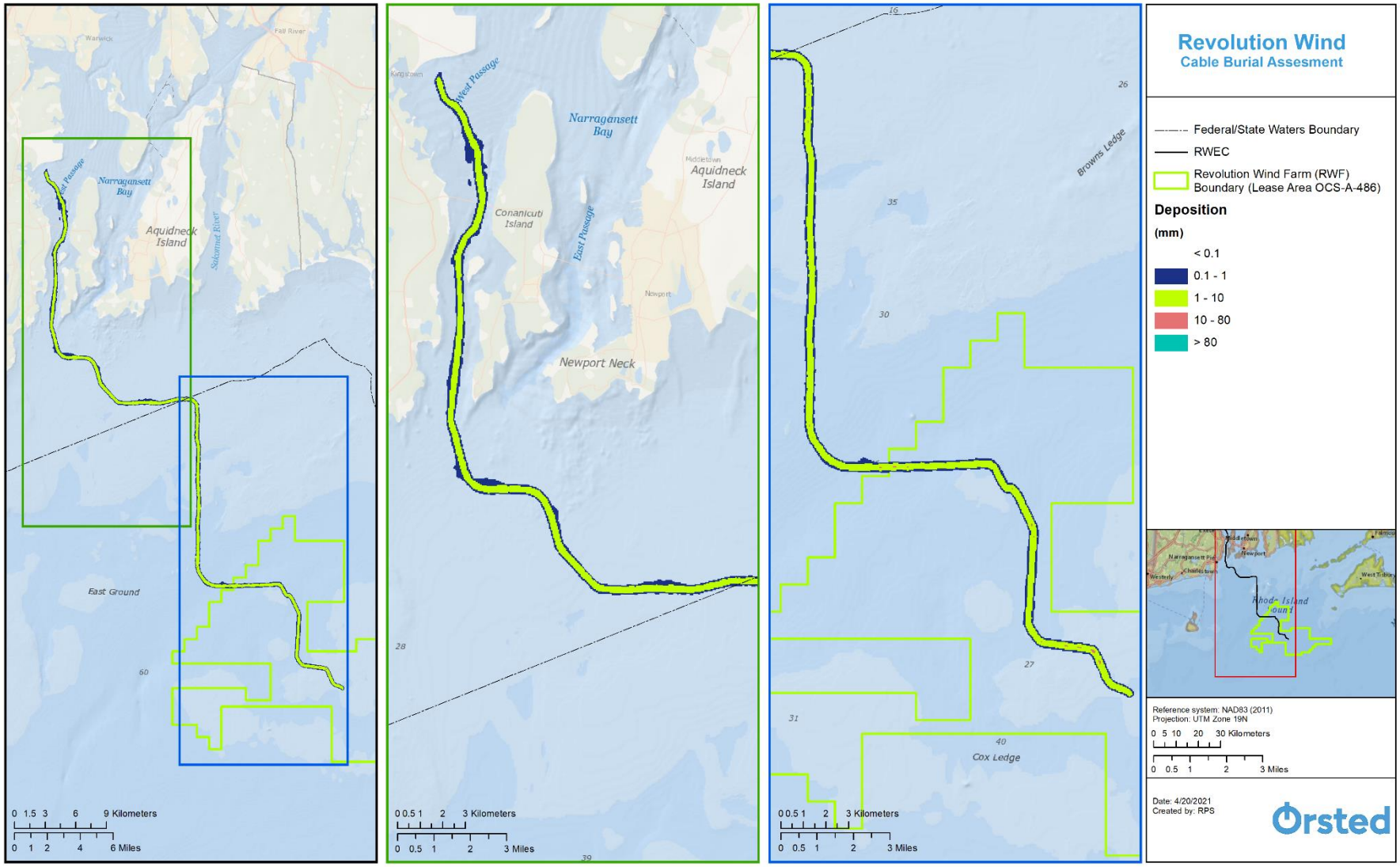

Figure 4.3-15. Map of Predicted Deposition Thickness Associated with RWEC Circuit 1 Cable Burial.

4.3.3 Study Component 3: Representative IAC Cable Burial

Two separate scenarios were modeled of the installation of a representative segment of the IAC. The two scenarios reflect two timeframes that would experience different current conditions. This was done to investigate the sensitivity to the currents, since the modeling of the representative segment simulates a relatively short installation period (<2 days) and does not capture a full spring/neap (more energy/less energy) cycle. One scenario was run during a timeframe that is representative of a spring tide and current (i.e., current regime 1), and the other was representative of a neap tide and current (i.e., current regime 2).

The results from the IAC simulations for two different current conditions are presented in Figure 4.3-16 through Figure 4.3-18. Figure 4.3-16 presents snapshots of instantaneous TSS concentrations with cross-sections for each scenario, Figure 4.3-17 presents the maximum TSS concentrations, and Figure 4.3-18 presents the associated deposition. The results are presented together such that they can be easily compared. These figures show that the two approaches result in the same order of magnitude of effects (e.g., TSS concentration plume extent). However, the location of the effect (plume or deposition) relative to the cable centerline will change in response to the currents.

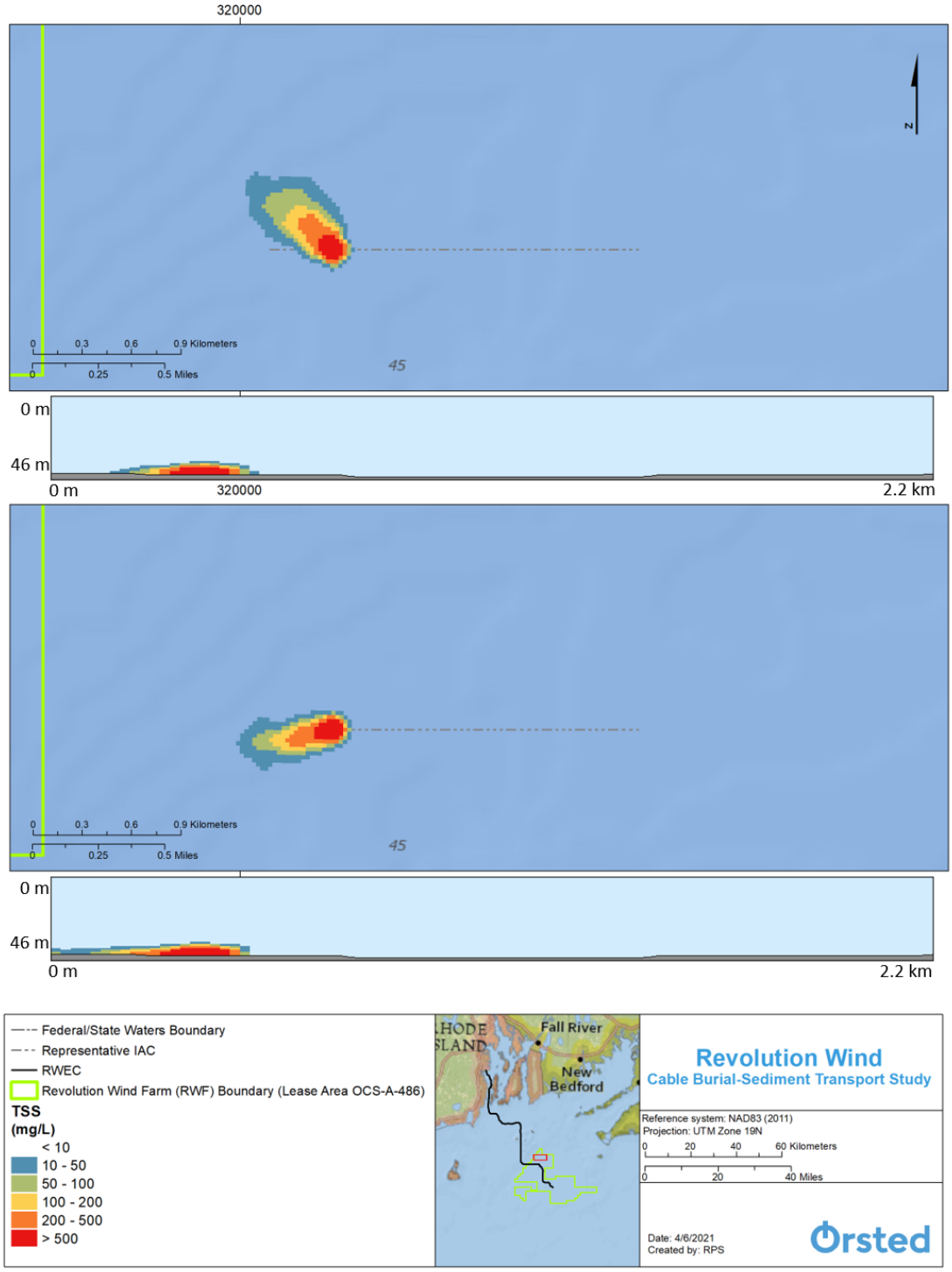

Figure 4.3-16. Snapshot of Predicted Instantaneous TSS Concentrations Associated with Representative IAC Cable Burial for Current Regime 1 (Top) and Current Regime 2 (Bottom).

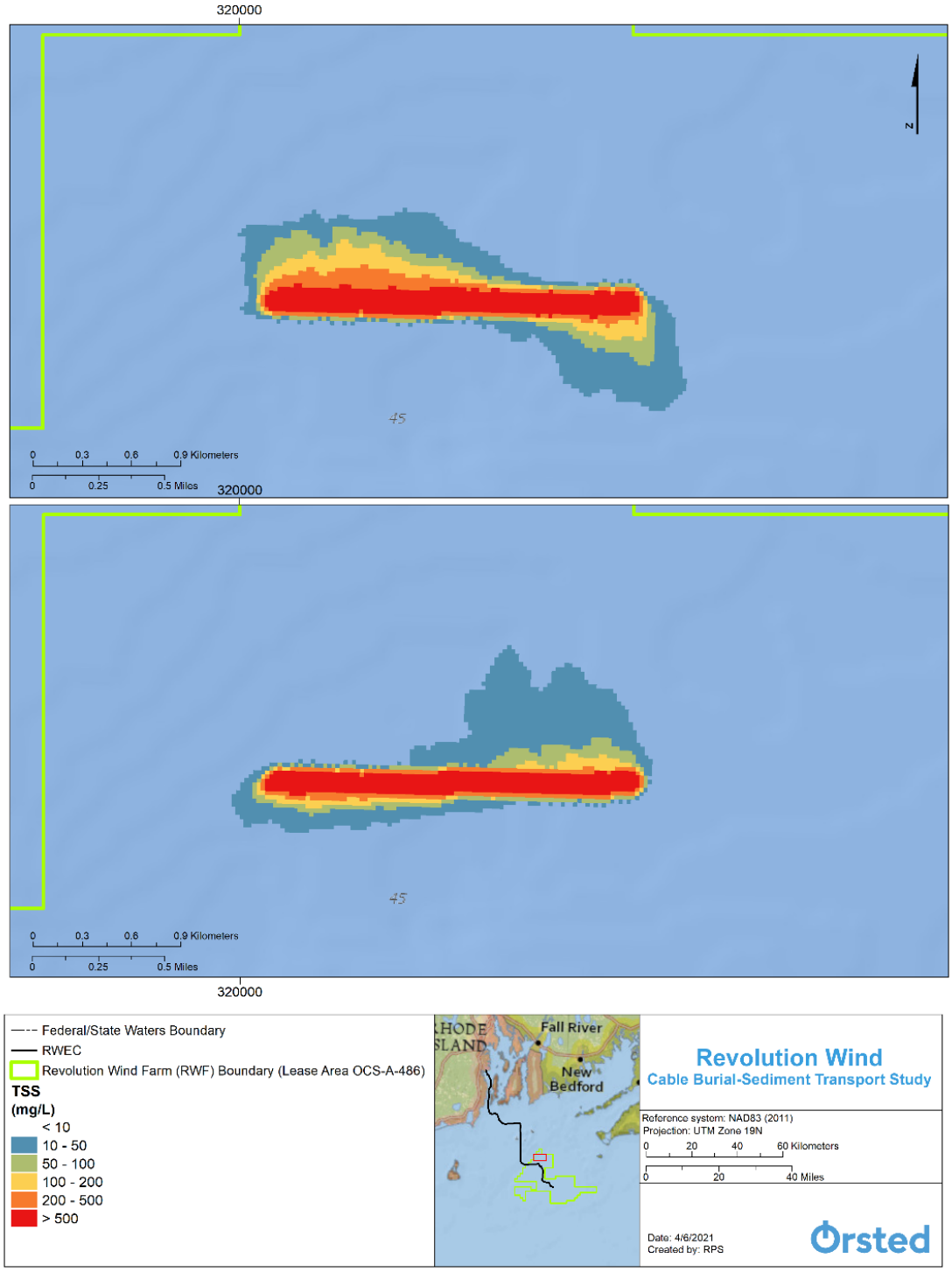

Figure 4.3-17. Map of Predicted Time-Integrated Maximum TSS Concentrations Associated with Representative IAC Cable Burial for Current Regime 1 (Top) and Current Regime 2 (Bottom).

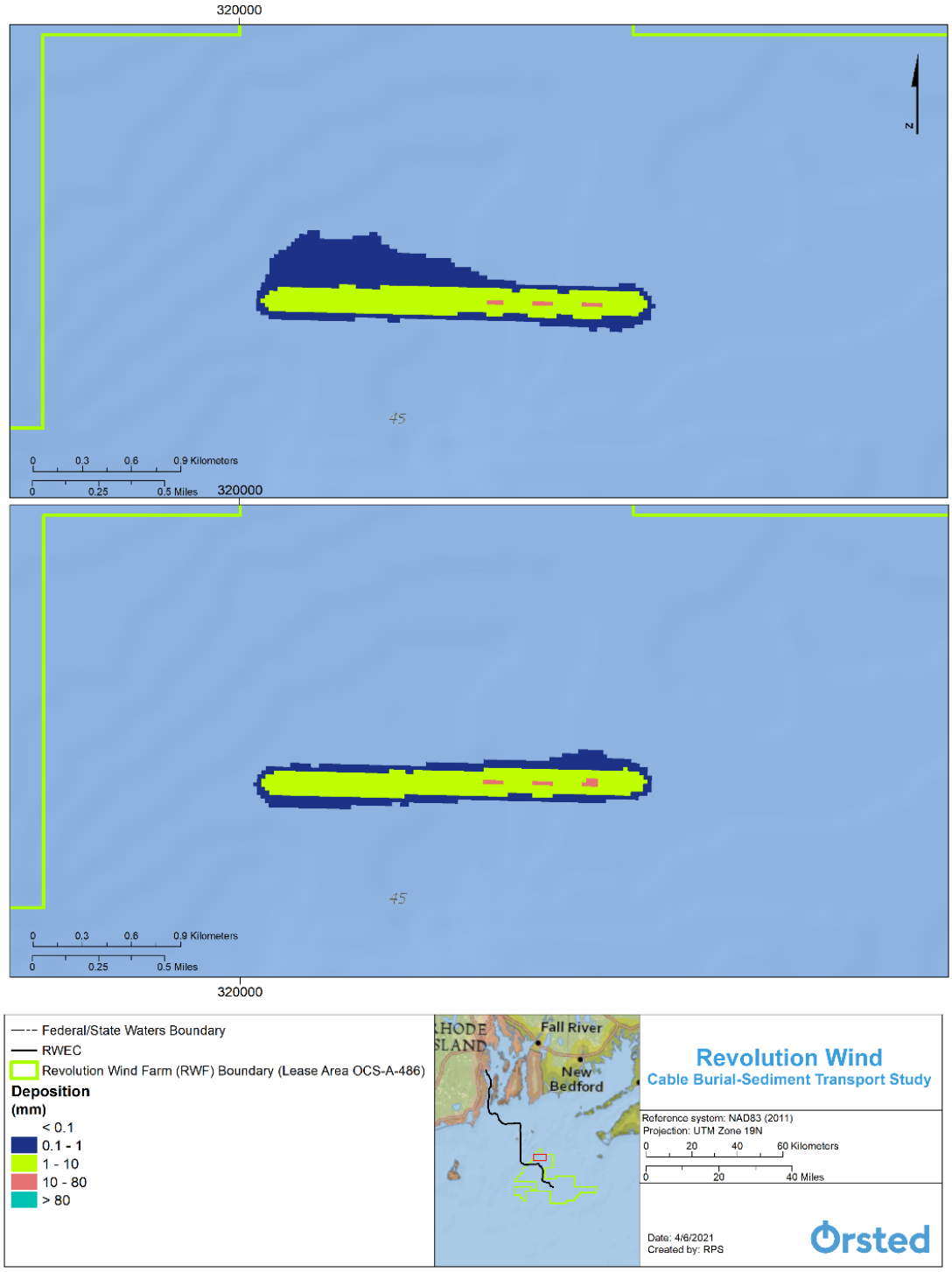

Figure 4.3-18. Map of Predicted Deposition Thickness Associated with Representative IAC Cable Burial for Current Regime 1 (Top) and Current Regime 2 (Bottom).

4.3.4 Study Component 4: RWEC Landfall

A snapshot of the instantaneous concentration from the RWEC landfall simulation is provided in Figure 4.3-19. The snapshot illustrates that highest concentrations are predicted to be directly adjacent to the route centerline, with lower concentrations extending further towards the northeast due to transport from local currents. The cross-sections, extending from the shoreline to just past the HDD exit pit, show sediment is introduced near the surface.

The time-integrated maximum TSS concentrations and deposition thickness results from the RWEC landfall simulation are presented in Figure 4.3-20 and Figure 4.3-21, respectively. Since the landfall analysis only includes clearance of the HDD exit pit, the concentration footprint is small, though exhibits fairly high concentrations due to the shallow depth and low currents of the site which reduce sediment transport extents.

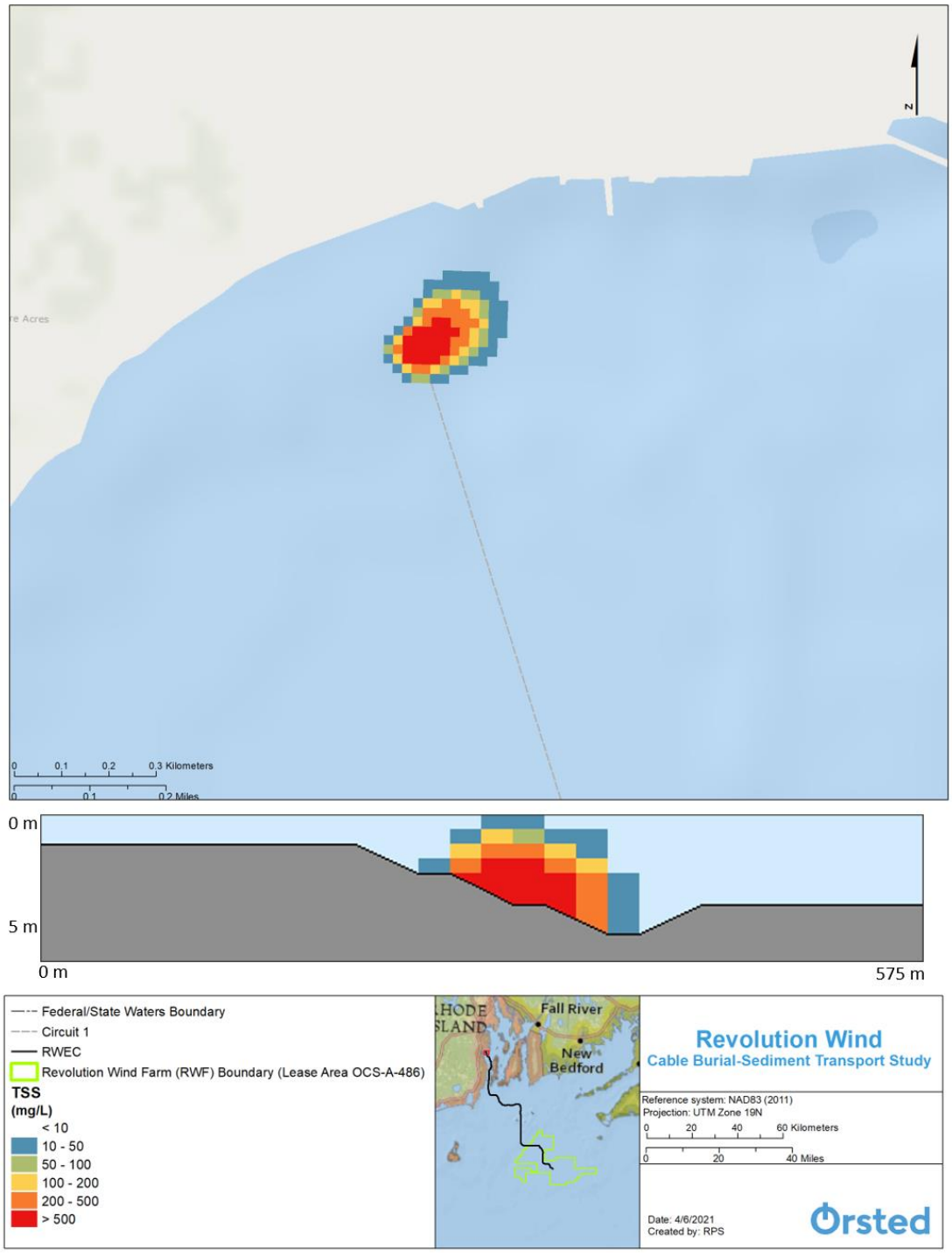

Figure 4.3-19 Snapshots of Predicted Instantaneous TSS Concentrations Associated with RWEC Landfall.

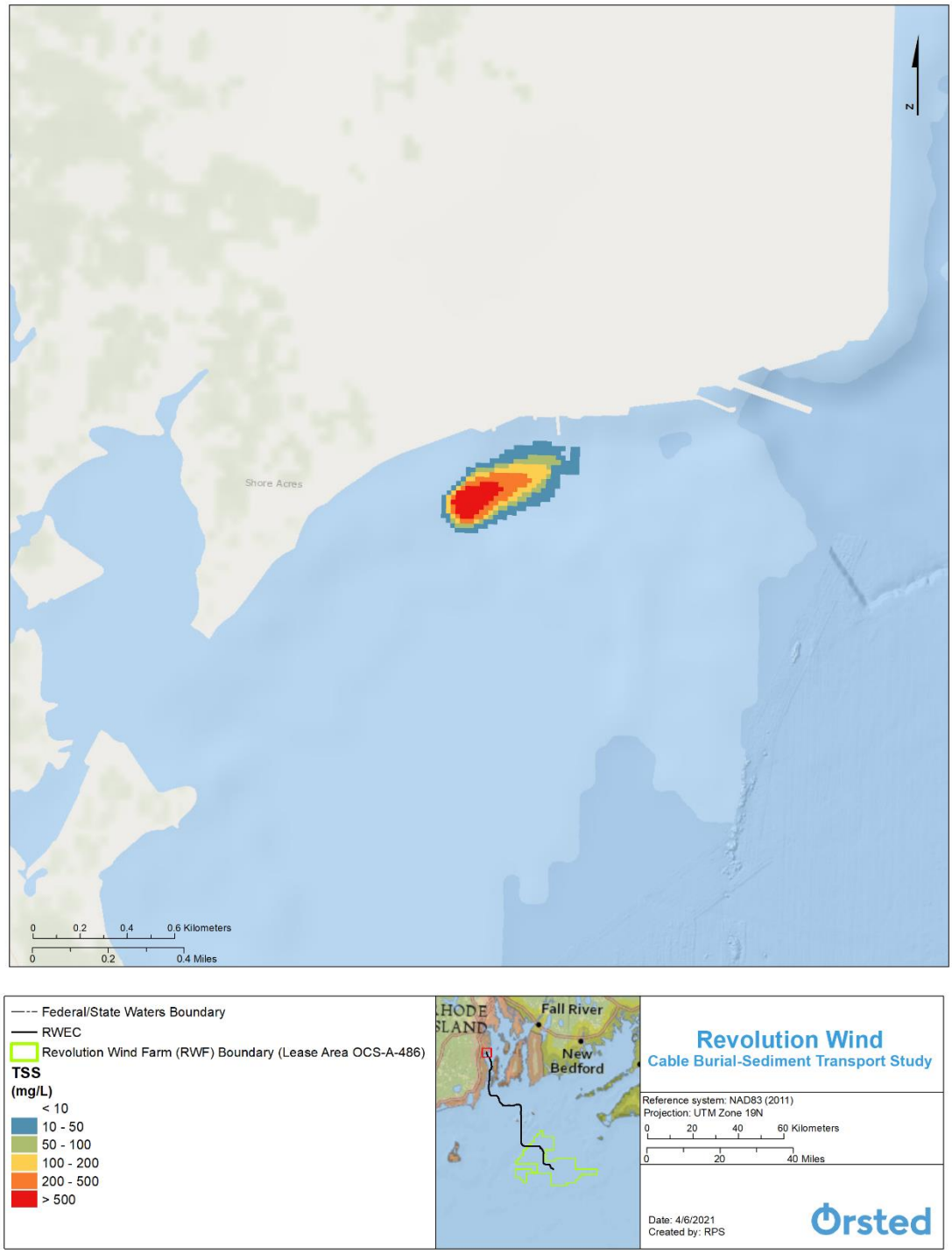

Figure 4.3-20. Map of Predicted Time-Integrated Maximum TSS Concentrations Associated with RWEC Landfall.

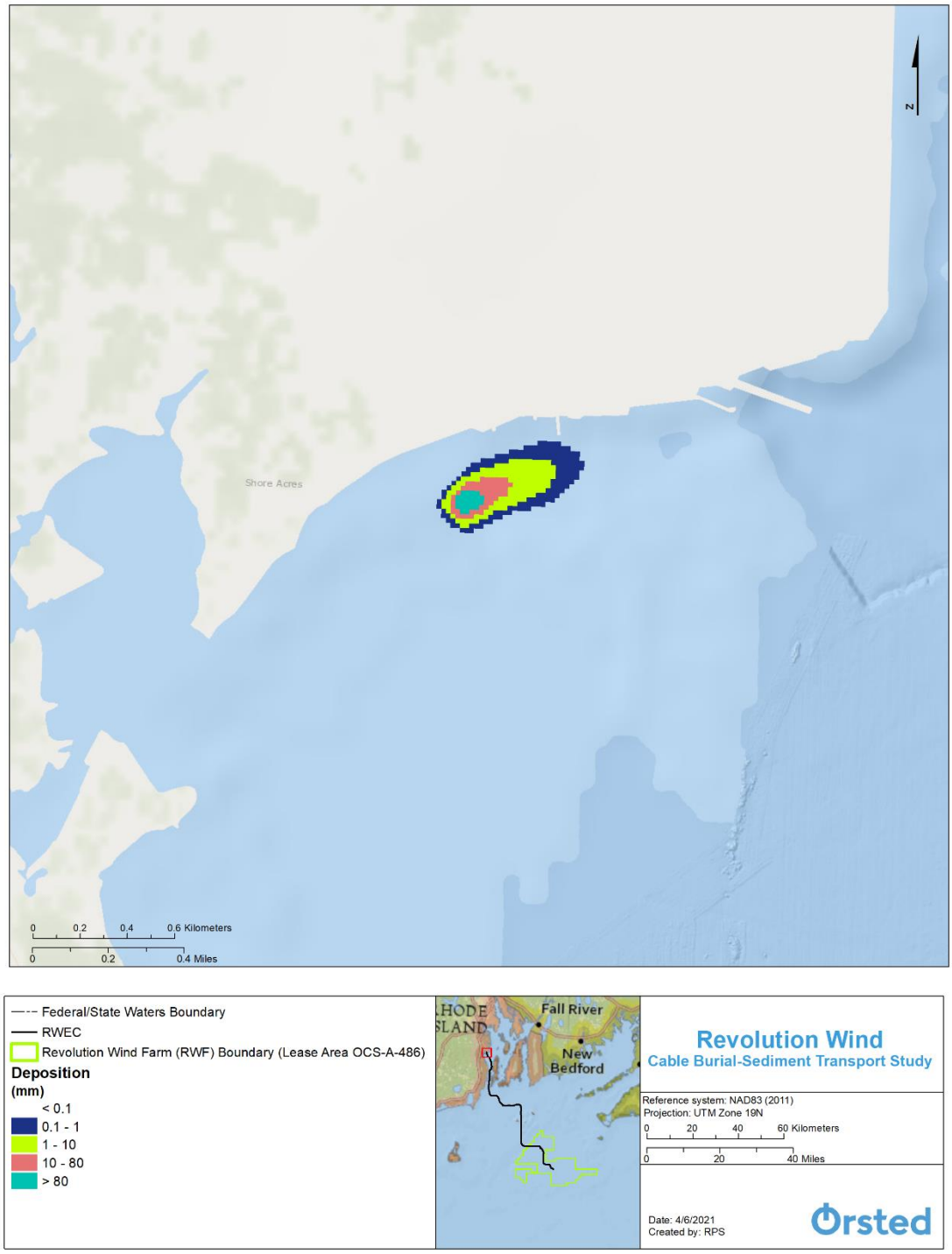

Figure 4.3-21. Map of Predicted Deposition Thickness Associated with RWEC Landfall.

4.4 Results Summary Tables

The results of the modeling showed that the cable burial activities will result in plumes of excess TSS in the water column and seabed deposition. The TSS plumes are limited to the bottom of the water column for the CFE seabed preparation method, RWEC Circuit 1 burial, and IAC burial because the construction methods modeled for these scenarios introduce sediment near the seabed. The TSS plumes for TSHD seabed preparation and the landfall are present throughout the majority of the water column due to sediment introduction at or near the water surface and, for the landfall, shallow depths. Each plume is temporary in any given location and was transported by local currents. Key metrics of each scenario are compiled and presented in the tables below. The bullets below describe the summary tables and discuss key results.

- Table 4.4-1 summarizes the total volumes resuspended for each scenario and the amount resuspended within RI state and federal waters.

Table 4.4-2 and Table 4.4-3 summarize the total area over different deposition thickness thresholds (0.1 mm, 1.0 mm, and 10 mm). The two tables present the same information (i.e., total area and area within RI state and federal waters above each threshold) as acres and hectares.

- Table 4.4-4 summarizes the maximum extent of deposition over three thickness thresholds (0.1 mm, 1.0 mm, and 10 mm). The extents were measured perpendicular to the modeled route centerline. Note that while the maximum extent is presented, the typical extent is often less than the scenario-specific maximum.
    - For the seabed preparation segments, deposition exceeding 10 mm is predicted to remain within 688.8 ft (210 m), 1,033.2 ft (315 m), and 852.8 ft (260 m) from the route centerline for CFE, TSHD split bottom, and TSHD continuous overflow seabed preparation activities, respectively.
    - For jet plow installation along the RWEC, deposition exceeding 10 mm is predicted to remain within 311.6 ft (95 m) from the route centerline.
    - For the IAC, deposition exceeding 10 mm is predicted to remain within 78.7 ft (24 m) and 88.6 ft (27 m) from the route centerline for current regime 1 and current regime 2, respectively.
    - Evaluation of the landfall showed that deposition exceeding 10 mm may extend up to 738 ft (225 m) from the exit pit location.
- Table 4.4-5 summarizes the maximum extent of the TSS plume over two different thresholds (50 mg/L and 100 mg/L). The extents were measured perpendicular to the modeled route centerline. Note that while the maximum extent is presented, the typical extent is often less than the scenario-specific maximum. The persistence of concentrations associated with the activities was investigated and the following points summarize those findings.
    - For the seabed preparation segments, the predicted concentrations above background (> 0 mg/L) do not persist in any given location (grid cell) for greater than 5.5 hours, 59.2 hours, and 85 hours for CFE, TSHD split bottom, and TSHD continuous overflow seabed preparation activities, respectively. In most locations (> 75% of the affected area) concentrations return to ambient within approximately 2.5 hours for CFE and approximately 26 hours for TSHD split bottom and 37 hours for TSHD continuous overflow. Predicted concentrations greater than 100 mg/L do not persist for greater than 2.2 hours, 19.2 hours, and 17.5 hours for CFE, TSHD split bottom, and TSHD continuous overflow seabed preparation activities, respectively.
    - For jet plow installation along the RWEC, predicted concentrations above background (> 0 mg/L) do not persist in any given location (grid cell) for greater than 69.7 hours. In most locations (> 75% of the affected area) concentrations return to ambient within approximately 24.5 hours. Predicted concentrations greater than 100 mg/L do not persist for greater than 4.5 hours.

- For the IAC, predicted concentrations above background (> 0 mg/L) do not persist in any given location (grid cell) for greater than 4.2 hours and 6.7 hours for current regime 1 and current regime 2, respectively. In most locations (> 75% of the affected area) concentrations return to ambient within approximately 3 hours and 4 hours for current regime 1 and current regime 2, respectively. Predicted concentrations greater than 100 mg/L do not persist for greater than 1.2 hours and 1.7 hours for current regime 1 and current regime 2, respectively.
- Evaluation of the landfall showed that predicted concentrations above background (> 0 mg/L) do not persist in any given location (grid cell) for greater than 70.3 hours. In most locations (> 75% of the affected area) concentrations return to ambient within approximately 6 hours. Predicted concentrations greater than 100 mg/L do not persist in for greater than 70.2 hours.

Table 4.4-1. Summary of Volume Resuspended for Modeling Scenarios.

Volumes Resuspended				
Study Component	Description of Scenario	Total Volume Resuspended, cy (m^3)	Volume Resuspended within RI State Waters, cy (m^3)	Volume Resuspended within Federal Waters, cy (m^3)
RWEC Seabed Preparation	Circuit 1 – Seabed Preparation, CFE	296,781.0 (226,905.4)	103,875.3 (79,418.4)	192,905.7 (147,487.0)
	Circuit 1 – Seabed Preparation, TSHD Split Bottom	296,279.2 (226,521.7)	103,163.2 (78,873.9)	193,116.0 (147,647.8)
	Circuit 1 – Seabed Preparation, TSHD Continuous Overflow	296,781.0 (226,905.4)	103,875.3 (79,418.4)	192,905.7 (147,487.0)
RWEC	Circuit 1 – Jet Plow	114,232.9 (87,337.3)	46,287.1 (35,388.9)	67,945.8 (51,948.4)
RWF – IAC	IAC – Current Regime 1, Jet Plow	2,292.2 (1,752.5)	0 (0)	2,292.2 (1,752.5)
	IAC – Current Regime 2, Jet Plow	2,292.2 (1,752.5)	0 (0)	2,292.2 (1,752.5)
Landfall	HDD Exit Pit – Backhoe Excavator followed by Venturi Eductor Device	3,097.8 (2,368.4)	3,097.8 (2,368.4)	0 (0)

Table 4.4-2. Summary of Areas (ac) Exceeding Deposition Thickness Thresholds.

Deposition Results: Area in Acres over Thickness Thresholds										
		Total Area (ac) of Deposition Exceeding Threshold			Area (ac) within RI State Waters of Deposition Exceeding Threshold			Area (ac) within Federal Waters of Deposition Exceeding Threshold		
Study Component	Description of Scenario	0.1 mm	1.0 mm	10 mm	0.1 mm	1.0 mm	10 mm	0.1 mm	1.0 mm	10 mm
RWEC Seabed Preparation	Circuit 1 – Seabed Preparation, CFE	2,621.8	1,955.8	1,195.4	992.1	727.1	453.4	1,629.7	1,228.7	742.0
	Circuit 1 – Seabed Preparation, TSHD Split Bottom	8,373.8	3,400.8	1,289.9	4,056.9	1,498.1	481.9	4,316.9	1,902.7	808.0
	Circuit 1 – Seabed Preparation, TSHD Continuous Overflow	8,459.0	3,419.9	1,271.4	4,270.0	1,677.8	480.0	4,189.0	1,742.1	791.4
RWEC	Circuit 1 – Jet Plow	8,354.6	5,094.7	25.9	4,017.3	2,335.8	0	4,337.3	2,758.9	25.9
RWF – IAC	IAC – Current Regime 1, Jet Plow	206.6	90.2	2.2	0	0	0	206.6	90.2	2.2
	IAC – Current Regime 2, Jet Plow	149.8	86.8	2.6	0	0	0	149.8	86.8	2.6
Landfall	HDD Exit Pit – Backhoe Excavator followed by Venturi Eductor Device	35.4	20.4	7.4	35.4	20.4	7.4	0	0	0

Table 4.4-3. Summary of Areas (ha) Exceeding Deposition Thickness Thresholds.

Deposition Results: Area in Hectares over Thickness Thresholds										
		Total Area (ha) of Deposition Exceeding Threshold			Area (ha) within RI State Waters of Deposition Exceeding Threshold			Area (ha) within Federal Waters of Deposition Exceeding Threshold		
Study Component	Description of Scenario	0.1 mm	1.0 mm	10 mm	0.1 mm	1.0 mm	10 mm	0.1 mm	1.0 mm	10 mm
RWEC Seabed Preparation	Circuit 1 – Seabed Preparation, CFE	1,061.0	791.5	483.8	401.5	294.3	183.5	659.5	497.2	300.3
	Circuit 1 – Seabed Preparation, TSHD Split Bottom	3,388.8	1,376.3	522.0	1,641.8	606.3	195.0	1,747.0	770.0	327.0
	Circuit 1 – Seabed Preparation, TSHD Continuous Overflow	3,423.3	1,384.0	514.5	1,728.0	679.0	194.3	1,695.3	705.0	320.2
RWEC	Circuit 1 – Jet Plow	3,381.0	2,061.8	10.5	1,625.8	945.3	0	1,755.2	1,116.5	10.5
RWF – IAC	IAC – Current Regime 1, Jet Plow	83.6	36.5	0.9	0	0	0	83.6	36.5	0.9
	IAC – Current Regime 2, Jet Plow	60.6	35.1	1.1	0	0	0	60.6	35.1	1.1
Landfall	HDD Exit Pit – Backhoe Excavator followed by Venturi Eductor Device	14.3	8.2	3.0	14.3	8.2	3.0	0	0	0

Table 4.4-4. Summary of Extent of Deposition Exceeding Thickness Thresholds as Measured Perpendicular from the Modeled Cable Centerline.

Deposition Extent							
		Maximum Extent of Deposition Exceeding Threshold within RI State Waters, ft (m)			Maximum Extent of Deposition Exceeding Threshold within Federal Waters, ft (m)		
Study Component	Description of Scenario	0.1 mm	1.0 mm	10 mm	0.1 mm	1.0 mm	10 mm
RWEC Seabed Preparation	Circuit 1 – Seabed Preparation, CFE	1,587.5 (484)	1,049.6 (320)	688.8 (210)	1,738.4 (530)	1,197.2 (365)	616.6 (188)
	Circuit 1 – Seabed Preparation, TSHD Split Bottom	6,553.4 (1,998)	3,017.6 (920)	1,033.2 (315)	5,641.6 (1,720)	2,633.8 (803)	846.2 (258)
	Circuit 1 – Seabed Preparation, TSHD Continuous Overflow	6,510.8 (1,985)	3,755.6 (1,145)	852.8 (260)	4,132.8 (1,260)	2,033.6 (620)	754.4 (230)
RWEC	Circuit 1 – Jet Plow	1,869.6 (570)	787.2 (240)	0 (0)	1,508.8 (460)	656.0 (200)	311.6 (95)
RWF – IAC	IAC – Current Regime 1, Jet Plow	N/A	N/A	N/A	1,453.0 (443)	367.4 (112)	78.7 (24)
	IAC – Current Regime 2, Jet Plow	N/A	N/A	N/A	659.3 (201)	324.7 (99)	88.6 (27)
Landfall	HDD Exit Pit – Backhoe Excavator followed by Venturi Eductor Device	1,771.2 (540.0)	1,377.6 (420.0)	738.0 (225.0)	N/A	N/A	N/A

Table 4.4-5. Summary of Extent of Plume Exceeding TSS Thresholds as Measured Perpendicular from the Modeled Cable Centerline

Plume Concentration Extent					
		Maximum Extent of Plume Concentration Perpendicular to Route Exceeding TSS Threshold within RI State Waters, ft (m)		Maximum Extent of Plume Concentration Perpendicular to Route Exceeding TSS Threshold within Federal Waters, ft (m)	
Study Component	Description of Scenario	50 mg/L	100 mg/L	50 mg/L	100 mg/L
RWEC Seabed Preparation	Circuit 1 – Seabed Preparation, CFE	1,754.8 (535)	1,443.2 (440)	1,836.8 (560)	1,731.8 (528)
	Circuit 1 – Seabed Preparation, TSHD Split Bottom	6,888.0 (2,100)	4,690.4 (1,430)	4,493.6 (1,370)	3,066.8 (935)
	Circuit 1 – Seabed Preparation, TSHD Continuous Overflow	6,560.0 (2,000)	5,838.4 (1,780)	3,378.4 (1,030)	2,984.8 (910)
RWEC	Circuit 1 – Jet Plow	3,673.6 (1,120)	2,345.2 (715)	4,920.0 (1,500)	1,754.8 (535)
RWF – IAC	IAC – Current Regime 1, Jet Plow	N/A	N/A	1,518.6 (463)	1,272.6 (388)
	IAC – Current Regime 2, Jet Plow	N/A	N/A	898.7 (274)	590.4 (180)
Landfall	HDD Exit Pit – Backhoe Excavator followed by Venturi Eductor Device	1,459.6 (445)	1,312.0 (400)	N/A	N/A

4.5 Results Discussion and Conclusions

Based on conservative assumptions for the modeled study components, the goal of this assessment was to bound the range of predicted movement, behavior, and potential for effects that may be expected during and following sediment-disturbing activities anticipated for the Project. Using SSFATE, developed jointly by the USACE ERDC and Applied Science Associates (now part of RPS), sediment transport modeling was conducted to predict the extent, magnitude, and duration of sediment plumes above background values.

Simulations of CFE seabed preparation predict a plume that is localized to the seabed due to the introduction of sediment near the bottom of the water column. Predictions show the plume of the CFE method tends to remain closer to the route centerline, with relatively higher concentrations, than the TSHD methods. The localization of sediment plumes for the CFE method is likely due to the introduction of sediment closer to the seabed and a faster installation rate. For CFE, the maximum extent of deposition exceeding 10 mm is predicted to remain within 688.8 ft (210 m) from the route centerline. In comparison, this maximum extent was approximately 344.4 ft (105 m) and 164 ft (50 m) smaller than the TSHD split bottom and TSHD continuous overflow, respectively. For the TSHD seabed preparation simulations, the predicted plume was present throughout the water column due to the introduction of sediment at or near the water surface. While the TSHD split bottom's instantaneous plume reflects the periodic overflow and split bottom disposal compared to the TSHD continuous overflow, the footprints of both TSHD methods appear alike. For example, the total area of deposition exceeding 10 mm within RI state waters differed by approximately 1.9 acres (0.7 ha). These similarities are due to the similar disposal locations within the water column and identical installation speed. The slight differences are most likely due to the periodic introduction of finer sediment at the surface and coarser sediment a few meters below the surface for the split bottom method,

whereas all sediment was disposed of at the surface for the continuous overflow method. The influence of the location where sediment is introduced to the water column (e.g., seabed vs. water surface) was highlighted by the TSHD methods larger duration of predicted concentrations above background (> 0 mg/L). For example, the predicted concentration above background for CFE was estimated to subside 53.7 hours and 79.5 hours before the TSHD split bottom and TSHD continuous overflow activities, respectively. Additionally, in > 75% of the affected area, concentrations are predicted to return to ambient within approximately 2.5 hours for CFE, approximately 26 hours for TSHD split bottom, and 37 hours for TSHD continuous overflow.

Simulations of RWEC Circuit 1 cable installation using jet plow installation parameters predict a plume that is localized to the seabed due to the introduction of sediment near the bottom of the water column. The response of the plume to the oscillating currents is evident in the footprint, particularly in sections where the route is perpendicular to the predominate current direction. Along the RWEC the maximum deposition exceeding 10 mm is predicted to remain within 311.6 ft (95 m) from the route centerline. The predicted concentrations above background (> 0 mg/L) do not persist in any given location (grid cell) for greater than 69.7 hours. In most locations (> 75% of the affected area) concentrations return to ambient within approximately 24.5 hours.

Simulations of IAC installation using jet plow installation parameters predict a plume that is localized to the seabed due to the introduction of sediment near the bottom of the water column. The response of the plume to the oscillating currents is evident when comparing the current regime 1 (i.e., spring tide) and current regime 2 (i.e., neap tide) footprints. Deposition exceeding 10 mm is predicted to remain within 78.7 ft (24 m) and 88.6 ft (27 m) from the route centerline for current regime 1 and current regime 2, respectively. The predicted concentrations above background (> 0 mg/L) do not persist in any given location (grid cell) for greater than 4.2 hours and 6.7 hours for current regime 1 and current regime 2, respectively. In most locations (> 75% of the affected area) concentrations return to ambient within approximately 3 hours and 4 hours for current regime 1 and current regime 2, respectively.

The landfall simulation predicts the concentration footprint is relatively small, though exhibits fairly high concentrations due to the shallow depth and low currents of the site which reduce sediment transport extents. Deposition greater than 10 mm may extend up to 738 ft (225 m) from the exit pit location. The predicted concentrations above background (> 0 mg/L) do not persist in any given location (grid cell) for greater than 70.3 hours. In most locations (> 75% of the affected area) concentrations return to ambient within approximately 6 hours.

SSFATE was used to effectively simulate four representative study components of the types of activities that are expected with the Project. The modeling predicted the potential TSS concentrations, deposition thicknesses, exposure durations, and corresponding areas and distances associated with each Project-related construction activity.

5.0 REFERENCES

Anderson, E.L., Johnson, B., Isaji, T., and E. Howlett, 2001. SSFATE (Suspended Sediment FATE), a model of sediment movement from dredging operations. WODCON XVI World Dredging Congress, 2-5 April 2001, Kuala Lumpur, Malaysia.

Codiga, D.L and D.S Ullman. (2010). Characterizing the Physical Oceanography of Coastal Waters Off Rhode Island, Part 1: Literature Review, Available Observations, and A Representative Model Simulation in the Rhode Island Ocean SAMP study area (p. 14). Technical Report 2.

Connecticut Department of Energy & Environmental Protection. (Accessed 2017). CT_TOWN.shp [Shapefile]. Retrieved from http://www.ct.gov/deep/gisdata/

Davies, A. M. (1977). The numerical solution of the three-dimensional hydrodynamic equations, using a B-spline representation of the vertical current profile. Elsevier Oceanography Series, 19, 1-25.

Egbert, G. D., Bennett, A. F., & Foreman, M. G. (1994). TOPEX/POSEIDON tides estimated using a global inverse model. *Journal of Geophysical Research: Oceans*, *99*(C12), 24821-24852.

Egbert, G. D., & Erofeeva, S. Y. (2002). Efficient inverse modeling of barotropic ocean tides. *Journal of Atmospheric and Oceanic Technology*, *19*(2), 183-204.

Gordon, R. B. (1982). *Wind-driven circulation in Narragansett Bay* (Doctoral dissertation, University of Rhode Island).

Grilli, S., Harris, J., Sharma, R., Decker, L., Stuebe, D., Mendelsohn, D., Crowley, D., & Decker, S. (2010). High resolution modeling of meteorological, hydrodynamic, wave and sediment processes in the Rhode Island Ocean SAMP study area (p. 119). Technical Report 6.

Isaji, T. H., Howlett, E, Dalton C. and Anderson E. (2001).,Stepwise-Continuous-Variable-Rectangular Grid. In *Proc. 24th Arctic and Marine Oil Spill Program Technical Seminar* (pp. 597-610).

Isaji, T., & Spaulding, M. L. (1984). A model of the tidally induced residual circulation in the Gulf of Maine and Georges Bank. *Journal of physical oceanography*, *14*(6), 1119-1126.

Johnson, B.H., E. Anderson, T. Isaji, and D.G. Clarke, 2000. Description of the SSFATE numerical modeling system. DOER Technical Notes Collection (TN DOER-E10). U.S. Army Engineer Research and Development Center, Vicksburg, MS. http: //www.wes.army.mil/el/dots/doer/pdf/doere10.pdf.

Lin, J.; Wang, H.V.; Oh, J-H.; Park, K.; Kim, S-C.; Shen, J., and Kuo, A.Y., 2003. A new approach to model sediment resuspension in tidal estuaries. Journal of Coastal Research, 19(1), 76-88.

MassGIS. (Accessed 2017). OUTLINE25K_POLY.shp [Shapefile]. Retrieved from https://www.mass.gov/get-massgis-data

NDBC. (Accessed 2019). Historic Meteorological Observations [ASCII Text Files]. Retrieved from http://www.ndbc.noaa.gov/station_page.php?station=buzm3

NOAA. (Accessed 2019a).ENC Data [Multiple geodatabase files]. Retrieved from https://encdirect.noaa.gov/

NOAA. (Accessed 2019b). Harmonic Constituents [ASCII Data]. Retrieved from https://tidesandcurrents.noaa.gov/

NY GIS Clearinghouse. (Accessed 2017). Counties_Shoreline.shp [Shapefile]. Retrieved from http://gis.ny.gov/gisdata/inventories/details.cfm?DSID=927

Owen, A. (1980). A three-dimensional model of the Bristol Channel. *Journal of Physical Oceanography*, *10*(8), 1290-1302.

Pawlowicz, R., Beardsley, B., & Lentz, S. (2002). Classical tidal harmonic analysis including error estimates in MATLAB using T_TIDE. *Computers & Geosciences*, *28*(8), 929-937.

RIGIS. (Accessed 2010). Towns.shp [Shapefile]. Retrieved from http://www.rigis.org/

Soulsby, R.L., 1998. Dynamics of Marine Sands. Thomas Telford, England.

Spaulding, M. L., & Gordon, R. B. (1982). A nested NUMERICAL tidal model of the Southern New England Bight. *Ocean Engineering*, *9*(2), 107-126.

Swanson, J.C., T. Isaji, M. Ward, B.H. Johnson, A. Teeter, and D.G. Clarke, 2000. Demonstration of the SSFATE numerical modeling system. DOER Technical Notes Collection (TN DOER-E12). U.S. Army Engineer Research and Development Center, Vicksburg, MS. http://www.wes.army.mil/el/dots/doer/pdf/doere12.pdf.

Swanson, C., and T. Isaji, 2004. Modeling Dredge-Induced Suspended Sediment Transport and Deposition in the Taunton River and Mt. Hope Bay, Massachusetts. Western Dredging Association Annual Meeting and Conference, March 26, 2004.

Swanson, C., T. Isaji, and C. Galagan, 2007. Modeling the Ultimate Transport and Fate of Dredge-Induced Suspended Sediment Transport and Deposition. Proceedings of WODCON 2007, Lake Buena Vista, Florida.

Teeter, A.M., 2000. Clay-silt sediment modeling using multiple grain classes: Part I: Settling and deposition. Proceedings in Marine Science, 3, 157-171.

Van Rijn L.C., 1989, *Sediment Transport by Currents and Waves,* Report H461, Delft Hydraul. Lab., Delft, Netherlands.